2007:09

DOCTORAL THESIS

Microwave Sensors for Scanning of Sawn Timber

Nils Lundgren

Luleå University of Technology
LTU Skellefteå
Division of Wood Science and Technology

2007:09 | ISSN: 1402-1544 | ISRN: LTU-DT -- 07/09 -- SE

Microwave Sensors for Scanning of Sawn Timber

by

Nils Lundgren

Luleå University of Technology
LTU Skellefteå
Division of Wood Science and Technology
Skeria 3, SE-931 87 Skellefteå, Sweden
http://www.ltu.se/ske
2007

Abstract

A microwave imaging sensor that measures the signal transmitted through a board was investigated with respect to the ability to predict the distribution of moisture and density in sawn lumber. Furthermore, the response from the sensor was related to strength properties of the boards. Multivariate statistics was used to relate the measured variables to various properties. A finite element model based on X-ray computed tomography images was developed to describe the interactions between microwaves and wood. The model made it possible to simulate the response from the sensor under varying conditions. The results show that microwaves can be used for prediction of density and moisture content. They can also be used for prediction of strength properties, mainly from the correlation to density, but also from the influence on microwaves of structural variations in the wood. The finite element model is useful in the evaluation of microwave sensors for wood, drying equipment or other applications where electromagnetic waves interact with wood.

Keywords: microwave scanning; wood; density; moisture content; strength grading; finite element.

Preface

I have learnt a lot about wood since I began my work as a PhD student in December 2002. I have worked with different scanning equipments based on X-rays, microwaves, infrared or visible light and learnt about how logs are turned into useful products at a sawmill. I have also learnt about microwaves and how they can be used to measure the properties of a dielectric material.

Other subjects that I have studied during the same period of time are how to navigate in the Kvarken archipelagos from Holmön in Sweden to Björkö in Finland, how to find my way in the mountains around Szczawnica in southern Poland and how to dance the polska, which is a traditional Scandinavian dance that is believed to have Polish roots. The results from these studies are not reported here.

The work presented in this thesis was carried out at Luleå University of Technology, Skellefteå Campus, under supervision of Professor Olle Hagman and Professor Anders Grönlund. The project was financially supported by the SkeWood program, through the Swedish Agency for Innovation Systems (Vinnova) and the Kempe foundation. It was also financed by the European Regional Development Fund, objective 1.

Thanks to Lars Hansson who made the first finite element model and to all my colleagues at Campus Skellefteå for the help that I have received. Also thanks to Mattias Brännström for his lectures on strength grading.

Tack till mina polska vänner.

Det är bra att det går framåt
– men det ska gå runt också!

Skellefteå in February 2007

Nils Lundgren

List of papers

I. Hansson, L., Lundgren, N., Antti, L. and Hagman, O. 2005. Microwave penetration in wood using imaging sensor. *Journal of International Measurement Confederation* 38(1):15–20.

II. Hansson, L., Lundgren, N., Antti, L. and Hagman, O. 2006. FEM simulation of interactions between wood and microwaves. *Journal of Wood Science* 52(5):406–410.

III. Lundgren, N., Hansson, L., Hagman, O. and Antti, L. 2006. FEM simulation of interactions between microwaves and wood during thawing. Mathematical Modelling of Wave Phenomena. Växjö University, Sweden. 14–19August 2005. In: *AIP Conference Proceedings* 834:260–267.

IV. Hansson, L., Lundgren, N., Antti, L. and Hagman, O. 2005. FEM simulation of heating wood in an industrial microwave applicator. *10th International Conference on Microwave and High Frequency Heating*. Modena and Reggio Emilia University, Modena, Italy, September12–15, 2005.

V. Lundgren, N., Hagman, O. and Johansson, J. 2006. Predicting moisture content and density distribution of Scots pine by microwave scanning of sawn timber II: evaluation of models generated on a pixel level. *Journal of Wood Science* 52(1):39–43.

VI. Lundgren, N., Brännström, M., Hagman, O. and Oja, J. 2007. Predicting the strength of Norway spruce by microwave scanning: A comparison with other scanning techniques. *Wood and Fiber Science* 39(1) (in press).

VII. Lundgren, N., Gerasimov, V., Kozlova, T. and Zorin, E. 2006. *An Online Microwave Scanner for Sawn Wood*. Technical report. Luleå University of Technology.

Contribution to the included papers

I – IV. The work was done by the author in collaboration with Lars Hansson with supervision and comments by Hagman and Antti.

V. Most of the work was done by the author with supervision and comments by the co-authors of the paper.

VI. The work was done by the author in collaboration with Mattias Brännström with supervision, comments and assistance in some measurements by Hagman and Oja.

VII. The co-authors have participated in measurements and data processing.

Contents

Små vågor av värme …

1. Introduction

1.1. Outline

This thesis is composed from work that has previously been presented in seven papers that are attached in an appendix. The introduction contains some notes on the background and the results from previous studies on microwave sensors in combination with wood. This part is followed by a description of materials and methods used, including a discussion about wood as a dielectric material and some electromagnetic theory. The next part is a summary of the papers, and finally there is a discussion about the results and a summary of the conclusions made. Figure 1 shows the working procedure for the papers included in the thesis, starting with a validation of the existing sensor in paper I. Finite element modelling (FEM) was used to simulate the response from the sensor in papers II–III. Heating of wood was simulated in paper IV, and multivariate models for prediction of moisture content (MC), density and strength properties were evaluated in papers V–VI. Preliminary tests with a new version of the sensor were performed in paper VII.

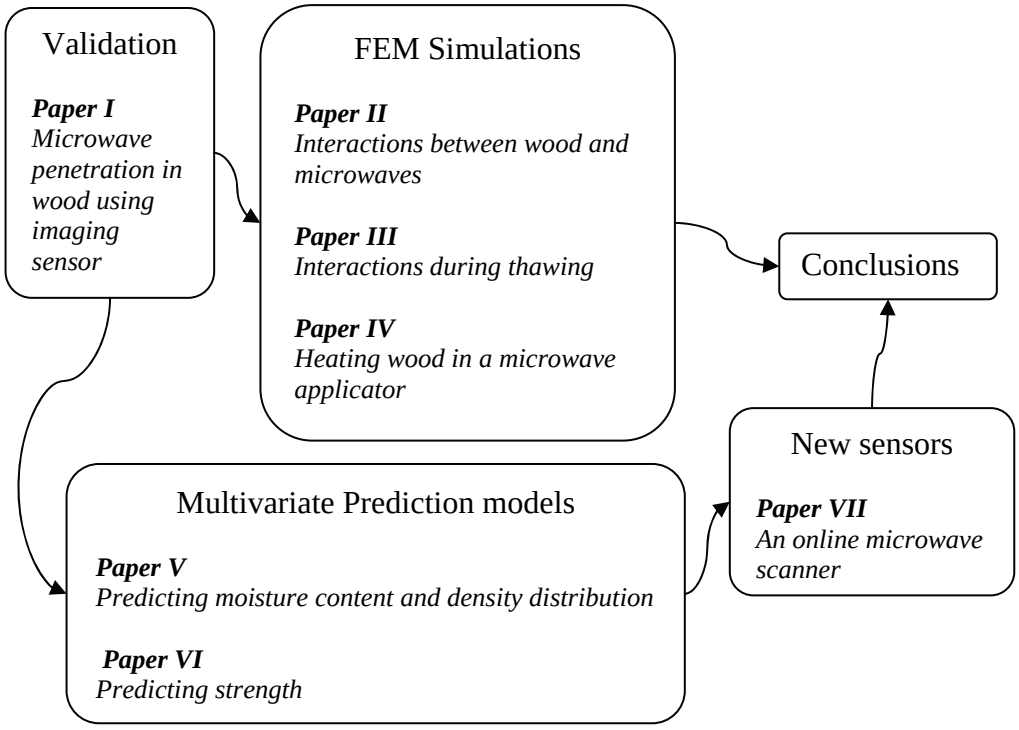

Figure 1. Schematic diagram for the papers included in the thesis.

1.2. Background

The starting point for the present work was a microwave scanning system, developed at LTU Skellefteå, and the licentiate thesis that was presented by Jan Johansson (2001). He shows that the microwave scanner in combination with multivariate statistics can be used for prediction of dry matter density and moisture content (MC) in sawn timber. Johansson also concludes that this technique has a high potential for prediction of strength in pine. The present work is mainly based on the scanning system used by Johansson and modulated scattering technique (MST). This technique makes it possible to measure the electromagnetic field with a high resolution (< 5 mm). Other kinds of microwave sensors and possible applications have been recapitulated by Nyfors and Vainikainen (1989) and in an updated review by Nyfors (2000). The most appealing qualities of microwaves can be summarized in the following points:

- Microwave sensors are fast enough for online measurements.
- The sensors do not need mechanical contact with the material.
- The tested material is unaffected by the measurement.
- Microwaves penetrate all materials except for metals, which makes it possible to measure interior properties.
- Electromagnetic radiation at low power levels is safe, in contrast with radioactive radiation.
- The multivariate character of the signal can be used to deduce more than one property of the measured object.

One drawback with microwaves is the shallow penetration in materials with high moisture content. Another problem is that small objects are invisible due to the long wavelength. A high or low microwave frequency can be chosen depending on whether high resolution or high penetration is preferred. It is possible to design microwave sensors with a short distance between the measurement points, but the resolution will still be limited by the wavelength. Very small objects (1/10 of the wavelength) can be detected if the contrast in dielectric properties is high or if the object is a single defect in a homogeneous material. For example, cracks can be detected in a metal surface (Zoughi 2000). The variations and low contrast in dielectric properties within wood mean that knots normally must have a size comparable to the wavelength to be detected by a microwave sensor.

1.3. Microwave sensors

A dielectric material will cause attenuation in a propagating microwave by absorption of energy. Wavelength and velocity of the wave will be reduced, and part of the wave will be reflected or scattered at boundaries where the dielectric properties change. The most straightforward approach is to measure the transmitted signal and predict, for example the moisture content of a bulk material passing on a conveyor belt (Nyfors and Vainikainen 1989). For some applications, it is more practical to measure the reflected signal. This is the case when ground-penetrating radar is used to detect underground objects or when the level of a surface is monitored. It is also possible to design cavities in waveguides where standing waves will be present when the material in the cavity has certain dielectric properties. This kind of sensor is useful for detection of small deviations in a homogeneous material.

1.4. Previous work

Several studies have been made on how microwave sensors can be used to measure different properties in wood. The possibility to use microwaves for online control in the wood and paper industries has, among others, been investigated by Lhiaubet et al. (1992) in a study in which amplitude and phase measurements were related to moisture content and density through polynomial models.

The direction of the grain is the angle between the wood fibres and the longitudinal axis of the lumber. The dielectric constant is normally greater along the grain than across the grain, which means that grain angle can be measured by two capacitance-type transducers mounted perpendicular to each other (Samson 1984). A method for grain angle measurements by the use of a rotating probe has been proposed by Shen et al. (1994).

Both grain angle and knots influence the strength of a board. Leicester and Seat (1996) used this circumstance to improve the results from a bending machine for stress grading by adding microwave sensors for detection of knots and measurement of grain angle. The Finnograder, tested by Boström (1994), uses a combination of microwaves, gamma rays and infrared light for grading of lumber without mechanical contact. This reduces the sensitivity to grading speed and makes it possible to grade the whole board but grading machines with microwave sensors have not yet been commercially successful.

The complex relations between wood and microwaves make it difficult to separate the influence from different wood properties on a transmitted microwave signal.

One way to deal with such problems is to calibrate multivariate models. Johansson et al. (2003) used this method to predict moisture content and density distribution in Scots pine (*Pinus sylvestris*) by microwave scanning. An extended study based on this work is presented in Paper V while the study on microwaves and strength in paper VI is based on preliminary results presented by Johansson (2001).

Several commercial systems for in-line measurement of the moisture content in wood are available, but most of these systems use electromagnetic waves in the radio frequency (RF) region. A test of four commercial in-line moisture measurement systems is reported by Esping (2003) where he states that their accuracy is lower than desired. Esping also suggests that the measurements should be improved by compensating for density variations.

Microwaves cannot penetrate into the centre of a living tree due to the high moisture content and shape of the trunk. Measurements on freshly cut logs by Eskelinen and Eskelinen (2000) show that information about the internal structure can be gathered in real time, but it is difficult to correlate the response to different properties. Possible applications are noninvasive detection of rot or cavities in living trees. Microwave measurements in wood are generally made in one or sometimes two dimensions. Three-dimensional microwave imaging has mainly been developed for medical applications, but some studies on microwave tomography of logs have been reported (Kaestner 2002).

1.5. Aim and Scope

The purpose of the present study was to evaluate whether high-resolution microwave sensors are suitable for prediction of wood properties and for grading of lumber. A further purpose was to analyze the interaction between wood and microwaves in order to propose improvements to the sensors and to the methods of interpretation of the measurements. The study is limited to one kind of microwave sensor using modulated scattering technique and a frequency of 9.375 GHz. A finite element model that describes how microwaves propagate in wood was developed in order to investigate the response from the sensor.

2. Multivariate calibration

Large amounts of data that consist of many variables or observations can be summarized by the use of multivariate methods (Martens & Næs 1989). Calibration involves relating known reference variables to data from another measurement, e.g., when density determined by measuring dimensions and weight is related to data from the microwave sensor. Variables with a large numerical range can be expected to have a large variance and to dominate over other variables. This is generally avoided by scaling all variables to unit variance prior to modelling. The standard procedure also includes mean centring of the data by subtracting the average value from each variable to improve interpretability of the model. Further preprocessing is sometimes done when the relations between variables are nonlinear or when a variable has a skewed distribution.

Principal component analysis (PCA) is used to reduce the dimensionality of the data by finding latent variables, the principal components (PCs) that explain the systematic variation. The first PC is fitted by the least squares method to the observations in order to explain as much of the systematic variation as possible. The second PC is then fitted to explain as much as possible of the systematic variation that is left orthogonal to the first PC. Each PC that is fitted will contribute less information and more noise as compared to the previous one. The number of PCs required to describe the data is lower than the number of variables unless all variables are uncorrelated. The projection of observations onto PCs is known as scores while the orientation of the PC plane with respect to the original variables is known as loadings. PCA is used for screening of data to find outliers, hidden patterns and relations between variables or observations.

Projection to latent structures by means of partial least squares (PLS) is a multivariate method wherein the data set is divided into predictors (X data) and responses (Y data). The PLS algorithm calculates PCs in such a way that the correlation between PC in X and Y is maximized. The scores in X and Y are connected by an inner relation that makes it possible to predict y-values from x-values in an observation.

The difference between predicted value, $\hat{y}$, and true value, y, of a response is called the residual, and the sample mean is denoted by $\bar{y}$. The sum of squares for Y data is defined as

$$SS_y = \sum_{i=1}^{N} (y_i - \bar{y})^2 \qquad (1)$$

where N is the number of observations.

The sum of square errors is defined as

$$SSE = \sum_{i=1}^{N} (\hat{y}_i - y_i)^2 . \quad (2)$$

How well the predicted values estimate the true values for Y data is given by the goodness of fit

$$R^2 y = \frac{SS_y - SSE}{SS_y} . \quad (3)$$

R^2y gives information about the ability of the model to describe the variations in the responses of the data set from the variations in the predictors, but its ability to describe the response for new observations has to be validated.

Cross validation is a standard procedure for testing the significance of a PLS model. Parts of the data are kept out of the model development and then predicted by the model and compared with the actual values. This procedure is repeated until every data element has been kept out once and only once. The prediction error sum of squares, *PRESS*, is calculated as the squared difference between observed Y and predicted values when the observations were kept out

$$PRESS = \sum_{i=1}^{N} (\hat{y}_i - y_i)^2 . \quad (4)$$

The goodness of prediction is then calculated as

$$Q^2 y = \frac{SS_y - PRESS}{SS_y} . \quad (5)$$

R^2 and Q^2 are also calculated for X data and used to validate PCA models. A general guideline is that values greater than 0.5 are regarded as good, but that depends on the application. The difference between R^2 and Q^2 should not be too large (preferably less than 0.2 – 0.3).

Another commonly used method for validation of models is to exclude 20% of the available observations when the models are generated and calculate R^2_y for predictions made when the model is applied to the excluded observations.

3. Microwaves and Wood

3.1. Electromagnetic Waves

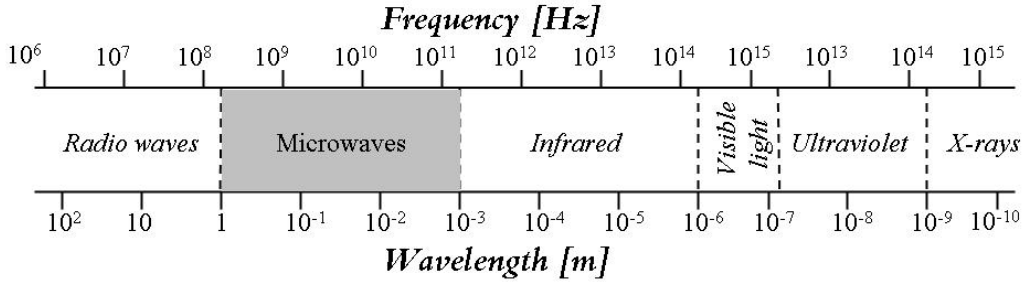

Figure 2. Electromagnetic spectrum with the wavelength in free space.

Visible light is just a small part of the electromagnetic spectrum shown in Figure 2. When the frequency changes, the properties of the electromagnetic waves will also change, but their behaviour is always governed by Maxwell's equations. Higher frequency means that each photon carries more energy and has a shorter wavelength. It also means that very short waves such as X-rays can be regarded as small particles with a size comparable to the size of atoms. Radio waves, on the other hand, have low frequencies and long wavelengths. The term microwave was introduced around 1930 to describe very short radio waves, although their wavelength (1 mm to 1 m in free space) is long compared to the wavelength of visible light. A special feature of microwaves is that the wavelength is of the same order of size as the components used for generation and detection of the waves. The wavelength, λ, is related to frequency, f, through the speed of propagation, c, by the relation

$$c = \lambda \cdot f \,. \tag{6}$$

The speed of propagation in free space is $3 \cdot 10^8$ m/s, but both the speed and the wavelength will be reduced when the wave enters a dielectric. Maxwell's equations and the behaviour of electromagnetic waves in dielectric media have been explained by von Hippel (1995) among others. The electric field, **E**, from a wave moving in the z direction at time t can be described by the equation

$$\mathbf{E} = \mathbf{E}_0 e^{j\omega t - \gamma \cdot z} \,. \tag{7}$$

If losses due to conductance and reflections are ignored, the attenuation and wavelength are governed by the factor $e^{-\gamma z}$, with the complex propagation constant,

$$\gamma = j\omega\sqrt{\varepsilon^*\varepsilon_0\mu^*\mu_0} = \alpha + j\beta \ , \qquad (8)$$

where

ω is the angular frequency of the wave,
$\varepsilon^* = \varepsilon' - j\varepsilon''$ is the complex permittivity (dielectric constant),
$\mu^* = \mu' - j\mu''$ is the complex permeability,
μ_0 is the permeability of free space and
$\varepsilon_0 = 1/(\mu_0 c_0^2)$ is the permittivity of free space where
c_0 is the speed of light in free space.

The real part of γ can be defined as an attenuation constant, α, and the imaginary part as a phase constant, β. The influence of attenuation and phase shift on the wave is shown in Figure 3.

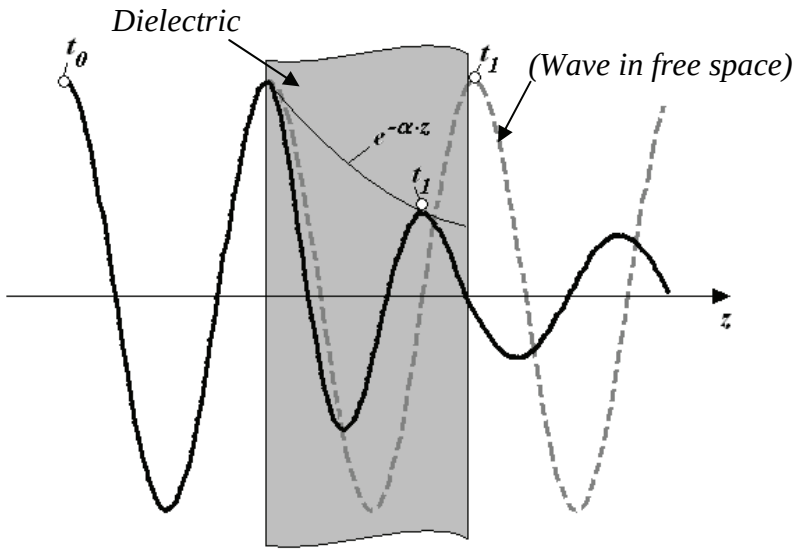

Figure 3. If a signal is initiated from a transmitter at time t_0, it will have travelled a shorter distance at time t_1 if it must pass through a dielectric. There will also be an attenuation of the signal.

3.2. Wood as a Dielectric

The dielectric properties of a material are given by its permittivity, ε^*, and permeability, μ^*, as described in equation 8. For wood and other nonmagnetic materials, the permeability is equal to μ_0. If we define the loss tangent as

$$\tan \delta = \varepsilon' / \varepsilon'' , \tag{9}$$

and the real and imaginary parts of equation 8 are equated, the expressions for the attenuation factor and phase factor will be

$$\alpha = \frac{\omega}{c_0}\left[\frac{\varepsilon'}{2}\left(\sqrt{1+\tan^2\delta}-1\right)\right]^{\frac{1}{2}} \tag{10}$$

and

$$\beta = \frac{\omega}{c_0}\left[\frac{\varepsilon'}{2}\left(\sqrt{1+\tan^2\delta}+1\right)\right]^{\frac{1}{2}} \tag{11}$$

This means that the dielectric properties of wood can be described by ε^* or by ε' and $\tan \delta$.

Dinwoodie (2000) defines timber as a low-density, cellular, polymeric composite. Many properties can be related to the macroscopic structure (knots, grain angle, etc.). The different features can also be identified at the microscopic level by variations in the cellular structure. One reason for the high degree of anisotropy in wood is that a majority of the cells are aligned in the vertical direction of the standing tree, with small deviations. In most cases, this deviation is shaped like a spiral around the trunk, where the magnitude of the angle varies with the distance to the pith.

Figure 4 illustrates the attenuation of an electromagnetic wave passing through a piece of wood. The electric field is perpendicular to the propagation direction of the wave, and the interactions depend on how the wave is polarized in relation to the fibres of the wood.

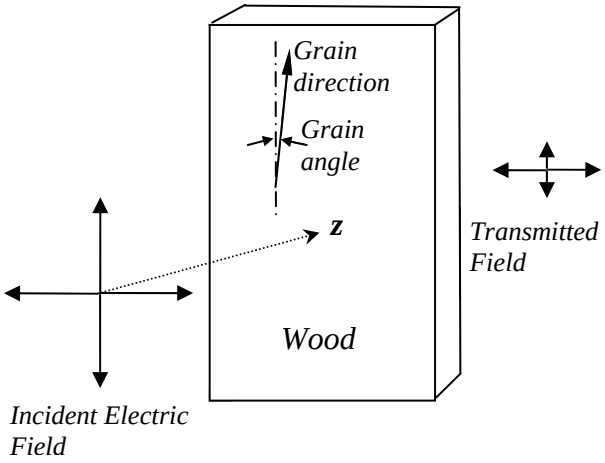

Figure 4. Electromagnetic wave propagating in the z direction. Attenuation of the electric field depends on whether the field is oriented parallel or perpendicular to the grain.

There will be more interactions when the electromagnetic field is oriented parallel to the fibres, and this causes anisotropy in the dielectric properties. The permittivity at 10 GHz is 1.1–2 times greater parallel to the grain direction (Torgovnikov 1993). A microwave sensor based on transmission will measure the average value of the grain angle through the board, which reduces the accuracy of the measurement.

Most of the variations in dielectric properties can be related to variations in grain angle, density and moisture content. Moisture is important, because water molecules will oscillate with the field and transform the energy into heat. The influence from moisture bound in the cell walls is somewhat less than the influence from free moisture in the cell cavities. Softwoods in green condition have an MC of 40%–50% in the heartwood, while the sapwood has an MC of 100%–150%. The relative amount of sapwood has to be estimated, especially when transmission sensors are being used for measurement on freshly sawn boards. The influences from abrupt changes in dielectric properties will be greater than the influence from a progressive change. A wet surface, for example, will reflect more of the incident wave, even if the relative amount of water is low.

4. Modulated Scattering Technique

All microwave measurements were performed with sensors based on modulated scattering technique (MST), also referred to as modulated scatterer technique as described by Bolomey and Gardiold (2001). The principle of MST is that a small probe is placed at the position where the field is to be measured. The probe picks up the signal and reradiates it towards a receiving antenna. A signal that modulates the local field with a low frequency is fed to the probe through high-resistivity wires. The modulated signal is then collected by the receiving antenna and demodulated to extract the field at the position of the probe. This reduces the perturbations on the field as compared to the antenna and transmission line that are required for a direct measurement of the field. James et al. (1985) describe a system using a moving probe. Such a system minimizes the perturbations on the measured field, but will be complicated and slow, since measurements generally are taken at a number of locations. A faster and less expensive method that is implemented in the sensors from Satimo (2007) is to set up a grid of stationary probes. The main advantages of MST are low disturbances to the field and that a single microwave receiver can be used to measure the field at all probe positions.

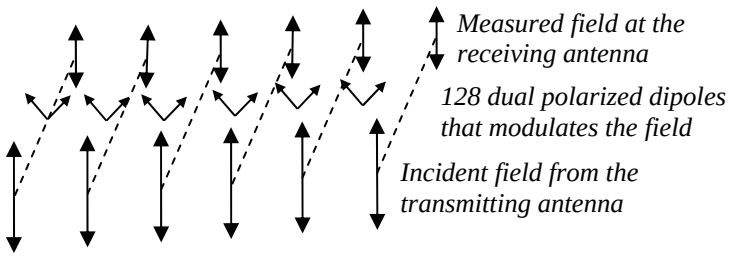

Figure 5. Positioning of the scattering dipoles in relation to the electric field.

The scanning system at LTU Skellefteå is based on a sensor that was used together with neural nets for prediction of wood properties by Portala (1992). A plane wave is transmitted through the wood. The microwave signal is modulated by a low-frequency signal at 128 dual polarized dipoles (probes) in the retina, positioned close to the receiving antenna. Figure 5 illustrates how the probes are oriented in relation to the electric field.

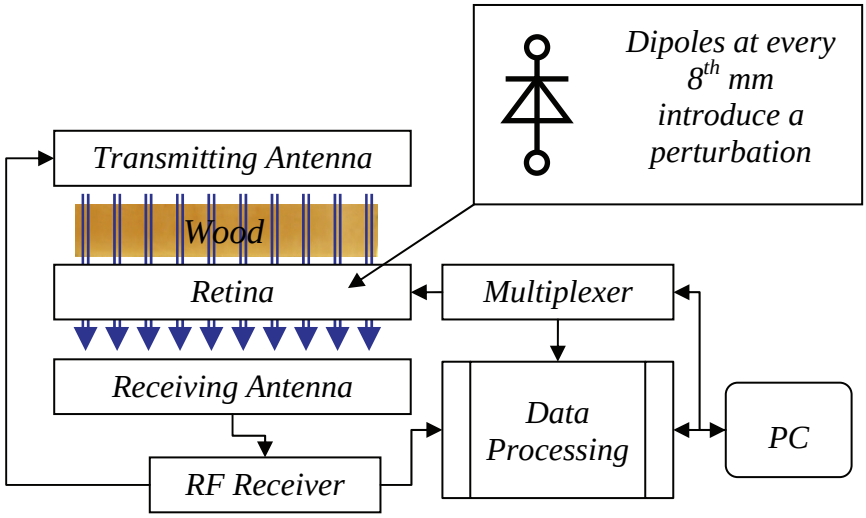

Figure 6. The microwave signal is modulated by a radio frequency (RF) signal at 128 probes (dipoles) in the retina. The electromagnetic field at each probe is then extracted from the signal.

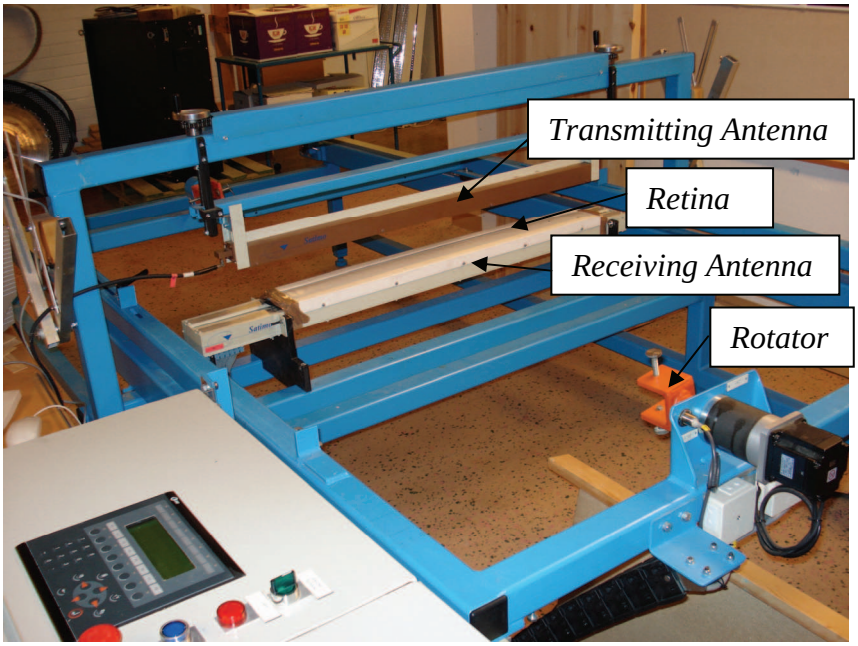

Figure 7. The measurement system is combined with a conveyer and a rotator in the microwave scanner at LTU Skellefteå.

A schematic drawing of the different parts in the sensor is shown in Figure 6. The sensor functions as a line-scan camera for the transmitted microwave signal at 9.375 GHz. It has been combined with a control system and a conveyer shown in Figure 7 (Johansson 2001) in order to produce two-dimensional images of the measured object.

The real and imaginary parts of the electromagnetic field at each probe are extracted from the signal in both polarization directions. The spacing between the probes is 8 mm, and each probe has two orthogonal polarization directions. The control system records 128 line scans in each image. If the conveyer is set to stop for a scan at every 8^{th} mm, the scanner will measure the electromagnetic field in two directions over a surface of 1 x 1 m with a pixel size of 8 x 8 mm. The scanner can also be used for microwave tomography, since it is possible to rotate the object during scanning.

All microwave measurements were made using the same technique, but a new version of the sensor described by Dréan et al. (2006) was used in paper VII. This new sensor was designed for measurements on stone wool and did not include a conveyer.

5. Finite Element Modelling

Interpretation of the results from microwave scanning of wood is complicated due to effects from reflections and scattering. Modelling of microwave propagation in wood gives information about how different variations can be detected from the measured signal. Figure 8 illustrates how finite element models were generated to describe the interactions that occur in the microwave scanner. The distribution of moisture and density can be measured in three dimensions by computed tomography (CT) scanning. Due to the deformations that will take place during drying, the images of dry wood have to be reshaped before the distribution of dielectric properties is calculated from the CT images. Transformation of the images was done by a process known as elastic registration.

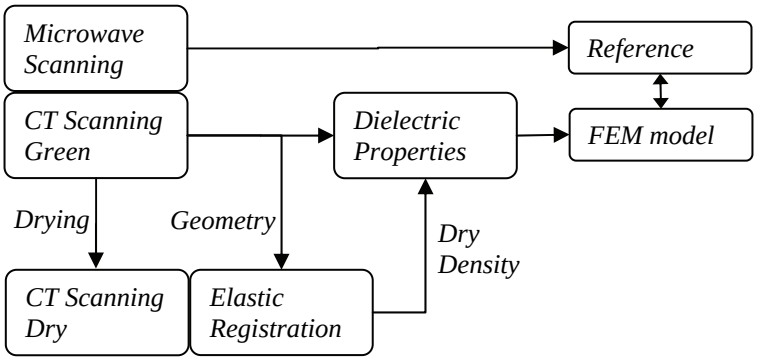

Figure 8. Working procedure for generation of the finite element models.

The dielectric properties were obtained from Torgovnikov's data (1993) and COMSOL (1997) software was used for generation of the models with the finite element method as described by, among others, Jin (2002). The intention was to keep information about the internal structure of the wood piece, and to do so requires a high resolution. The available computational power was not sufficient for three-dimensional simulations. Influence from variations in the third dimension was ignored, and the simulations were done to describe interactions in a two-dimensional cross-section of the wood.

5.1. X-ray Computed Tomography

A medical CT scanner (Siemens Somatom AR.T.) was used to measure the internal three-dimensional density distributions of the wood pieces. These measurements give an accuracy of ±1 kg/m^3 in wood density for a voxel size of 2 x 2 x 1.5 mm (Lindgren 1992). The variation in density within annual rings will

not be fully resolved in this kind of scanning, but the main variation of the internal structure is still visible in the images.

5.2. Elastic Registration

The degree of shrinkage in timber during drying is different on the three principal axes (Dinwoodie 2000), and the presence of knots or compression wood will cause local variations in shrinkage. Furthermore, there will be a twist in some boards, depending on the structure and direction of the cells. The density image of the dry board has to be transformed back into the shape of the green board before the dielectric properties are calculated. This was done by elastic registration using an algorithm described by Sorzano et al. (2005). The algorithm is able to identify patterns in the source image and stretch different parts until the geometry is aligned with a target image. Figure 9 shows the transformation for a cross-section of wood that has been dried from 18% MC to 0% MC.

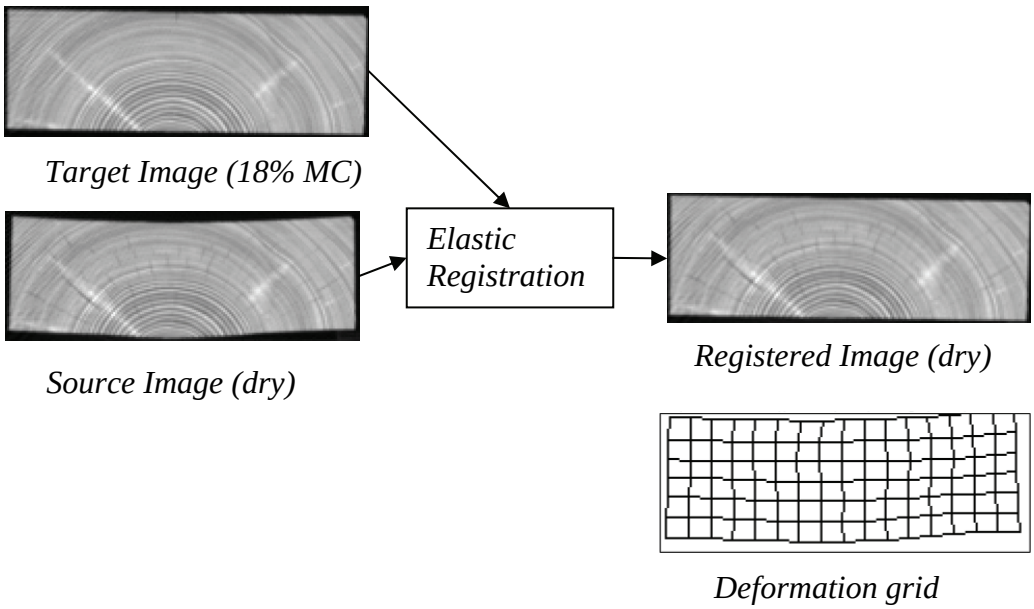

Figure 9. Elastic registration. The algorithm calculates the deformation grid and transforms the geometry of the source image.

5.3. Moisture content calculations

The moisture content will be underestimated when green and dry density images are used to calculate the moisture distribution. The moisture content is defined as

$$u = \frac{m_u - m_0}{m_0} \tag{12}$$

where m_u is the initial mass of a sample and m_0 is the mass in dry condition. The estimated MC is calculated from green density, $\rho_{u,u}$ and dry density, $\rho_{0,0}$ as

$$u_e = \frac{\rho_{u,u} - \rho_{0,0}}{\rho_{0,0}} = \frac{\frac{m_u}{V_u} - \frac{m_0}{V_0}}{\frac{m_0}{V_0}}. \tag{13}$$

The relation between the true MC, u and estimated MC, u_e is given by

$$u_e = (1+u)\frac{(1-\beta)}{\left(1-\beta\left(\frac{u_{fsp}-u}{u_{fsp}}\right)\right)} - 1, \qquad u < u_{fsp} \tag{14.a}$$

$$u_e = (1+u)(1-\beta) - 1, \qquad u > u_{fsp} \tag{14.b}$$

where the volumetric shrinkage, β, is assumed to be linear from the volume V_{fsp} at fibre saturation point, u_{fsp}, to the volume V_0 at u = 0. The shrinkage is then calculated as

$$\beta = \frac{V_{fsp} - V_0}{V_{fsp}}. \tag{15}$$

The estimated MC has to be compensated for the error caused by shrinkage according to the relation described in Equation 14.

6. Results

6.1. Validation of the sensor

The dielectric properties of wood have been studied since the beginning of the 20th century. Several researchers have contributed to knowledge about how these properties are related to moisture content, dry wood density and temperature at different frequencies. The results have been compiled by Torgovnikov (1993) in tables where the values of ε' and $\tan\delta$ are given. These values can be used in computer simulations but it should be confirmed that they will give the same attenuation and phase shift as measurements with the microwave scanner. Paper I describes how Torgovnikov's data was compared to measurements made with the microwave sensor on a piece of birch wood at different MC and temperatures. Thickness of the piece, shown in Figure 10 varied between 0 and 31 millimetres.

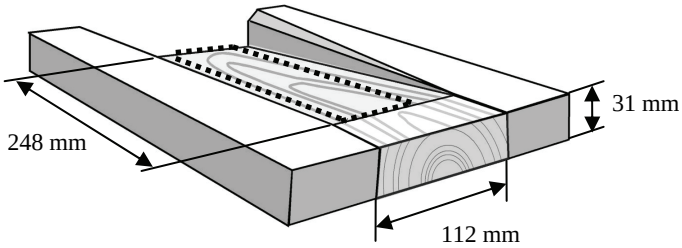

Figure 10. Pieces of birch were glued to the edges of the measured object to reduce boundary effects. The measured region is indicated by the dotted line.

The distribution of dry wood density within the piece was decided from CT scanning in dry condition. The desired moisture content was established by placing the wood in a climate chamber long enough to assume a uniform distribution of moisture and verified by weighing of the piece. Dielectric properties were interpolated from tabulated values, and after insertion into equations 10 and 11 it was possible to calculate the attenuation constant, α, and the phase constant, β. The attenuation and phase shift given by α and β were compared to values obtained from measurements with the microwave scanner.

Figure 11 shows the calculated attenuation compared to measured values, while calculated and measured phase shift is shown in Figure 12. There was good agreement in the values even if measured values were lower and contained more variations. The level of noise was about 3 dB in measured attenuation due to effects from reflections and scattering. This indicates that the signal-to-noise ratio will be low if the measured object is thin or has low MC. The result shows that the

data compiled by Torgovnikov can be used to model interactions between wood and microwaves in order to predict the response from the scanner.

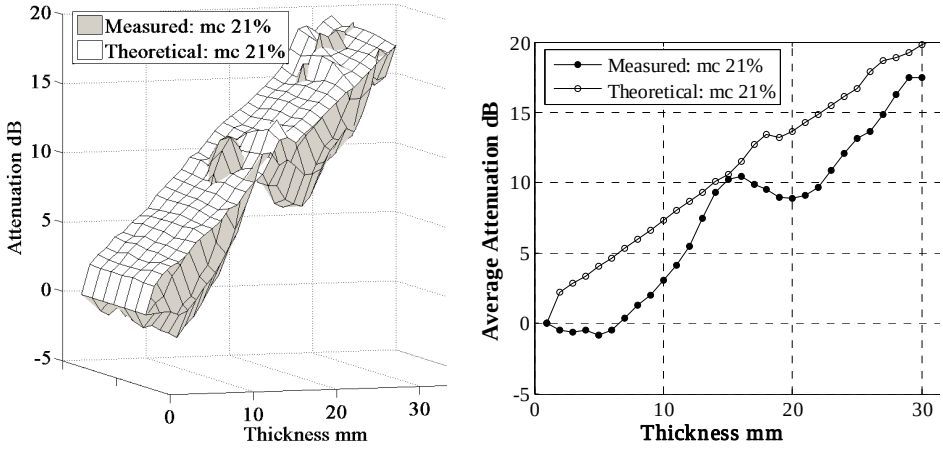

Figure 11. Distribution (left) and average values (right) of attenuation of microwaves penetrating a piece of wood with varying thickness over a width of 64 mm.

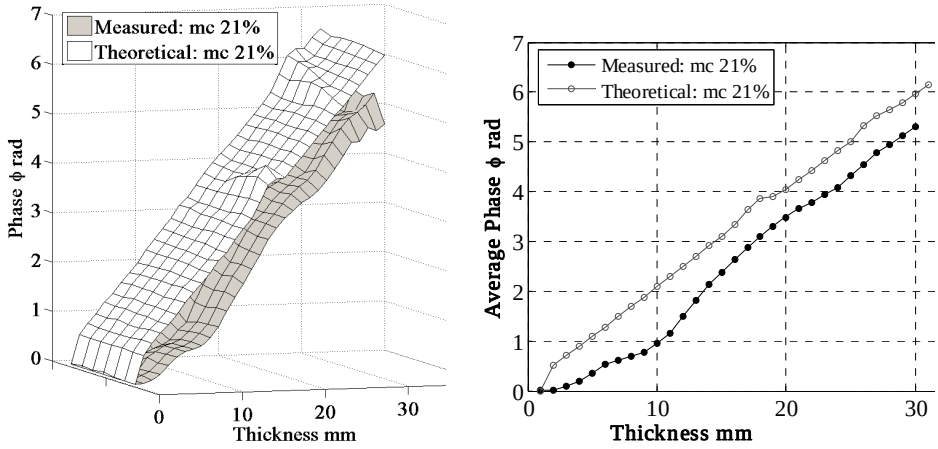

Figure 12. Distribution (left) and average values (right) of phase shift of microwaves penetrating a piece of wood with varying thickness over a width of 64 mm.

6.2. Modelling the field

The behaviour of a plane monochromatic electromagnetic wave propagating through an infinite linear medium is described by equation 7. The interactions are more complicated in an inhomogeneous medium such as wood, because the value of γ will then depend on the spatial position. Even worse is that the normal dimensions for sawn lumber make it necessary to include boundary effects at the board edges. Paper II describes how a finite element model of the interactions between wood and microwaves was developed in two dimensions. This model is based on the distribution of moisture and dry wood density in cross-sections of the board, in contrast to Paper I, in which average values of density through the board over a volume were used.

The density distribution in a piece of wood was measured by X-ray CT scanning in green and dry condition. The moisture distribution could then be calculated as the difference between these two scans, but first the dry wood image was aligned to the green wood image. The moisture content was not corrected for the error in estimated values due to shrinkage as given by Equation 14. This means that attenuation and phase shift should be expected to have lower values in the finite element model compared to measured values in green condition. The distributions of dielectric properties within the wood were calculated and imported into the model. By using the geometry of the microwave scanner in the model, it was possible to compare the modelled and measured fields. Figure 13 shows the pattern in attenuation that occurred when scanning of a piece of pinewood was simulated compared to measured values.

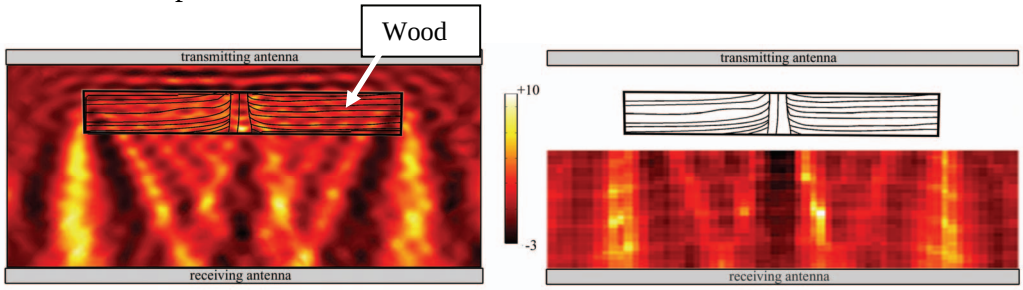

Figure 13. Simulated attenuation (left) and measured values (right) in decibels. The measurements were made by moving the receiving antenna and taking scans at various distances to the wood.

The limitation to two dimensions in the model introduced errors at small objects such as the knot in the centre of the wood in Figure 13. The patterns caused by adjacent objects will interfere at the receiving antenna. This complicates the interpretation of measurements on inhomogeneous objects.

6.3. Modelling frozen wood

The temperature dependence in dielectric properties has to be considered during the winter when the wood is frozen. The water molecules are locked to each other and will absorb less energy from the electromagnetic field. The change in dielectric properties when moist wood changes from frozen to nonfrozen condition was investigated in Paper III. This was done both in the model and by placing a frozen piece of freshly sawn birch wood in the scanner where the transmitted signal was measured during thawing at room temperature. The dimensions of the piece were 21 x 175 x 305 mm, and the simulated cross-section was 21 x 305 mm in the centre of the piece. Heat transfer was included in the previously described model in order to simulate how heat energy is transported from the surface into the wood. Some simplifications were made, such as ignoring the convective heat flow and energy losses due to evaporation. Heating caused by the electromagnetic field in the scanner could also be ignored. Figure 14 shows that the simulated temperature in the centre of the piece behaves similar to measured values. The temperature will be constant at 0 °C for a period of time when water changes into liquid condition.

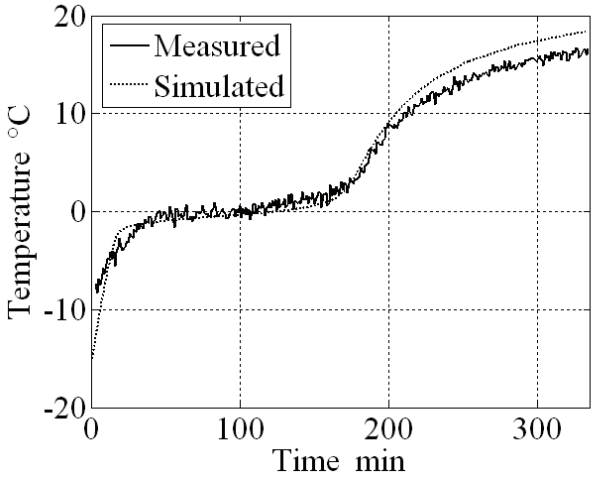

Figure 14. Measured and simulated core temperature.

The influence from moisture on a transmitted microwave signal is considerably lower at temperatures below 0 °C. The measured attenuation and phase shift depend on how large a proportion of the wood is frozen, as can be seen in Figure 15, where the phase shift in a piece of pinewood was measured during thawing by Hagman et al. (2004). The sapwood with high moisture content has a steep change in phase shift at the freezing point, while the changes in heartwood rise more evenly with the temperature, due to lower moisture content. It is impossible to

calibrate prediction models for wood properties at temperatures close to 0°C, since the result will depend on the mixture of frozen/nonfrozen material.

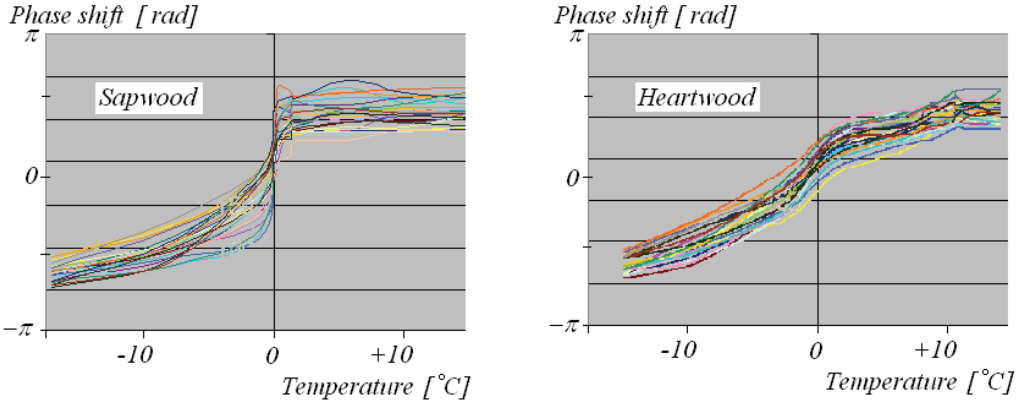

Figure 15. Variation in phase shift of a microwave signal transmitted through a piece of green pinewood at different temperatures. (Hagman et al. 2004).

Penetration depth is increased in frozen wood due to the low interaction with water. This gives an opportunity to measure the density in green wood with high moisture content. The obvious drawback is that such equipment only can be used when the wood is frozen.

6.4. Modelling heating

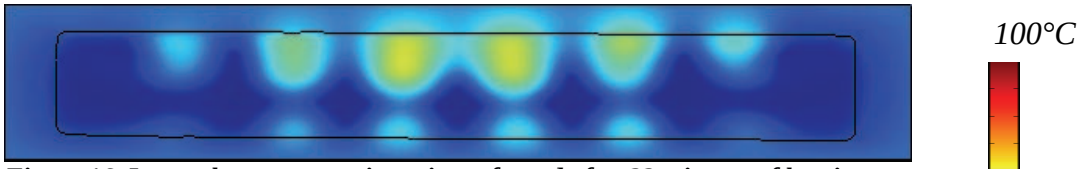

Figure 16. Internal temperature in a piece of wood after 22 minutes of heating. Initial temperature was 0°C.

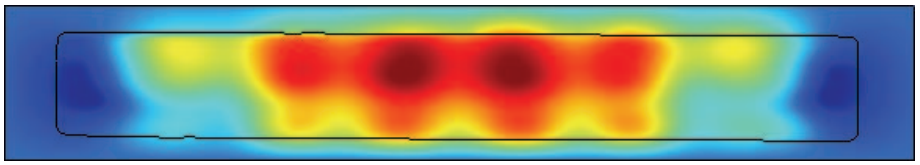

Figure 17. Internal temperature after 50 minutes of heating.

Focus of the present work is set on microwave sensors, but the model developed can also be used to describe electromagnetic heating if heat energy transferred from the electromagnetic field is included. The amount of energy that is absorbed depends on the dielectric properties of the material, while the distribution of

electromagnetic energy depends on the shape of the cavity and the shape of the incident field. It is important to monitor the variations in energy and temperature distribution, because local hot spots may cause damage to the heated material.

Paper IV describes how the incident field was adjusted in the model to simulate the field in the cavity of an industrial microwave drier. Birch wood with an average MC of 84% was placed in the drier, and the temperature was registered during heating. The surface temperature was measured using an infrared camera, and the internal temperature was measured using a fibre optic sensor. These temperatures were compared to the temperatures in the finite element model during heating to 100ºC. At that temperature, the losses due to evaporation become too large to be ignored, and a more complicated model is required.

Results from heating simulations as described in Paper IV are shown in Figure 16 and Figure 17. The measured temperature followed the simulated values in the core, while there was a difference in the surface temperature due to physical processes that were not included in the model, e.g., evaporation.

6.5. Prediction of moisture content and density

Uneven distribution of moisture in a board leaving the sawmill will cause problems for the end user and variations in density are related to quality and strength of a board. MST sensors are interesting since they have a potential for concurrent prediction of both moisture and density distributions.

The work presented in Paper V was carried out in order to evaluate a microwave scanner for sawn lumber, its ability to penetrate wood and to resolve spatial variations in density and moisture content. Boards of Scots pine (*Pinus sylvestris*), 25 and 50 mm thick, were scanned with microwaves and X-rays at three different moisture contents. Raw data from the microwave scanner, i.e. the complex amplitude in two polarization directions where used as predictors in a PLS model. CT scanning and weighing of the boards were used to decide the distribution of moisture and dry wood density and these variables were used as responses. Models based on randomly selected 8- x 8-mm pixels were compared to models based on average values from manually selected homogeneous regions from the boards. Pixels from regions with high density (knots) introduced noise, as can be seen in Figure 18, while the model is better adapted to predict the density variations in clearwood.

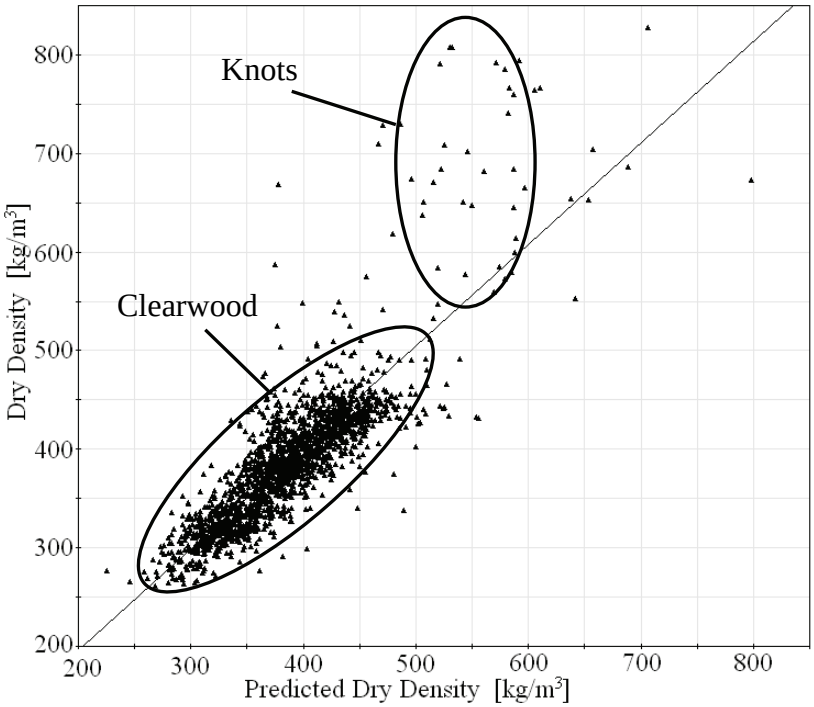

Figure 18. Dry density predicted for randomly selected pixels.

The microwave sensor measures the transmitted signal, and average values of MC and density are predicted, but variations such as those illustrated in Figure 19 will influence the signal. A model that is calibrated on boards with a uniform moisture distribution will not give correct predictions if the moisture is unevenly distributed, as is the case for the second board in Figure 19 where the sapwood has a higher MC than the heartwood. The third board in the figure is sawn from the centre of the log. The pith in the middle of the board will affect the signal, and the standing annual rings on the sides will act as waveguides.

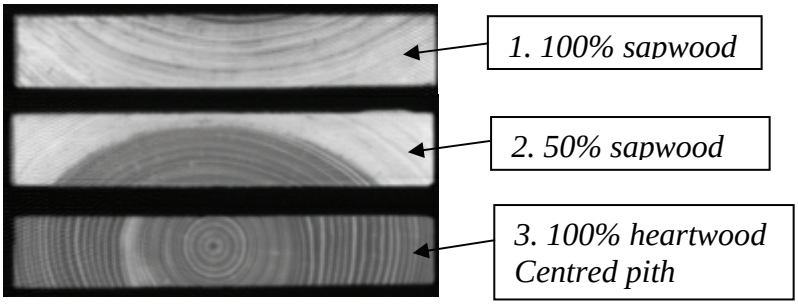

Figure 19. CT image showing density variations in green condition for some of the boards with 25 mm thickness. Dark pixels represent low density values.

The results show that phase shift of the signal can be used as a strong predictor of density when moisture distribution is uniform. Variations in MC give variations in phase shift of more than one period. This makes it complicated to find a relation between MC and phase shift, and models for prediction of MC were mainly based on attenuation of the signal. It was also noted that measured attenuation is affected by reflections and scattering. Averages have to be taken over larger regions to get reliable values of attenuation. There is less spatial noise in measurements of phase shift.

The main conclusion from paper V was that dry density could be predicted for each pixel from microwave scanning, while reliable models for prediction of moisture content had to be based on average values from larger regions.

6.6. Predicting strength

The boards with a thickness of 50 mm, described in the previous section, were used in a preliminary study of how the microwave signal is related to strength properties (Lundgren 2005). Destructive four-point bending was used to measure modulus of rupture (MOR) and modulus of elasticity (MOE) on the boards with MC = 7%.

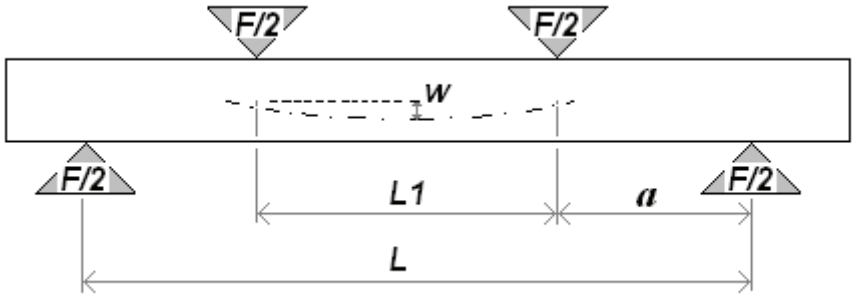

Figure 20. Test arrangement in four point bending. L and L1 is the distance between supports and w is the deformation when the load, F was applied.

Figure 20 shows the test arrangement according to the European standard EN408 (Anon. 2003). The setup had to be adapted to the dimensions of the boards (150 x 50 x 1600 mm) by reducing the distances *L* and *L1*, and this caused deformations at the supporting points and cracks from the board edges. The local modulus of elasticity was calculated using the expression

$$MOE = \frac{aL1^2(F_3 - F_2)}{16I(w_3 - w_2)} \qquad (16)$$

where *a* is the distance from a loading position to the nearest support and *I* is the second moment of area (b x h^3 / 12) where *b* is the width and h is the height of the cross section of the board. F_3 and w_3 are the load and deformation at 40% of maximum load while F_2 and w_2 are the load and deformation at 10% of maximum load.

The modulus of rupture was calculated as

$$MOR = \frac{3F_4 \cdot L}{2bh^2}, \qquad (17)$$

where F_4 is equal to the maximum load before rupture.

The deformations of the wood that occurred at the supports affected the measurements of elasticity, and no correlation was found between MOE and other variables. Models for prediction of MOR from microwaves had a correlation coefficient $R^2 = 0.44$. When a model for prediction of MOR from X-ray scanning was calibrated, a value of $R^2 = 0.39$ was attained.

In Paper VI, an extended study of the relation between microwaves and strength properties is described. The response from the microwave scanner was related to elasticity and bending strength of 90 boards of Norway spruce (*Picea abies*). Average values of the different variables from microwave scanning, X-ray scanning, grain angle and annual ring width measurements were assessed for each board, and the correlation in different variables was examined by principal component analysis (PCA).

The results confirm that the correlation to density is the most important factor when microwaves are used to predict strength or elasticity. This can be seen in the PCA loadings plot shown in Figure 21 where P1 and P2 represent the first two principal components.

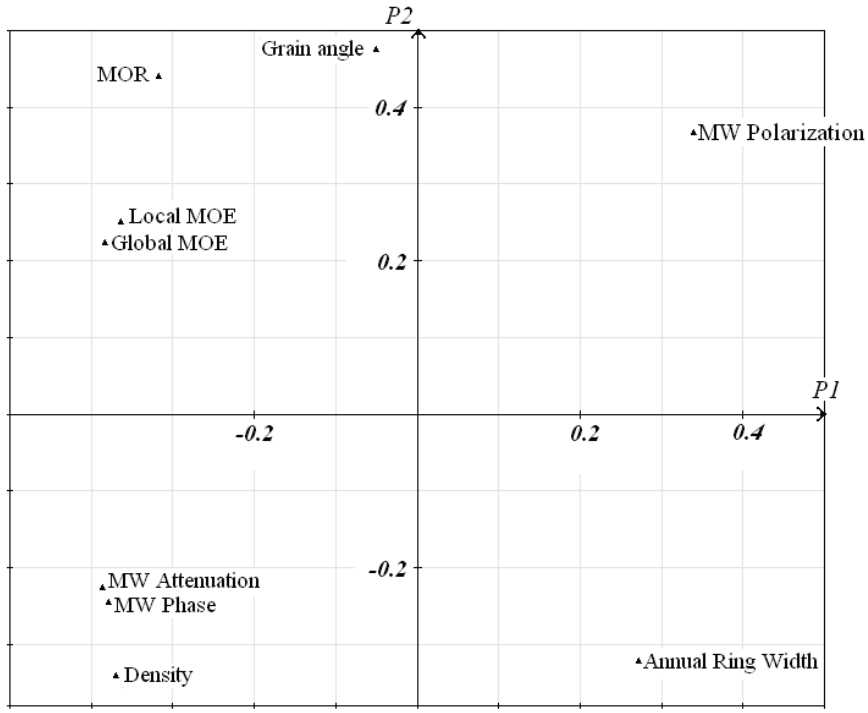

Figure 21. Principal component analysis showing the correlations between measured variables.

Most of the variation is explained by the horizontal component, P1 which means that the highest correlation exists between the variables with large positive or negative values in P1. These variables are Modulus of rupture (MOR), modulus of elasticity (MOE), attenuation, phase, density and annual ring width. The influence from grain angle is low in P1. The remaining variation, explained by P2 in Figure 21, is less important in the models for prediction of MOE and MOR.

It was also noted that microwaves gave a better prediction of elasticity than X-rays. This indicates that structural variations in the wood with influence on elasticity can be detected by microwaves. The correlation coefficients were R^2 = 0.55 for microwaves and R^2 = 0.50 for X-rays. These results can be compared to a study by Hanhijärvi et al. (2005) in which several grading techniques were tested. For example, they reported R^2 = 0.67 when the Finnograder was used for prediction of MOE in spruce.

6.7. New sensors

The last paper in this thesis (Paper VII) presents the results from preliminary tests on wood with a new sensor based on the same technique as the sensor used in the previous papers. These tests indicate that the quality of the images is approximately the same as was obtained from the old sensor. The main improvement is that the new measurement system is fast enough to perform online scanning in real time. The graphs in Figure 22 show that measurements with the new sensor give similar results as compared to the old sensor. Deviations in the results may reflect differences in positioning of the piece in the two sensors. The new sensor provides increased scanning speed at a lower cost, which is important for industrial implementations. It will be possible to measure thicker materials if the measurement noise is reduced. This can increase the number of applications for scanning of green wood.

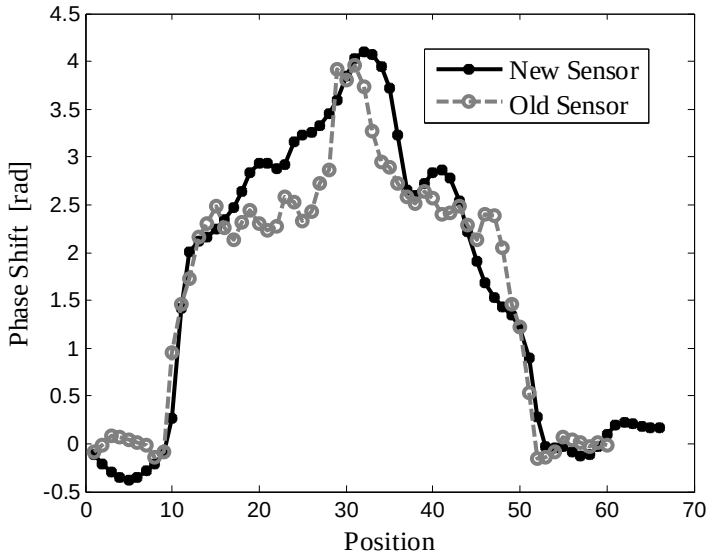

Figure 22. Phase shift in a piece of pine measured with the new sensor compared to measurements that were made with the old sensor in Paper II.

Measured amplitude of the signal when a section from a board of Scots pine was scanned is compared in Figure 23. It should be noted that these images are the results from preliminary tests and could be misleading. The quality of images obtained by the new sensor would have been improved by a shorter distance to the receiving antenna and a conveyer to ensure a constant feeding.

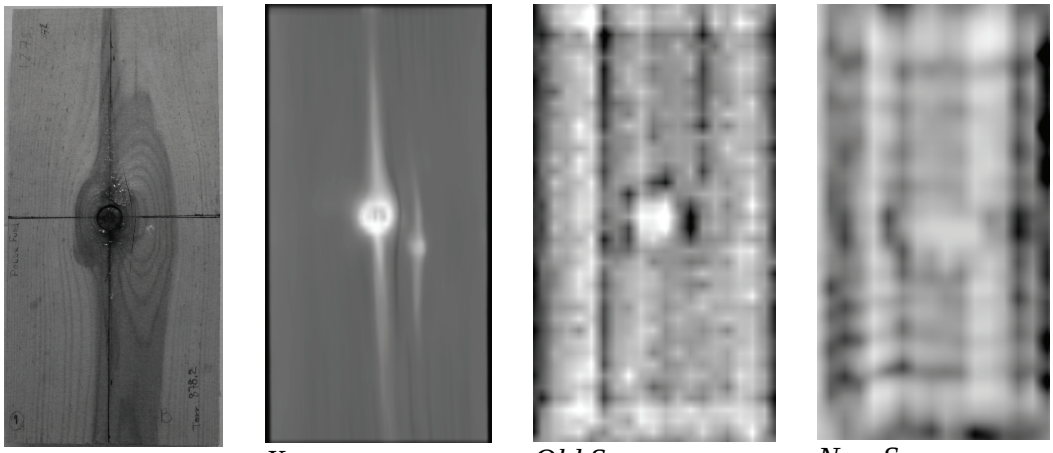

Photo *X-ray* *Old Scanner* *New Scanner*

Figure 23. Photography and X-ray of a knot compared to amplitude measurements performed with the old and the new microwave scanner.

7. Discussion

Microwave sensors are fast, rugged and noninvasive. The attenuation, reflection, phase shift and polarization of waves can be used for prediction of several properties of wood in one single measurement. Standard waveguide antennas can be used to measure the reflected or transmitted signal, but the use of MST will give a higher resolution and reduce the perturbations on the measured field.

The size of the smallest detectable object is related to the wavelength in combination with the contrast in dielectric properties for wood. Figure 24 illustrates the relation between resolution and frequency if the resolution is assumed to be half of the wavelength in free space. The scanners used in this study work at a frequency of 9.375 GHz, which means that a legible knot passing straight through the board and with a diameter of 16 mm can be detected.

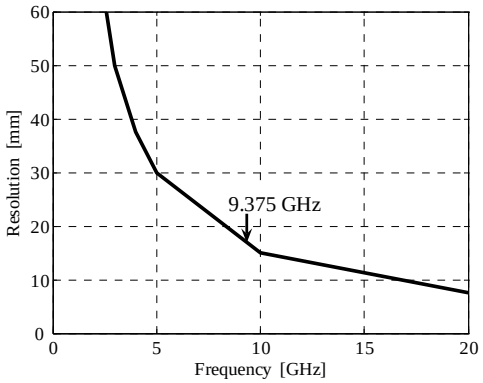

Figure 24. Resolution (λ/2) in relation to frequency.

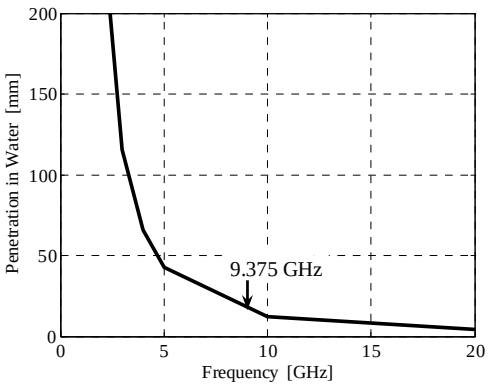

Figure 25. Penetration depth in water (40 dB attenuation) in relation to frequency.

Penetration depth is reduced considerably by moisture, which is a limitation in the measurements of green boards. Insertion of the dielectric properties of water (Lide 2003) at different frequencies into equation 10 gives the attenuation constant that makes it possible to calculate attenuation when the wave travels a certain distance through the water. Figure 25 shows how deep a microwave signal is transmitted into water when the attenuation of the signal reaches 40 dB. This is a level at which the signal is still easy to detect. The penetration dept in dried wood with a moisture content of less than 18% is at least 200 mm.

Another important issue is the accuracy of the measurements. The error was not estimated in the predictions of MC in Scots pine (paper V) but a recent study by Schajer and Orhan (2006) uses microwaves to predict MC in hemlock and Douglas fir with standard errors of 1.2% and 1.9% respectively in the range from

7% to 28%. Furthermore, they were able to measure dry density and the rotational angle of the samples. The accuracy of MC measurements is comparable to commercially available equipment for on-line scanning (Esping 2003), but such equipment is generally based on less expensive technology working at radio frequencies. The extra cost of microwave components and MST is motivated when more information is extracted from the signal. Some examples of useful data are variations in the distribution of MC and dry density over a board and localization of knots.

The sensor examined in this study measures the transmitted field in two orthogonal directions, which should make it possible to calculate the polarization. However, no correlations to grain angle were found from the measurements in paper VI. One explanation for this is the variations in polarization as the wave penetrates the board, and another explanation is that the incident wave was linearly polarized in the longitudinal direction of the boards. The best approach when microwaves are to be used for measurement of grain angle is to measure the reflected signal, and a preliminary study has been performed in which this was done on pieces of sapwood from Scots pine with angles in the range of -1 to +13.6 degrees. A model for prediction of grain angle was calibrated with $Q^2 = 0.7$. Different parts of the same board were used for each angle which means that there might be influence from variations in the material. The use of rotating probes improves accuracy and makes it possible to detect variations within a few degrees (Shen et al. 1994; Sjödén et al. 2005), but the low anisotropy in dielectric properties makes it difficult to reach the precision required for prediction of twist during drying.

The possibility of using the sensor for microwave tomography of wood has been tested in a measurement in which a small bottle of water was placed inside a plastic container with a diameter of 150 mm. The container was filled with sawdust and rotated during scanning. The cross-section was then reconstructed by applying the inverse Radon transform. The influence of the water bottle was visible in the reconstructed image, but it would not have been possible to localize knots inside a log. An FEM simulation of the measurement produced similar results. Water gives a high contrast in the dielectric properties, and a material with lower contrast would not have been detected in this measurement. Furthermore the patterns from several knots will interfere with each other when a log is scanned.

To detect and classify knots with microwaves requires special care as knots are represented by both high and low pixel values in microwave images, depending on knot size and where the pixel is positioned in the knot. Knots (as well as holes)

of a certain size will act as waveguides, causing patterns such as those shown in Figure 26. There will also be wave shaped patterns due to reflections at other boundaries where dielectric properties change. This introduces noise in linear models. The wave pattern is related to the wavelength and can be reduced by filtering out a certain frequency. Another option is to amplify the pattern and use it for detection of edges and knots.

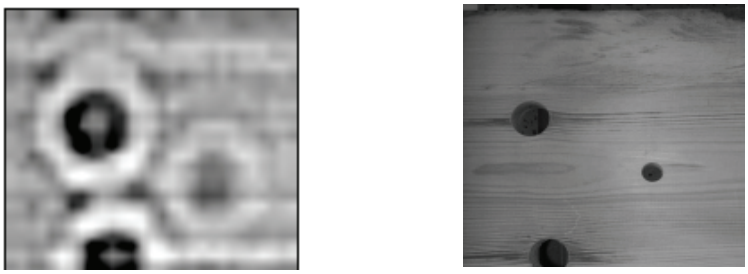

Figure 26. Two holes with a diameter of 30 mm and one hole with a diameter of 16 mm drilled in a 30-mm-thick piece of wood. Microwave image (left) and photo (right).

Multivariate calibration is useful in relating the different properties of wood to measured variables. There is a limitation in the number of properties that can be decided simultaneously by microwave scanning. This can be handled by restrictions on the material to be scanned or by adding other kinds of sensors (X-ray, infrared, visible light, etc).

There is a complex relation between wood properties and the microwave signal. It is possible to find correlations and generate prediction models by the use of multivariate calibration, as was done in papers V and VI. The models generated in those papers for prediction of MC, density and strength can be improved by pretreatment of the measured data. The raw data from the scanner gives several variables, but some of those only contribute noise. The software for multivariate statistics will identify such variables, but they should be examined and removed if there is no information about the response. The remaining predictors should, if possible, be transformed to maximize correlation to the responses. This requires a proper description of the interactions between wood and microwaves. The results in papers II – IV show that it is possible to use FEM for simulation of these interactions. The influence of edges, knots, temperature and distance to the receiving antenna are some factors that have been examined. The results in paper II show that unwrapping of phase shift when variations in dielectric properties are large is practically impossible without more information. Measurements at more than one frequency or measurements of both the transmitted and reflected signal are examples of ways information can be added. Such measurements can be

simulated in the finite element model in order to evaluate their contribution in the predictions.

The finite element models that are presented in this thesis describe the interactions between microwaves and wood and can be used to:

- Understand how microwaves are scattered and reflected by variations in the wood.
- Verify models for prediction of properties in wood.
- Generate new prediction models for properties in wood from microwave scanning by changing the properties in the finite element model.
- Describe other processes in which a heterogeneous material with known dielectric properties interacts with microwaves (e.g., microwave heating).

The new sensor tested in paper VII has a scanning speed of about 30 lines/s. This means that each line will be measured over a length of 10 cm if the feeding speed is 180 m/min. This is enough for moisture and density measurements and can also be used in prediction of MOE and MOR, but it will not be possible to detect knots. Transverse feeding can be used to decrease feeding speed, but the maximum length of the sensor is limited by the length of the cables to the dipoles in the retina, and the scanning speed will be lower for a longer sensor. An industrial application of the sensor can be designed for lengthwise feeding (80 cm wide) or transverse feeding (4–5 m wide). Two sensors must be combined for scanning the full length of longer boards in the transverse direction.

8. Conclusions

Microwaves can be used to measure MC and dry density of sawn lumber after drying. The use of MST will increase resolution and the possibility to detect knots. Edges, knots and other regions where properties change will cause errors in prediction of MC and density. These errors can be reduced by averaging the measurements over a larger area or by classifying the regions and using different prediction models for different regions. Penetration depth in green lumber is increased if the lumber is scanned in frozen condition, but it is not possible to calibrate prediction models for temperatures close to the freezing point.

Reflections and scattering cause noise in measured attenuation, and the proportion of noise will be higher at low moisture content. There is less noise in measured phase shift, but the measurements have to be unwrapped when the shift is more than 360 degrees.

Strength properties can be predicted from microwave scanning, mainly from the influence from density on electromagnetic waves, but microwaves are also affected by structural variations.

Equipment based on X-rays, infrared or visible light has greater potential to locate knots and small defects in wood, but microwaves and MST can be used to measure the distribution of moisture and dry density over a board. The influence of structural variations in the wood on microwaves and the ability of microwaves to penetrate below the surface add information that is invisible to other noninvasive sensing techniques.

9. Future work

The model developed in this study will be useful in further investigations of microwave scanning. It can also describe the interactions in microwave drying of wood or high frequency hardening of glue. The influence of structural variations and gradients in moisture content and density should be investigated to find out how to interpret the measured signal.

The advantages of MST compared to conventional microwave sensors in combination with new systems for data acquisition and signal processing make it possible to perform online measurements in a sawmill with microwave sensors. Such experiments could reveal if microwaves are competitive for verification of moisture content after drying and how the information can be used for grading of lumber. The information in phase shift is important for the results, and the measured phase shift must be unwrapped.

10. References

Anon. 2003. *Timber structures - Structural timber and glued laminated timber - Determination of some physical and mechanical properties.* European Standard EN408: 2003.

Bolomey, J. C. and Gardiol, F. E. 2001. *Engineering Applications of the Modulated Scatterer Technique*. Boston: Artech House Inc.

Boström, L. 1994. *Machine Strength Grading - Comparison of Four Different Systems*. Swedish National Testing and Research Institute, SP Report 1994:49.

Comsol AB. 2007. Tegnérgatan 23 SE-11140 Stockholm. Home page: http://www.comsol.se (cited Feb. 2007)

Dinwoodie, J. D. 2000. *Timber: Its nature and behaviour*. London: E & FN Spon.

Dréan, J., Duchesne, L. and Norén, P. 2006. Non Invasive Electromagnetic Quality Control System. In: *9th European Conference on Non-Destructive Testing*. Berlin: September 25–29, 2006.

Eskelinen, P. and Eskelinen, H. 2000. A K-Band Microwave Measuring System for the Analysis of Tree Stems. *Silva Fennica* 34(1):37–50.

Esping, B. 2003. *Test av Kommersiella Fuktkvotsmätare In-line*. SP-Trätek. Rapport P 0309026 (In Swedish)

Hagman, O., Lundgren, N. and Johansson, J. 2004. *Calibration for Frozen/Non-Frozen Conditions When Predicting Moisture Content and Density Distribution of Wood by Microwave Scanning of Sawn Timber.* Forest Products Society 58th Annual meeting. Grand Rapids, Michigan, USA, June 27–30, 2004.

Hanhijärvi, A., Ranta-Maunus, A. and Turk, G. 2005. *Potential of strength grading of timber with combined measurement techniques*. VTT Publications 568, Espoo, Finland.

James, W. L., Yen, Y. H. and King, R. J. 1985. *A microwave method for measuring moisture content, density and grain angle of wood.* USDA Forest Products Laboratory, Research Note FPL-0250.

Jin, J. 2002. *The Finite Element Method in Electromagnetics*. New York: John Wiley & Sons, Inc.

Johansson, J. 2001. *Property Predictions of Wood Using Microwaves.* Licentiate Thesis, Luleå University of Technology. LIC 2001:35.

Johansson, J., Hagman, O. and Fjellner, B. A. 2003. Predicting Moisture Content and Density Distribution of Scots pine by Microwave Scanning of Sawn Timber. *Journal of Wood Science* 49:312–316.

Kaestner, A. 2002. *Non-Invasive Multidimensional Imaging Applied on Biological Substances.* PhD Thesis, Chalmers University of Technology, Gothenburg, Sweden, September, 2002. ISBN 91-7291-2049.

Leicester, R. H. and Seat, C. A. 1996. Microwave Scanners in Stress Grading Operations. In: *Proc. 25th Forest Products Research Conference*. CSIRO Division of Forestry and Forest Products. Clayton, Victoria, Australia, November 18–21, 1996.

Lhiaubet, C., Cottard, G., Ciccotelli, J., Portala, J. F. and Bolomey, J. C. 1992. On-Line Control in Wood and Paper Industries By Means of Rapid Microwave Linear Sensor. In: *Proc. 22nd European Microwave Conference*, Espoo, Finland. August 24–27, 1992, Topic 16.

Lide D. R. (Editor) 2003. *CRC Handbook of Chemistry and Physics 84th Ed.* London: CRC Press.

Lindgren, O. 1992. *Medical CT-Scanners For Non-Destructive Wood Density and Moisture Content Measurements*. Doctoral Thesis, Luleå University. 1992:111 D.

Lundgren, N. 2005. *Modelling Microwave Measurements in Wood.* Licentiate Thesis, Luleå University of Technology. LIC 2005:61.

Martens H. and Næs T. 1989. *Multivariate Calibration.* New York: John Wiley & Sons Inc.

Nyfors, E. and Vainikainen, P. 1989. *Industrial Microwave Sensors*. Norwood, MA: Artech House.

Nyfors, E. 2000. Industrial Microwave Sensors – A Review. *Subsurface Sensing Technologies and Applications* 1(1):23–43.

Nyström, J. 2002. *Automatic measurement of compression wood and spiral grain for the prediction of distortion in sawn wood products.* Doctoral Thesis, Luleå University of Technology. 2002:37.

Portala, J. F. 1992. *Caracterisation du Bois par Intercorrelation de Mesures Multisensorielles*. These présentée pou l'obtention du Doctorat de L'institut National Polytechnique de Lorraine. CNRS URA 821 (in French).

Samson, M. 1984. Measuring general slope of grain with the slope-of-grain indicator. *Forest Products Journal* 34:27–32.

Satimo France. 2007. 22 Avenue de la Baltique Z.A. Courtaboeuf 91953 France. Home page: http://www.satimo.com (cited Feb 2007).

Schajer, G. S. 2001. Lumber strength grading using x-ray scanning. *Forest Products Journal* 51(1):43–50.

Schajer, G. S. and Orhan, F. B. 2006. Measurement of wood grain angle, moisture content and density using microwaves. *Holz als Roh und Werkstoff* 64:483-490.

Shen, J., Schajer, G. and Parker, R. 1994. Theory and practice in measuring wood grain angle using microwaves. *IEEE Transactions on instrumentation and measurement* 43(6):803–809.

Sjödén T., Nilsson B., Nordebo S. 2005. Microwave Modelling and Measurements for Early Detection of Spiral Grain in Wood. In: *Proc. Of the 14th International Symposium on Nondestructive Testing of Wood.* Aachen: Shaker.

Sorzano CÓS, Thévenaz P, Unser M. 2005. Elastic Registration of Biological Images Using Vector-Spline Regularization, *IEEE Transactions on Biomedical Engineering*, 52:652-663

Torgovnikov, G. I. 1993. *Dielectric Properties of Wood and Wood-Based Materials*. Berlin: Springer.

Von Hippel, A. 1995. *Dielectrics and waves. New ed.* London: Artech House.

Zoughi, R. 2000. *Microwave non-destructive testing and evaluation*. Dordrecht, Netherlands: Kluwer.

Paper I

Available online at www.sciencedirect.com
SCIENCE DIRECT®
Measurement 38 (2005) 15–20
Measurement
www.elsevier.com/locate/measurement

Microwave penetration in wood using imaging sensor

L. Hansson [a,*], N. Lundgren [b], A.L. Antti [a], O. Hagman [b]

[a] Luleå University of Technology, Division of Wood Physics, Skellefteå Campus, SE-93187 Skellefteå, Sweden
[b] Luleå University of Technology, Division of Wood Technology, Skellefteå Campus, SE-93187 Skellefteå, Sweden

Received 10 May 2004; received in revised form 14 March 2005; accepted 16 March 2005
Available online 22 June 2005

Abstract

It is possible to determine properties of wood using microwave scanning techniques. The purpose of this study was to verify the measured values from a microwave imaging sensor. Attenuation and phase shift of an electromagnetic wave transmitted through birch wood were measured and compared with theoretical calculated values. A test piece with varying thickness was measured with a scanner based on a microwave sensor (Satimo 9.375 GHz) at different temperatures and moisture contents. The density distribution of the test piece was determined by computer tomography scanning. The result showed good correspondence between measured and theoretical values. The proportion of noise was higher at low moisture content due to lower attenuation. There is more noise in attenuation measurement than in measurement of phase shift. A reason for this could be that wood is an inhomogeneous material in which reflections and scattering affect attenuation more than phase shift. The microwave scanner has to be calibrated to a known dielectric to quantify the error in the measurement.

Keywords: Microwave scanning; Wood; Dielectric properties; Modulated scattering technique

1. Introduction

It is known that the dielectric properties of wood are affected by density, moisture content (mc), temperature and frequency [1]. For many applications, such as drying, sorting and strength grading, it is necessary to detect mc or density distribution in wood. These parameters can be detected by nondestructive testing using microwaves. This technique has been investigated by Portala [2] among others. The scanner used in the present work is based on the same microwave sensor (Satimo 9.375 GHz) as in Portala's study [2] where several types of sensors for measurements on wood were investigated. The sensor uses modulated scattering technique [3] with 128 fixed probes. The frequency corresponds to a wavelength of 32 mm in vacuum and gives an acceptable ratio between resolution and

* Corresponding author.
E-mail address: lars.hansson@tt.luth.se (L. Hansson).

0263-2241/$ - see front matter © 2005 Elsevier Ltd. All rights reserved.
doi:10.1016/j.measurement.2005.03.007

penetration. A similar technique has been used by James et al. [4]. The main difference in his method is frequency and probe construction. Johansson [5] has shown that simultaneous prediction of moisture content and density is possible using a scanner system based on the sensor from Satimo where scanner data was used as input for calibration of a multivariate model. These models have to be compensated for variations in temperature and thickness of the wood. Johanssons [5] study does not compare the multivariate model with a physical model.

The present study was carried out in order to examine how measurements from the microwave sensor vary at different mc, thickness and temperatures for birch wood. This provides a more detailed study of the sensor in comparison to Portala's [2]. The experimental scanner data was compared to theoretical values of phase shift and attenuation of the signal.

2. Theory

Electromagnetic waves have an electric field strength ($\boldsymbol{E}$) and a magnetic field strength ($\boldsymbol{H}$) that oscillate perpendicular to each other. When the wave is moving in the z-direction it can be described mathematically with the harmonic wave equation as:

$$\boldsymbol{E}(x,y,z,t) = \boldsymbol{E}_0 \cdot \mathrm{e}^{-\mathrm{j}\cdot\omega\cdot t-\gamma\cdot z}, \tag{1}$$

$$\boldsymbol{H}(x,y,z,t) = \boldsymbol{H}_0 \cdot \mathrm{e}^{-\mathrm{j}\cdot\omega\cdot t-\gamma\cdot z}, \tag{2}$$

where $\boldsymbol{E}_0$ and $\boldsymbol{H}_0$ are the amplitudes of the electric field and the magnetic field strength. They are transverse to the z-direction and move through space with a complex distribution factor:

$$\gamma = \mathrm{j}\cdot\omega\cdot\sqrt{\varepsilon\cdot\mu} = \alpha + \mathrm{j}\cdot\beta, \tag{3}$$

where ω is angular frequency and μ is the complex permeability, which is equal to the permeability μ_0 of the free space, since wood is not a magnetic material. Furthermore, α is the attenuation factor and β is the phase factor of the wave. ε is the relative complex permittivity defined as:

$$\varepsilon = \varepsilon_0 \cdot (\varepsilon' - \mathrm{j}\cdot\varepsilon''), \tag{4}$$

where ε_0 is the absolute permittivity for vacuum, ε' is the relative permittivity and ε'' is the relative loss factor. The absolute permittivity and the relative loss factor have been thoroughly investigated by Torgovnikov [1]. These investigations have shown that the absolute permittivity and the relative loss factor of wood depend on moisture content (mc), density, material temperature, direction of electric field relative to the fibre direction and wave frequency.

If the real and imaginary parts of Eq. (3) are equated, the expression for the attenuation factor and phase factor will be:

$$\alpha = \omega\cdot\sqrt{\varepsilon_0\cdot\mu_0}\cdot\left(\frac{\varepsilon'}{2}\cdot\left(\sqrt{1+\left(\frac{\varepsilon''}{\varepsilon'}\right)^2}-1\right)\right)^{1/2}, \tag{5}$$

$$\beta = \omega\cdot\sqrt{\varepsilon_0\cdot\mu_0}\cdot\left(\frac{\varepsilon'}{2}\cdot\left(\sqrt{1+\left(\frac{\varepsilon''}{\varepsilon'}\right)^2}+1\right)\right)^{1/2}. \tag{6}$$

Insertion of Eq. (3) into wave Eq. (1) shows that the wave amplitude is attenuated exponentially with the factor $\mathrm{e}^{-\alpha\cdot z}$ as the wave penetrates the dielectric wood material (Fig. 1).

If the electric field strength decreases from $\boldsymbol{E}(0)$ to $\boldsymbol{E}(z)$, over the length Δz of wood (Fig. 1), the attenuation expressed in decibel is defined as:

$$\log\left(\frac{\boldsymbol{E}(0)}{\boldsymbol{E}(z)}\right) = \log(\mathrm{e})\cdot\alpha\cdot\Delta z\ [\mathrm{dB}], \tag{7}$$

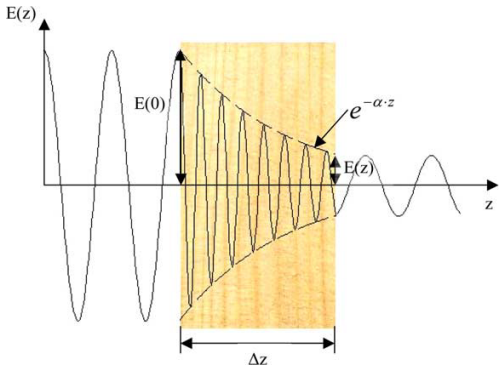

Fig. 1. An electromagnetic wave transmitted into wood.

and the phase shift ϕ over a length Δz as it penetrates wood instead of empty space is defined as:

$$\phi = \beta \cdot \Delta z \text{ [rad]}. \quad (8)$$

3. Material and methods

The study was based on one piece of birch wood with dimensions as shown in Fig. 2. The thickness increases linearly from 0 to 31 mm over a length of 248 mm. This will give a theoretical maximum attenuation of about 12 dB at 25% mc, which is within the dynamic range for the scanner system, which is stated to be about 40 dB. Measurements were excluded within 24 mm from the wood edges to reduce boundary effects on the field. The region of interest is inside the dotted line in Fig. 2.

The values of measured attenuation and phase shift over a width of 64 mm were compared with theoretical values calculated from Eqs. (7) and (8). For each moisture level the object was held at equilibrium mc in a climate chamber until the calculated target weight was reached. Initially the object was dried to 5% mc. By placing the piece in the climate chamber, the mc could be raised to a maximum of 21%. An intermediate measurement was taken at 13% mc. At each of these three levels, the object was scanned at room temperature using both the microwave and Computer Tomograph (CT) scanner. Then the object was dried to zero mc and scanned. Finally, the mc was raised once more to 21% and then the object was kept in a refrigerator for 48 h. Then a microwave scan was done with the object frozen to −20 °C.

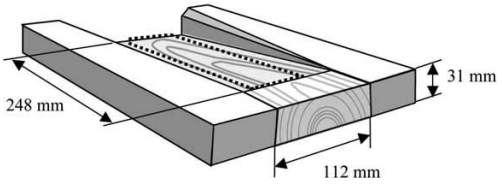

Fig. 2. Test object with birch pieces glued to the edges.

4. CT scanner

A CT scanner (Siemens Somatom AR.T.) was used to measure the density distribution in the test object. A scan was taken at every 8 mm with a 5 mm-wide X-ray beam. The 3D images from the CT scanner were transformed to 2D images with a pixel size of 8 mm × 8 mm.

5. Microwave scanner

Fig. 3 shows a schematic drawing on the main part of the microwave scanning system. The sensor (Satimo 9.375 GHz) is based on modulated scattering technique, MST, which makes it possible to measure the field at many points without a moving probe or microwave multiplexer [3]. The wood is illuminated by a quasi plane wave generated by a slotted waveguide that acts as a transmitting antenna. The transmitted wave is locally perturbed in the retina by a low frequency signal applied sequentially to 128 dual-polarised nonlinear dipoles loaded by PIN diodes. This will cause a modulation of the radio frequency (RF) signal that is proportional to the electromagnetic field. The modulated signal is collected by another slotted waveguide. The signal that reaches the RF receiver consists of a carrier wave modulated at the diode switching frequency. Down-conversion of the RF signal is done in a homodyne receiver that produces the real and imaginary parts of the electromagnetic field at the position of the dipoles. The

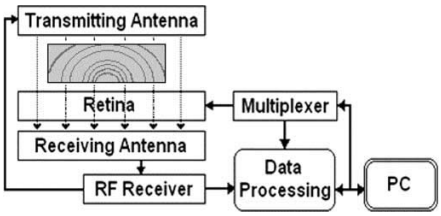

Fig. 3. Sensor system for the microwave scanner. The microwave signal is modulated by a low frequency signal at 128 probes in the retina. The electromagnetic field at each probe is then extracted from the signal.

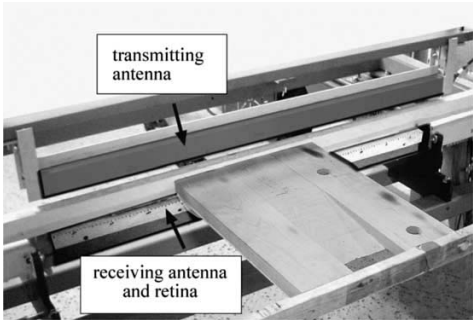

Fig. 4. Conveyer for the microwave scanner with antennas.

antennas are mounted on opposite sides of a conveyer shown in Fig. 4.

The conveyer position is controlled by programmable logic connected to the PC [5]. The distance between dipoles in the retina is 8 mm, which corresponds to one quarter of a wavelength. Since there are 128 dipoles, the resulting image covers a width of one meter. By setting the conveyer to stop for scanning every 8 mm, the same resolution is attained in both directions. From the collected data two images are extracted. One image describes the phase shift of the electromagnetic wave, and the other image describes the attenuation of the signal in dB after passing through the wood. There is a difference in level between sensors and also a small variation between measurements. These errors were minimized by setting the level in air to zero at every measurement.

6. Results and discussion

Fig. 5 shows the distribution of experimental and theoretical values for attenuation over the test object at 0% mc. The theoretical values are calculated with Eq. (7) using empirical values from Torgovnikov [1] and the density distribution obtained from CT scanning. Here the noise is about half of the maximum attenuation.

The measured surface has the same shape at 21% mc in Fig. 6, and the noise level is the same. The maximum attenuation has increased, which gives a better signal to noise ratio.

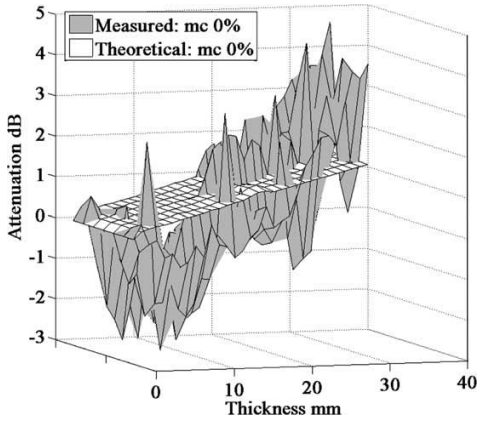

Fig. 5. Distribution of attenuation over a width of 64 mm in birch at 0% mc as thickness increases from 0 to 31 mm.

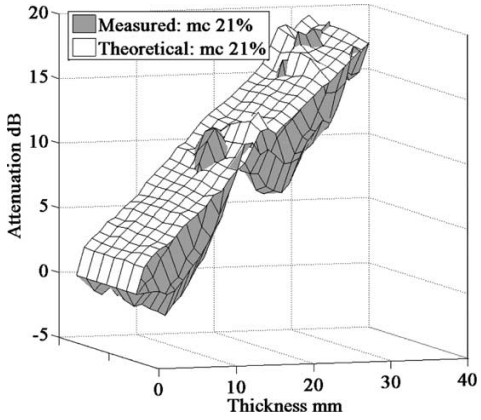

Fig. 6. Distribution of attenuation over a width of 64 mm in birch at 21% mc as thickness increases from 0 to 31 mm.

Figs. 7 and 8 show the corresponding distribution of phase shift at 0 and 21% mc where theoretical values have been calculated with Eq. (8) using empirical values from Torgovnikov [1] and the density distribution obtained from CT scanning.

Variations from the plane in Figs. 5–8 correspond to density variations as shown in Fig. 9. Different annual ring patterns or small regions with high density may cause reflections at bound-

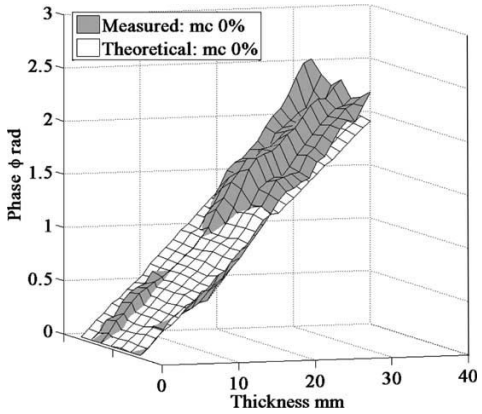

Fig. 7. Distribution of phase shift over a width of 64 mm in birch at 0% mc as thickness increases from 0 to 31 mm.

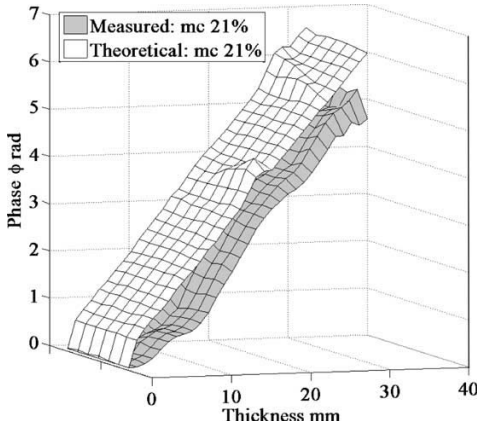

Fig. 8. Distribution of phase shift over a width of 64 mm in birch at 21% mc as thickness increases from 0 to 31 mm.

aries because of different dielectric properties. This will give deviations in attenuation from theoretical values, since theoretical values do not include effects from reflections. Attenuation is more affected by multiple reflections and mismatch losses than is the phase shift [6], and hence the deviations from theoretical values are smaller in phase shift than for attenuation. Another factor which may influence attenuation and phase shift is the variation of grain angle.

Fig. 10 shows the average over the area inside the dotted line in Fig. 2 of theoretical and measured values of attenuation versus thickness at mc 13% at room temperature and frozen at mc 21%. The water molecules in the frozen wood will not oscillate with the field, and the influence of water is decreased. This means that the attenuation in

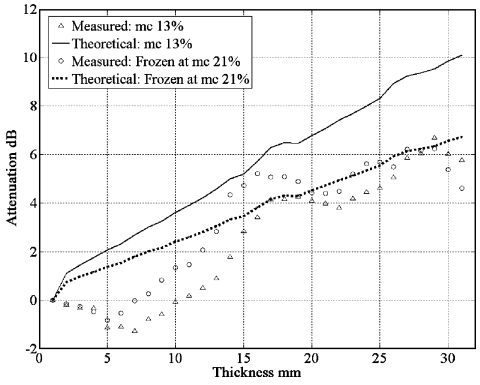

Fig. 10. Average values of attenuation versus thickness for microwaves at 9.375 GHz in birch wood. Measured and theoretical values.

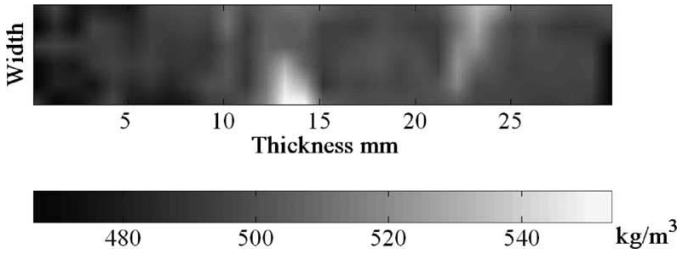

Fig. 9. Density distribution over the measured region. Two small regions have about 10% higher density.

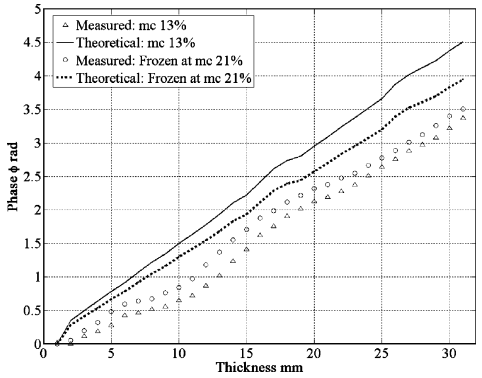

Fig. 11. Average values of phase shift versus thickness for microwaves at 9.375 GHz in birch wood. Measured and theoretical values.

frozen birch with mc 21% is almost the same as in room temperature with mc 13%. The same goes for phase shift in Fig. 11.

The influence of thickness on measured values is lower than on theoretical values, which may be caused by systematic errors in the microwave scanner. There could be gradients in the moisture distribution that cause deviations from theoretical values at some moisture levels. Another possible error is that theoretical values do not involve effects from reflections and scattering. These errors increase in dry wood.

7. Conclusions

- Good correspondence in measured and theoretical values of phase shift.
- The microwave scanner has to be calibrated with a known dielectric to quantify the error in the measurement.
- Reflections and scattering create more noise in attenuation measurement than in measurement of phase shift.
- The proportion of noise is higher at lower moisture content due to lower attenuation.

References

[1] G.I. Torgovnikov, Dielectric Properties of Wood and Wood-Based Materials, Springer, Berlin, 1993.
[2] Jean-F. Portala, Characterisation Du Bois Par Intercorrelation de Measures Multisensorielles. These, Institut National Polytechnique de Lorraine, 1992.
[3] J.C. Bolomey, F.E. Gardiol, Engineering Applications of the Modulated Scatterer Technique, Artech House Inc., 2001, ISBN 1-58053-147-4.
[4] W.L. James, You-Hsin Yen, R.J. King, A microwave method for measuring moisture content, density and grain angle of wood. USDA Forest Products Laboratory, Research Note FPL-0250, 1985.
[5] J. Johansson, Property Predictions of Wood Using Microwaves. Licentiate Thesis, Luleå University of Technology. LIC 2001, 35, 2001.
[6] E. Nyfors, P. Vainikainen, Industrial Microwave Sensors, Artech House, Norwood MA, 1989, pp. 207–212.

Paper II

J Wood Sci (2006) 52:406–410
DOI 10.1007/s10086-005-0794-8

ORIGINAL ARTICLE

Lars Hansson · Nils Lundgren · Anna-Lena Antti
Olle Hagman

Finite element modeling (FEM) simulation of interactions between wood and microwaves

Received: April 4, 2005 / Accepted: November 11, 2005 / Published online: April 25, 2006

Abstract The aim of this study was to use finite element modeling (FEM) as a tool to analyze microwave scattering in wood and to verify the model by measurements with a microwave scanner. A medical computed tomography scanner was used to measure distribution of density and moisture content in a piece of Scots pine (*Pinus sylvestris*). Dielectric properties were calculated from measured values for cross sections from the piece and used in the model. Images describing the distribution of the electric field and phase shift were obtained from the FEM simulation. The model was verified by measurements with a scanner based on a microwave sensor. The results show that simulated values correspond well to measured values. Furthermore, discontinuities in the material caused scattering in both the measured and the simulated values. The greater the discontinuity in the material, the greater was the need for computational power in the simulation.

Key words Microwave scanning · Wood · Dielectric properties · Modulated scattering technique · Finite element modeling

Introduction

Microwave scanning is a fast and nondestructive method of measuring internal properties, such as density and moisture content (MC) of wood. This method has previously been studied, for example, by Johansson et al.[1] The aim of the present study was to use finite element modeling (FEM) as a tool to analyze microwave scattering in wood and to verify the model by measurements with a microwave scanner. Values of phase shift and attenuation from the measurements were compared with the FEM model.

By transforming the Maxwell equations into second-order partial differential equations (PDEs) it is possible to solve electromagnetic wave propagation problems. Because wood is an inhomogeneous and anisotropic dielectric material, the wave scatters in different directions as it propagates. Moisture and heat flow during microwave drying of wood have been modeled by Antti,[2] Perre and Turner,[3] and Zhao and Turner.[4] No previous models have been made of electromagnetic wave propagation inside wood because of difficulties in ascertaining the internal structure and because of the need of computational power. In the present analysis, the internal structure of density and moisture content in wood was determined by computed tomography (CT) scanning, as described by Lindgren.[5] From these density and moisture content values, the distribution of dielectric properties was determined. The finite element modeling electromagnetic module in FEMLAB[6] version 3.1 software was used to solve PDEs that describe the wave propagation.

Theory

The dielectric properties of wood depend on moisture content, density, frequency, grain angle, and temperature. The real and imaginary part of the dielectric permittivity, ε' and ε'', perpendicular to the grain versus moisture content and density are shown in Figs. 1 and 2. The free water in the cell cavities, when above the fiber saturation point (FSP), seems to affect permittivity values somewhat differently from water that is bound in the cell walls. Parallel to the grain, the values are 1.1–2 times higher.[7]

Simulation models were constructed with the finite element method as described by, among others, Jin[8] using FEMLAB[6] 3.1. The models describe how a transverse electric (TE) wave propagates through a piece of wood surrounded by air. The variations in the material require a three-dimensional model to obtain a correct solution. How-

L. Hansson · A.-L. Antti
Division of Wood Physics, Luleå University of Technology, Skellefteå Campus, Skellefteå SE-931 87, Sweden

N. Lundgren (✉) · O. Hagman
Division of Wood Technology, Luleå University of Technology, Skellefteå Campus, Skellefteå SE-931 87, Sweden
Tel. +46-910-58-5707; Fax +46-910-58-5399
e-mail: nils.lundgren@ltu.se

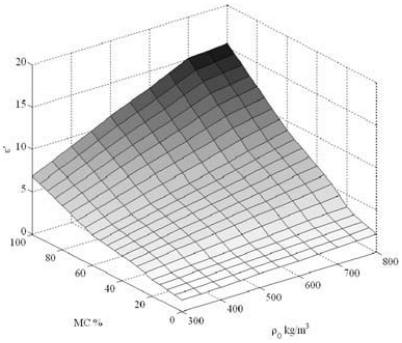

Fig. 1. The relative permittivity ε' at 10 GHz and room temperature, perpendicular to the grain versus moisture content and density[7]

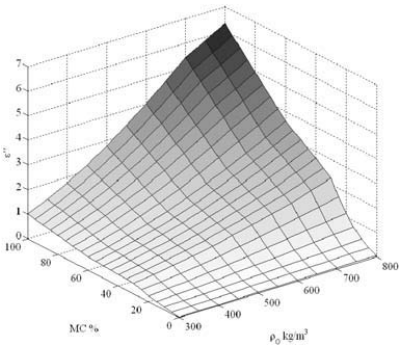

Fig. 2. The relative loss factor ε'' at 10 GHz and room temperature, perpendicular to the grain versus moisture content and density[7]

ever, insufficient computational power made it necessary to restrict the simulation to a two-dimensional model. Variations of dielectric properties in the z direction were neglected, which may increase the errors in the final solution. In the model domain, the z component of the $\boldsymbol{E}$ field is solved by the following equation:

$$\nabla\times\left(\frac{1}{\mu_r}\nabla\times\boldsymbol{E}_z\right)-\left(\varepsilon^*-j\cdot\frac{\sigma}{\omega}\cdot\varepsilon_0\right)\cdot k_0^2\cdot\boldsymbol{E}_z=0, \quad (1)$$

where μ_r is the relative permeability, which is equal to the permeability μ_0 of the free space in the total model domain, because wood is not a magnetic material. Furthermore, ω is the angular frequency, σ is the conductivity, and k_0 is the wave number in free space. In this case σ is close to zero. ε^* is the dielectric permittivity defined as:

$$\varepsilon^*=\left(\varepsilon'-j\cdot\varepsilon''\right), \quad (2)$$

where ε' is the relative permittivity and ε'' is the relative loss factor. Tables from Torgovnikov[7] that describe ε^* at varying moisture content, density, and temperature are included in the model and values for ε' and ε'' are interpolated for each grid point and time step by the solver. The model uses a low-reflectance boundary condition on the transmitting and receiving antennas, with electric field $\boldsymbol{E}_z = 1$ on the transmitting antenna and with a source field of zero on the receiving antenna. The low-reflectance boundary to free space is defined as:

$$\boldsymbol{e}_z\cdot\left(\boldsymbol{n}\times\boldsymbol{H}\right)+\boldsymbol{E}_z=2\cdot\boldsymbol{E}_{0z}, \quad (3)$$

where $\boldsymbol{H}$ is the magnetic field and $\boldsymbol{E}_{0z} = \boldsymbol{E}_z$ is the electric field.

Because the incoming wave to the domain is propagated parallel to the vertical boundaries and the magnetic field is perpendicular to these boundaries, a perfect magnetic conductor (PMC) boundary condition is used. PMC is defined as:

$$\left(\boldsymbol{n}\times\boldsymbol{H}\right)=0, \quad (4)$$

where $\boldsymbol{n}$ is a unit vector normal to the boundary.

Fig. 3. The piece of Scots pine that was used in the study

Material and methods

The material chosen for the study was one piece of Scots pine (*Pinus sylvestris*) shown in Fig. 3 with dimensions 40 × 150 × 320 mm. Close to the center of the piece was a cone-shaped knot with a diameter varying from 18 to 25 mm.

A CT scanner (Siemens Somatom) was used to measure the density in the cross sections. The geometric shape, dielectric properties, and moisture distribution in the green condition for each cross section were calculated from the measured density.

Density data from CT scanning was used to calculate variations in the dielectric properties of the wood and of the moisture distribution in the green condition. The difference between CT images in green and dry conditions was calculated and the resulting image was assumed to describe the moisture distribution in the cross section. Cross sections of the piece, as shown in Fig. 4, were scanned with microwaves and CT both parallel and perpendicular to the grain in green and dry conditions.

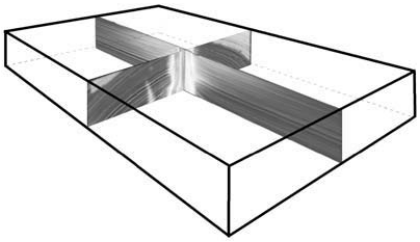

Fig. 4. Two cross sections from the object were scanned. One section was parallel to the grain and the other section was perpendicular to the grain. Regions with low density are darker in the computed tomography (CT) images

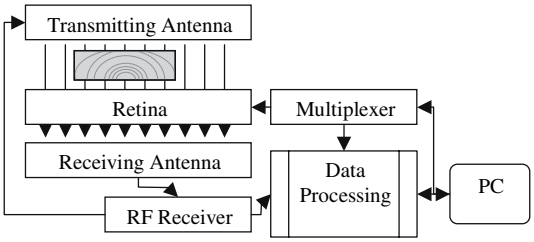

Fig. 6. Sensor system for the microwave scanner. The microwave signal is modulated by a low-frequency signal at 128 probes in the retina. The electromagnetic field at each probe is then extracted from the signal. *RF*, radio frequency; *PC*, personal computer

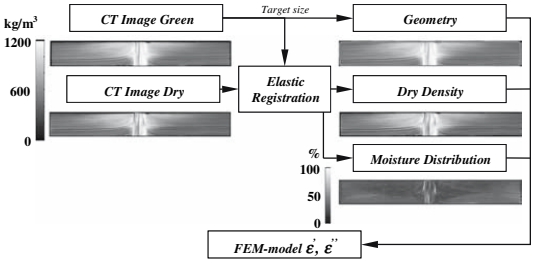

Fig. 5. Brief description of the working procedure in the generation of finite element models

Before the moisture content was calculated from the CT images, it was necessary to compensate the image of dry wood for shrinkage and deformation. Transformation of the CT image of dry wood to the shape of green wood was done by using elastic registration as described by Sorzano et al.[9] Figure 5 shows how the FEM model was generated using density images in green and dry conditions when the electric field (E-field) was oriented perpendicular to the grain (Fig. 4). The same procedure was used when the E-field was parallel to the grain, but the values for ε^* were multiplied with a moisture-dependent factor.[7] Within the knot, the E-field was perpendicular to the grain in both models.

A microwave scanning system described by Johansson[10] that measures attenuation and phase shift of the transmitted electromagnetic field every 8 mm was used for the measurements. Figure 6 shows a schematic drawing on the main part of the system. The wood is illuminated by a quasiplane wave generated by a slotted waveguide that acts as a transmitting antenna where the electrical field is perpendicular to the sensor (9.375 GHz).[11] The wave is locally perturbed at dipoles in the retina by a low frequency signal. This will cause a modulation of the radio frequency (RF) signal that is proportional to the electromagnetic field at the dipoles. This technique, known as modulated scattering technique (MST), has been described by Bolomey and Gardiol[12] among others. The measured values of attenuation and phase shift in the microwave signal after passing through the wood were compared with finite element simulations performed in two dimensions.

Results

The results show that simulated values correspond well to measured values. Figures 7–10 show attenuation and phase angle in the simulated and measured field after transmittance through dry wood. The measured values were obtained by repeated measurements with increasing antenna distance. Figures 11 and 12 show the attenuation when the E-field is oriented perpendicular and parallel to the grain. A clear pattern from the knot in the phase shift for dry wood is shown in Figs. 13 and 14. The phase shift perpendicular to the grain for green wood in Fig. 15 also shows a pattern caused by the knot. The knot is not visible in simulated or measured data for green wood parallel to the grain (Fig. 16).

Discussion

The phase shift is periodic and can only be measured and simulated in the interval $(-\pi, \pi)$. The vectors were unwrapped by changing absolute jumps greater than π to their 2π complement. This only works when the phase shift between adjacent points is less than 2π. The measurements that deviated from the model were attenuation in green wood with the E-field perpendicular to the grain and phase shift in dry wood with the E-field parallel to the grain. The first case can be explained by variations in the z direction. The moisture content was higher on both sides of the scanned cross section. In the second case, the result is very sensitive to changes in the correction factor for permittivity when the E-field is parallel to the grain.

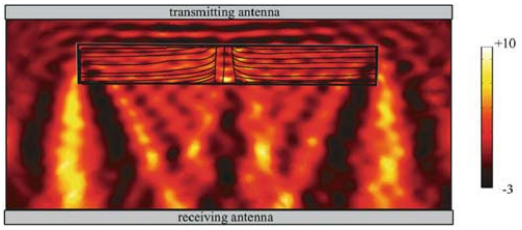

Fig. 7. Simulated attenuation of the electric field (E-field) in dB

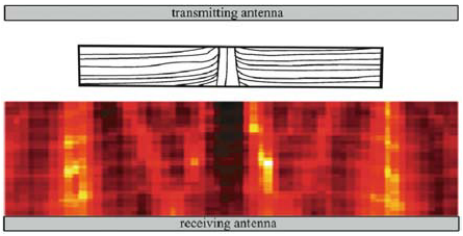

Fig. 8. Measured attenuation of the transmitted E-field

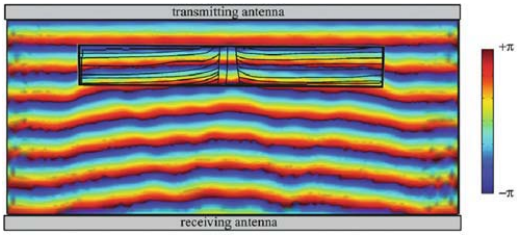

Fig. 9. Simulated phase angle of the E-field in radians

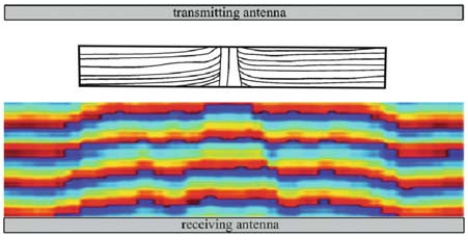

Fig. 10. Measured phase angle of the transmitted E-field

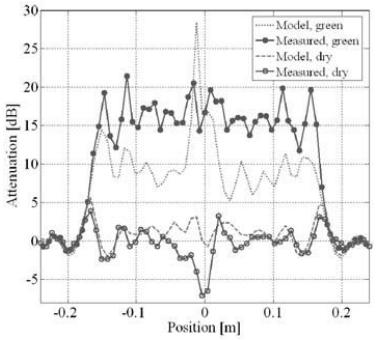

Fig. 11. Simulated and measured attenuation of electromagnetic (EM) wave with the E-field oriented perpendicular to the grain after transmittance through green and dry wood

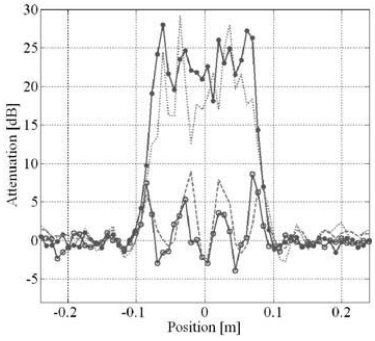

Fig. 12. Simulated and measured attenuation of EM wave with the E-field oriented parallel to the grain after transmittance through green and dry wood

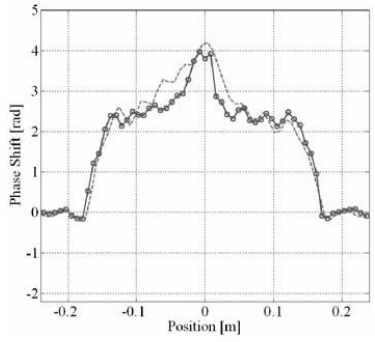

Fig. 13. Simulated and measured phase shift of EM wave with the E-field oriented perpendicular to the grain after transmittance through dry wood

Conclusions

The model corresponds well to the measured values, which show that the FEM simulation could be a useful tool for analyzing microwave scattering in wood. Because wood is an inhomogeneous material, there are discontinuities in density and moisture content in the wood pieces that result in a huge scattering in the measured and simulated values. The greater the discontinuities, the greater is the need for computational power in the simulation. Variations in the *z* direction give errors if the models are restricted to the *xy*

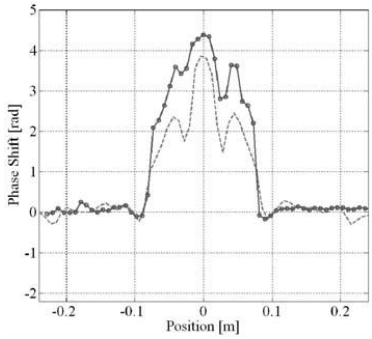

Fig. 14. Simulated and measured phase shift of EM wave with the E-field oriented parallel to the grain after transmittance through dry wood

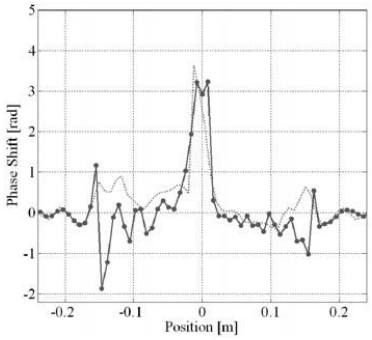

Fig. 15. Simulated and measured phase shift of EM wave with the E-field oriented perpendicular to the grain after transmittance through green wood

plane. The model for dry wood is sensitive to changes in the correction factor for permittivity.

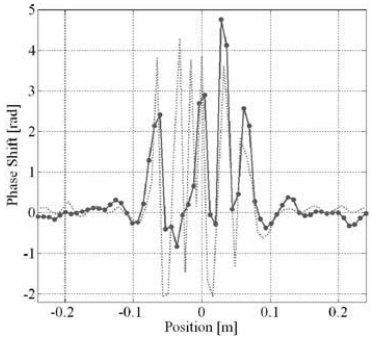

Fig. 16. Simulated and measured phase shift of EM wave with the E-field oriented parallel to the grain after transmittance through green wood

References

1. Johansson J, Hagman O, Fjellner BA (2003) Predicting moisture content and density distribution of Scots pine by microwave scanning of sawn timber. J Wood Sci 49:312–316
2. Antti L (1999) Heating and drying wood using microwave power. Doctoral Thesis, Luleå University of Technology
3. Perre P, Turner IW (1997) Microwave drying of softwood in an oversized waveguide: theory and experiment. AIChE J 43:2579–2595
4. Zhao H, Turner IW (2000) Use of a coupled computational model for studying the microwave heating of wood. Appl Math Model 24:183–197
5. Lindgren O (1992) Medical CT-scanners for non-destructive wood density and moisture content measurements. Doctoral Thesis, Luleå University of Technology
6. Comsol AB (2005) Comsol home page. http://www.comsol.se. Cited 31 Oct 2005
7. Torgovnikov GI (1993) Dielectric properties of wood and wood-based materials. Springer, Berlin Heidelberg New York
8. Jin J (2002) The finite element method in electromagnetics. Wiley, New York
9. Sorzano COS, Thévenaz P, Unser M (2005) Elastic registration of biological images using vector-spline regularization. IEEE Trans Biomed Eng 52:652–663
10. Johansson J (2001) Property predictions of wood using microwaves. Licentiate Thesis, Luleå University of Technology
11. Satimo France (2005) Satimo home page. http://www.satimo.com. Cited 31 Oct 2005
12. Bolomey JC, Gardiol FE (2001) Engineering applications of the modulated scatterer technique. Artech House, Boston

Paper III

FEM Simulation Of Interactions Between Microwaves And Wood During Thawing

N. Lundgren, L. Hansson, O. Hagman, A.L. Antti

Luleå University of Technology, Division of Wood Science and Technology, Skellefteå Campus, SE-93187 Skellefteå, Sweden

Abstract. Dipole polarization of water molecules is an important factor when microwaves interact with moist wood. Hence there will be a considerable change in dielectric properties when the wood changes from frozen to nonfrozen condition. The aim of this study was to develop a model that simulates measurements with a microwave scanner based on a sensor working at 9.4 GHz. Two-dimensional finite element modelling (FEM) was implemented to analyze interactions between microwaves and green wood during thawing of frozen wood at room temperature. A medical computed tomography scanner was used to measure the internal structure of density in a piece of wood in green and dry condition. From these density images the distribution of dry weight moisture content was calculated for a cross section of the piece and used in the model. Images describing the distribution of the electric field and phase shift at different temperatures where obtained from the FEM simulation. The results show that simulated values correspond well to measured values. This confirms that the model presented in this study is a useful tool to describe the interaction between microwaves and wood during microwave scanning at varying conditions.

Keywords: microwave scanning, wood, dielectric properties, finite element modelling, thawing, phase transition.

PACS: 41.20.Jb

INTRODUCTION

The dielectric properties of dry wood and water can be used to determine the distribution of moisture or density in sawn lumber, as has been described by Hansson et al. [1], among others. It has also been proposed that microwaves should be used to measure grain angle in wood [2]. Depending on geographical location and the properties being measured, it might be necessary to consider temperature dependence. Especially at temperatures around 0°C, there is a steep change in the way water molecules will interact with the electromagnetic field, and the influence of moisture content is small for measurements on frozen wood. Hansson et al. [3] have simulated the interaction between wood and microwaves at a constant temperature by finite element modelling (FEM). The heating of wood in an industrial microwave applicator has also been modelled [4]. A microwave system for scanning of sawn lumber has been developed at Luleå University of Technology. The aim with the present study

was to simulate the response from the microwave sensor when measurements are made on a piece of wood during thawing at room temperature. The model includes heat conduction in wood and the temperature dependence of dielectric properties.

MATERIALS AND METHODS

The study was based on one piece of frozen green birch wood, with dimensions 21 x 175 x 305 mm. The object was frozen to a temperature of about –15°C. After that, the frozen test piece was allowed to thaw out at room temperature. The test piece was microwave scanned every half hour in the centre in axial direction during thawing until almost the whole object had reached room temperature. The microwave scanning system described by Johansson [5], measures attenuation and phase shift of the transmitted electromagnetic field every eight millimetres. The wood is illuminated by a quasiplane wave generated by a slotted waveguide that acts as a transmitting antenna. The sensor [6] (9.375 GHz) is based on modulated scattering technique (MST) as described by Bolomey and Gardiol [7]. The internal temperature during thawing was measured continuously using a fibre-optic sensor (ASEA 1110) placed in centre of the object. After each microwave measurement, the sample was removed from the microwave scanner, and the heat distribution at the surface was captured using an infrared (IR) camera (AGEMA 550). A CT scanner (Siemens Somatom AR.T.) was used to measure green and dry density of the wood specimen.

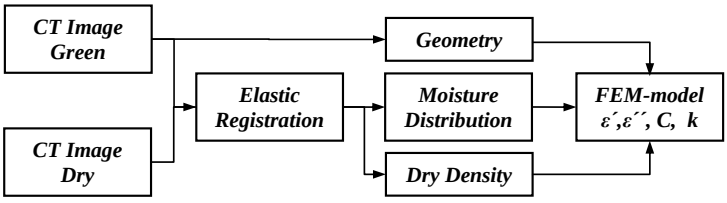

FIGURE 1. Description of the working procedure for generating the FEM model. Dielectric properties (ε', ε''), thermal heat conductivity (k) and specific heat capacity (C) were calculated as functions of temperature, dry density and dry weight moisture distribution in the model.

A schematic description of how the model was generated is shown in figure 1. Transformation of the CT image of dry wood to the shape of green wood was done using elastic registration as described by Sorzano et al [8]. Dry weight moisture distribution was calculated as the difference between these images. The thawing process was then simulated in a two-dimensional section by FEM using the software FEMLAB [9] version 3.1, where the dry weight moisture distribution and the transformed dry wood density images were used as input to estimate values for thermal heat conductivity, specific heat capacity and the dielectric properties for the object. The dielectric properties were calculated from empirical data given by Torgovnikov [10].

ELECTROMAGNETIC WAVE PROPAGATION IN WOOD

When a plane electromagnetic wave is exposed in y-direction through a dielectric material such as wood, the wave can be described as:

$$\mathbf{E}(x, y, z, t) = \mathbf{E}_0 \cdot e^{-j\cdot\omega\cdot t-\gamma\cdot y} \quad , \tag{1}$$

$$\mathbf{H}(x, y, z, t) = \mathbf{H}_0 \cdot e^{-j\cdot\omega\cdot t-\gamma\cdot y}, \tag{2}$$

where $\mathbf{E}_0$ and $\mathbf{H}_0$ are the amplitudes of the electric and the magnetic field and γ is the complex distribution factor:

$$\gamma = j\cdot\omega\cdot\sqrt{\varepsilon\cdot\mu} = \alpha + j\cdot\beta, \tag{3}$$

where ω is angular frequency and μ is the complex permeability. Since wood is not a magnetic material, the complex permeability is equal to the permeability μ_0 of the free space. Furthermore, ε is the relative complex permittivity defined as:

$$\varepsilon = \varepsilon_0\cdot(\varepsilon' - j\cdot\varepsilon''), \tag{4}$$

where ε_0 is the absolute permittivity for vacuum, ε' is the relative permittivity and ε'' is the relative loss factor. These factors for wood are dependent on the dry weight moisture content, density, frequency, temperature and grain angle. They have been thoroughly investigated by Torgovnikov [10]. If the electric field is parallel to the grain, the dielectric values are about 1.1–2 times higher. If the real and imaginary parts of equation 3 are equated, the expression for the attenuation factor α and the phase factor β of the wave will be:

$$\alpha = \omega\cdot\sqrt{\varepsilon_0\cdot\mu_0}\cdot\left(\frac{\varepsilon'}{2}\cdot\left(\sqrt{1+\left(\frac{\varepsilon''}{\varepsilon'}\right)^2}-1\right)\right)^{1/2}, \tag{5}$$

$$\beta = \omega\cdot\sqrt{\varepsilon_0\cdot\mu_0}\cdot\left(\frac{\varepsilon'}{2}\cdot\left(\sqrt{1+\left(\frac{\varepsilon''}{\varepsilon'}\right)^2}+1\right)\right)^{1/2}, \tag{6}$$

Insertion of equation 3 into equation 1 shows that the amplitude is attenuated exponentially with a factor $e^{-\alpha\cdot y}$ as the wave propagates. If the magnitude of the electric field decreases from $\mathbf{E}(0)$ to $\mathbf{E}(y)$, the attenuation per metre is defined as:

$$\frac{20\cdot\log\left(\frac{\mathbf{E}(0)}{\mathbf{E}(y)}\right)}{y} = 20\cdot\log(e)\cdot\alpha \quad \text{[dB/m]}, \tag{7}$$

The phase shift per metre is defined as:

$$\frac{\phi}{y} = \beta \quad \text{[rad/m]}. \tag{8}$$

The attenuation and phase shift per metre versus dry weight moisture content and density when the electric field is perpendicular to the grain are shown in figures 2 and 3. The free water in the cell cavities above the fibre saturation point affects attenuation and phase shift values somewhat differently than water that is bound in the cell walls.

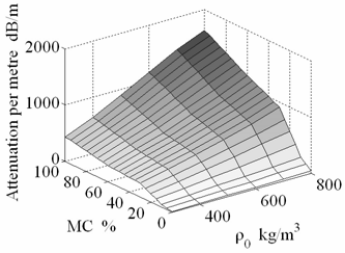

FIGURE 2. Attenuation per metre as a function of dry wood density and dry weight moisture content at room temperature.

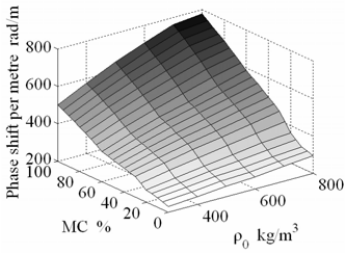

FIGURE 3. Phase shift per metre as a function of dry wood density and dry weight moisture content at room temperature.

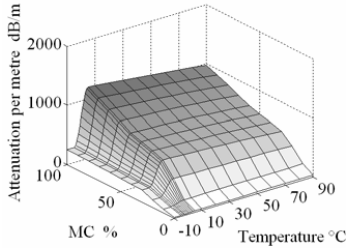

FIGURE 4. Attenuation per metre as a function of temperature and dry weight moisture content at a dry density of 600 kg/m^3.

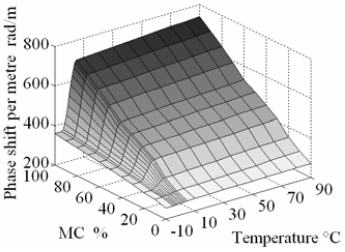

FIGURE 5. Phase shift per metre as a function of temperature and dry weight moisture content at a dry density of 600 kg/m^3.

The attenuation and phase shift per metre versus dry weight moisture content and temperature, when the electric field is perpendicular to the grain, are shown in figures 4 and 5. There is a step transition for the attenuation and for the phase shift when the temperature is zero. To emulate these steps, a smoothed Heaviside function with continuous first derivative [9] is used in the model in order to improve numerical reliability and convergence. The model uses a low-reflectance boundary condition on the transmitting and receiving antennas, with an electric field E_z = 1 on the transmitting antenna and with a source field of zero on the receiving antenna. The low-reflectance boundary [11] to free space used in Femlab's electromagnetic module is defined as:

$$\mathbf{e}_z \cdot (\boldsymbol{n} \times \boldsymbol{H}) + E_z = 2 \cdot E_{0z}, \tag{9}$$

where $\mathbf{e}_z$ is a unit vector, $\boldsymbol{H}$ is the magnetic field, $\boldsymbol{n}$ is the normal to the boundary and $E_{0z} = E_z$ is the electric field at the boundary. Since the incoming wave to the domain is propagated parallel to the vertical boundaries, and the magnetic field is perpendicular to these boundaries, a perfect magnetic conductor (PMC) boundary condition is used. PMC is defined as:

$$(\boldsymbol{n} \times \boldsymbol{H}) = 0, \tag{10}$$

where $\boldsymbol{n}$ is a unit vector perpendicular to the boundary.

HEAT TRANSFER IN WOOD

The temperature variation in a given region over time can be described mathematically with a partial differential equation. This heat equation describes the heat transfer by conduction and convection. In this model, heat transfer by convection is ignored and the heat equation has the form:

$$\rho \cdot C \cdot \frac{\partial T}{\partial t} - \nabla \cdot (k \cdot \nabla T) - Q = 0, \tag{11}$$

where T is the temperature, ρ is the density, t is time, C is the specific heat capacity for constant volume or constant pressure, k is the thermal conductivity and Q is heat-source or sink. In this case, the heat term is zero, because the microwave energy is ignored. In the region of the model, the density of wood,

$$\rho = \rho_0 \cdot \frac{1+u}{1+s_u}, \tag{12}$$

is a function of given dry weight moisture content u, the dry density ρ_0 and also the volumetric swelling or shrinking coefficient, s_u [12]. This coefficient has approximately linear behaviour below the fibre saturation point:

$$s_u = \frac{s_{\max}}{u_{fsp}} \cdot u \tag{13}$$

whereas above the fibre saturation point it is constant:

$$s_u = s_{\max}, \tag{14}$$

where u_{fsp} is the dry weight moisture content at the fibre saturation point at room temperature, and $s_{\max}$ is the maximum volumetric swelling or shrinking coefficient for birch [13]. The specific heat capacity for wood [12] is temperature and dry weight

moisture content dependent, as shown in figure 6. The thermal conductivity of wood [14] is temperature and dry weight moisture content dependent, but also density dependent (figure 7). Furthermore, thermal conductivity in the longitudinal direction is, in the dry weight moisture content range from about 0.06 to 0.15, approximately 2.25 to 2.75 times the conductivity across the grain [12].

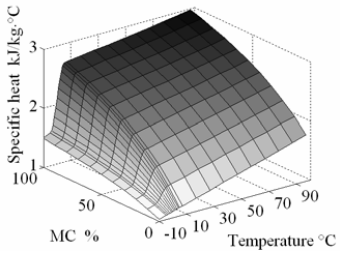

FIGURE 6. Specific heat as a function of temperature and dry weight moisture content.

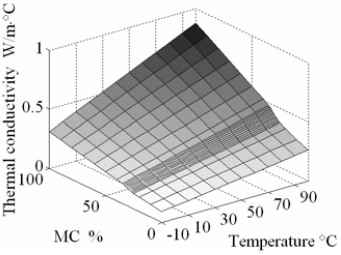

FIGURE 7. Thermal conductivity as a function of temperature and dry weight moisture content at dry density 600 kg/m^3.

Figures 6 and 7 show step transition for specific heat and thermal conductivity respectively when the temperature is zero and the dry weight moisture content has reached the fibre saturation point. These steps were emulated with a smoothed Heaviside function in the same way as the dielectric properties. The model uses a prescribed temperature boundary condition on the transmitting, receiving antennas and on the free space boundary, with a room temperature of T = 20°C. The generalized boundary heat flux condition between the air and the wood surface is defined as:

$$\mathbf{n} \cdot (k \cdot \nabla T) = q_0 + h \cdot (T_{\inf} - T) + C_{const} \cdot (T_{amb}^4 - T^4), \qquad (15)$$

where q_0 represent the heat flux due to evaporation from the surface and is ignored. The second term on the right hand side in equation (15) is the convective heat flux with the surrounding environment, where h is the heat transfer coefficient and T_{inf} is the ambient bulk temperature calculated as the mean value of the prescribed temperature and surface temperature. In general, the geometry and the ambient flow condition are used to determine the value of the heat transfer coefficient. Here, simplified equations are used for the free convection on the wood. The last term in equation (15) is the radiation heat flux with the surrounding environment, where T_{amb} is the surrounding environment temperature; i.e., the prescribed temperature. C_{const} is a product of the surface emissivity and the Stefan-Boltzmann constant.

RESULTS AND DISCUSSION

Figures 8 and 9 show the measured and simulated surface temperature. Energy loss due to evaporation is not included in the simulated model. The mass loss during thawing was 21.3 g. Hence there are some differences in the values.

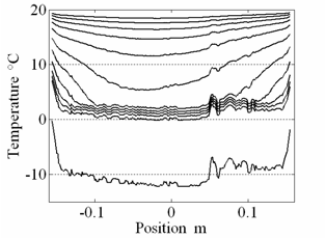

FIGURE 8. Measured surface temperature every 30 min during thawing.

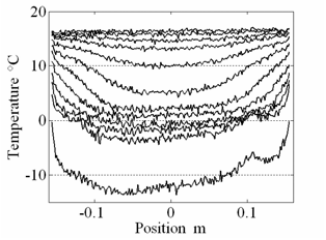

FIGURE 9. Simulated surface temperature every 30 min during thawing.

At low temperatures, the surface temperature is higher on the right hand side in both figures. This is due to lower moisture content in the right side of the wood, as can be seen in figure 10.

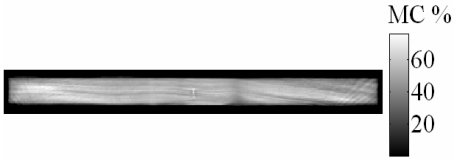

FIGURE 10. Moisture content distribution in the cross section.

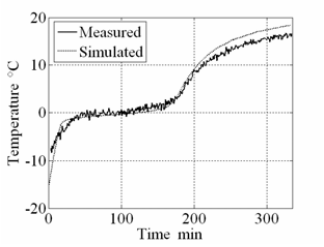

FIGURE 11. Measured and simulated core temperature.

Figure 11 shows measured and simulated core temperature. There is a small deviation in the end of the thawing process that also originates from evaporation that is not included in the model. Figures 12–15 show that the simulated values correspond well to measured values during thawing, both for attenuation and phase shift.

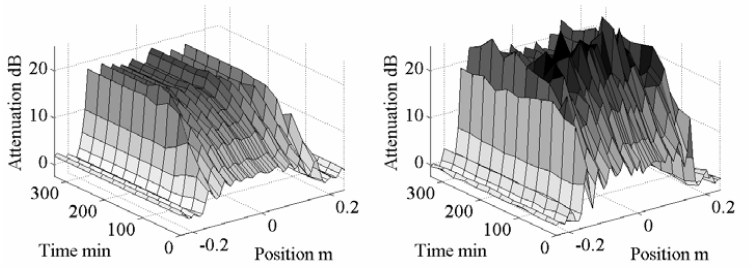

FIGURES 12 - 13. Simulated (left) and measured (right) attenuation.

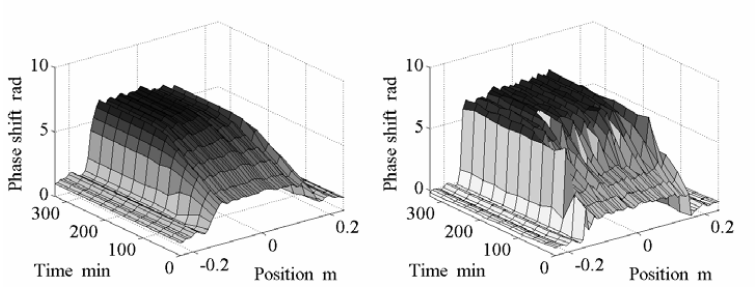

FIGURES 14 - 15. Simulated (left) and measured (right) phase shift.

The agreement in simulated and measured values implies that the FEM model provides a reliable description of the scanner system and that the tabulated values for dielectric and thermal properties on which the model is based are correct.

CONCLUSIONS

The simulated attenuation and phase shift corresponds well to measured values. The model can be used to develop and verify algorithms for scanning of frozen or non-frozen lumber. No reliable predictions of wood properties can be made at temperatures around the freezing point. The response from different types of wood or from knots can easily be simulated by changing the dielectric properties in the model.

REFERENCES

1. L. Hansson, N. Lundgren, A. L. Antti and O. Hagman, *Microwave Penetration in Wood Using Imaging Sensor*, Journal of International Measurement Confederation 38 pp15–20 (2005).
2. J. Shen, G. Schajer and R. Parker, *Theory and Practice in Measuring Wood Grain Angle Using Microwaves*, IEEE Transactions on Instrumentation and Measurement 43(6) pp 803–809 (1994).
3. L. Hansson, N. Lundgren, A. L. Antti and O. Hagman, *FEM Simulation of Interactions Between Wood and Microwaves*, Accepted for publication in Journal of Wood Science (November 2005).
4. L. Hansson, N. Lundgren, A. L. Antti and O. Hagman, *FEM Simulation of Heating Wood In an Industrial Microwave Applicator*, Proceedings from 10th International Conference on Microwave and High Frequency Heating pp 415–418 (2005).
5. J. Johansson, *Property Predictions of Wood Using Microwaves*, Licentiate Thesis Luleå University of Technology, LIC-2001:35 (2001).
6. Satimo France. 22 Avenue de la Baltique Z.A. Courtaboeuf 91953 France. Home page: www.satimo.com.
7. J. C. Bolomey and F. E. Gardiol, *Engineering Applications of the Modulated Scatterer Technique*, Artech House Inc. ISBN: 1-58053-147-4, 2001.
8. C. O. S. Sorzano, P. Thévenaz and M. Unser, *Elastic Registration of Biological Images Using Vector-Spline Regularization*, IEEE Transactions on Biomedical Engineering: 2005. Vol. 52:652–663.
9. Comsol AB. Tegnérgatan 23 SE-11140 Stockholm. Home page: www.comsol.se
10. G. I. Torgovnikov, *Dielectric Properties of Wood and Wood-Based Materials*, Berlin: Springer, 1993.
11. Anonymous, *FEMLAB3 Electromagnetic Module Users Guide*, January 2004
12. F. F. P. Kollman and W.A. Côté, *Principle of Wood Science and Technology (Vol. 1. Solid wood)*, New York: Springer, 1984.
13. J. B. Boutelje, *Träfakta 2nd ed*. Stockholm: Trätek, 1989.
14. J. D. MacLean, *Thermal conductivity of wood*, Heating, Piping and Air Conditioning Vol. 13:380–391 (1941).

Paper IV

FEM SIMULATION OF HEATING WOOD IN AN INDUSTRIAL MICROWAVE APPLICATOR

Lars Hansson, Nils Lundgren, Lena Antti, Olle Hagman
Luleå University of Technology, Division of Wood Technology, SE-931 87 Skellefteå, Sweden, www.ltu.se

ABSTRACT
The aim with this study was to use two-dimensional finite element modelling to investigate microwave heating of a heterogeneous material such as wood. Dielectric properties of wood depend on moisture content, density, frequency, grain angle and temperature. A CT scanner (medical computer tomography) was used to detect density and, with that, moisture content in birch wood. Dielectric properties were calculated within a wood cross section and used in the model. Heat distribution in wood was simulated and verified by measuring temperatures at specific locations in the wood during the process. A specially designed industrial microwave drier equipped with 1 kW magnetrons, 2.45 GHz, was used in the tests. The results show that finite element modelling is a powerful tool in estimation of heat distribution when microwave heating is applied to a well-described porous material such as wood.
KEYWORDS: Wood, FEM, Phase transition, Heating, CT-scanning

INTRODUCTION

Wood is a complex material composed of cellulose, lignin hemicelluloses and minor amounts of extractives. The variation in characteristics and volume of these components as well as differences in cellular structure makes the wood heavy or light, stiff or flexible and hard or soft. These properties are relatively constant in the same kind of wood. A living tree generally has a moisture content exceeding 30%, which means that the cell walls are fully saturated. The higher the moisture content is, the more water will be filled in the cell cavities. The use of microwave heating for drying of wood has been investigated and developed, among others, by Perré and Turner [1] and by Antti [2]. Uneven distribution of the field and material properties will lead to uneven distribution of the heat energy, which also has been studied by Zielonka and Dolowy [3]. When wood is placed in an electric field, the field will be influenced by wood properties such as temperature, density, moisture content, and fibre direction. Finite element modelling (FEM) has been used by Hansson et al. [4] to visualize the interior field when wood is exposed to microwaves. For simulation models of microwave heating it is also necessary to take into account temperature dependence. Especially for frozen wood there is a large change in dielectric properties during the phase transition from ice to water (Hagman et al. [5]). The dielectric and thermal properties of moisture within wood depend on whether the water is bound in the cell walls or free in the cavities. The relative dielectric constant and the loss factor values for the model are based on the literature such as, for instance, Torgovnikov [6]. The heat conductivity of wood depends on density, moisture content and direction of the heat flow with respect to the grain (MacLean [7]). The specific heat of wood is low as compared to other materials. It depends on moisture content and temperature of the wood (Kollman & Côté [8]). The purpose of the present study was to generate an FEM model for microwave heating of wood based on the internal structure and the external field distribution.

MATERIAL AND METHODS

Three pieces of birch wood with the dimensions 55 x 100 x 440 mm where heated in a microwave drier (Hansson and Antti [9]) as shown in Fig. 1. The drier is equipped with a 1 kW magnetron working at 2.45 GHz.

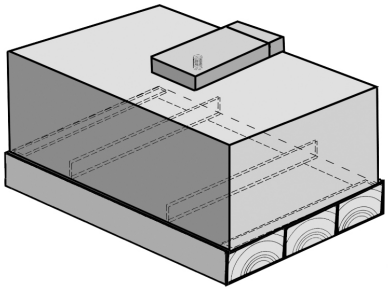

Fig. 1: Microwave drier used for heating of green birch wood from frozen to 100 C.

The internal temperature during the heating process was measured continuously using a fibre-optic sensor (ASEA 1110) placed at the maximum of the electric field. Every five minutes the samples were removed from the applicator for about 30 seconds, and the heat distribution at the surface was captured using an IR camera (AGEMA 550).

A CT scanner (Siemens Somatom AR.T.) was used to measure green and dry density of the wood specimen. Transformation of the CT image of dry wood to the shape of green wood was done using elastic registration as described by Sorzano et al. [10] Moisture distribution was calculated as the difference between these images. From density and moisture content it was possible to estimate values for heat conduction, heat capacity and the dielectric properties. The heating process was then simulated in a two-dimensional section by the use of finite element modelling (FEM) using the software FEMLAB [11] version 3.1. A schematic description of the procedure is shown in Fig. 2.

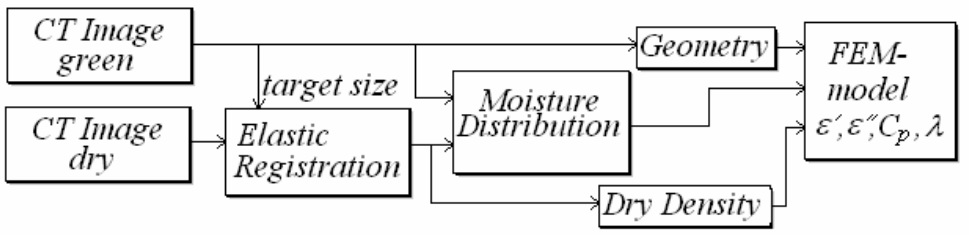

Fig. 2: Description of the working procedure for generation of the FEM models. Dielectric properties (ε´, ε´´), heat conduction (λ) and heat capacity (C_p) were calculated as functions of temperature, dry density and moisture distribution in the model.

At the phase transition from ice to water there is a step function both in dielectric (Fig. 3 and 4) and in thermal properties. Convergence problems due to this step are avoided by using a smoothed Heaviside function. The latent heat that is consumed when ice transforms into liquid water also has to be taken into account. The specific heat around the transition temperature is calculated by multiplying the latent heat with a normalized Gaussian pulse. A fine spatial grid is required for the whole cross section since the phase transition will move during thawing.

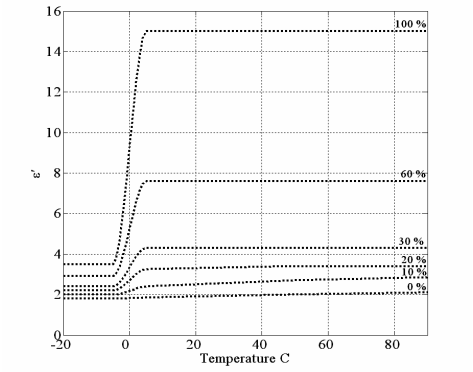

Fig. 3: Relative dielectric constant for wood as a function of temperature with different moisture contents at a density of 600 kg/m^3.

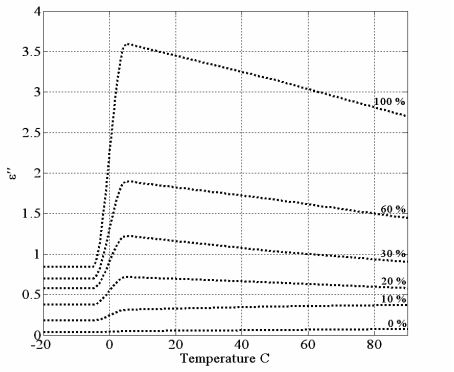

Fig. 4: Relative loss factor for wood as a function of temperature with different moisture contents at a density of 600 kg/m^3.

RESULTS

The simulated core temperature describes the heating process of wood from frozen to 100°C, but also the phase transition at 0°C and 100°C. At the end of the heating process there is a difference between the simulated and the measured core temperature. This difference is probably caused by the water movement in the wood piece, which is not included in the model. The weight of the pieces decreases about 0.1 kilogram during the heating process. Measured and simulated core temperatures are shown in Fig. 5.

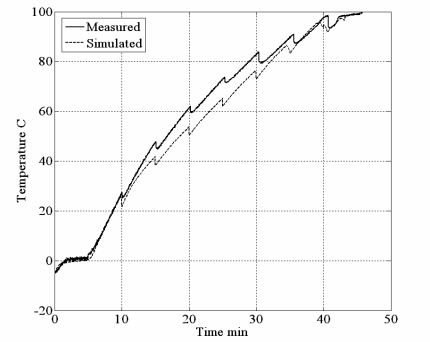

Fig. 5: The measured and the simulated core temperature.

The measured surface temperature at different moments is displayed in Fig. 6. Furthermore, the simulated surface temperature at the same point in time is displayed in Fig. 7. A comparison of the figures shows a difference between the simulated and the measured surface temperature. This difference is due to the fact that the model only approximately handles evaporation, which has a large influence on the surface temperature. The wood pieces used in this model had an average moisture content of about 0.43. Also the fact that the model is only made in 2D causes differences between the measured results and the simulated results. As wood is an inhomogeneous material, there can be discontinuities in density and moisture content in the wood pieces. This causes microwave scattering in all directions, which in turn affects the heating process.

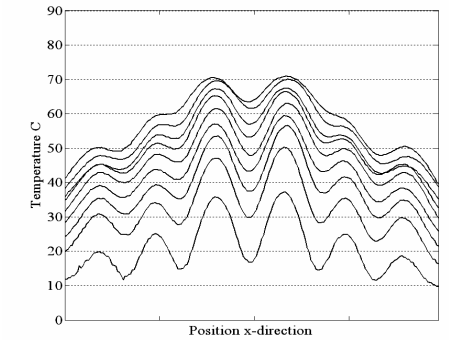

Fig. 6: Measured surface temperature every 5 min during the heating.

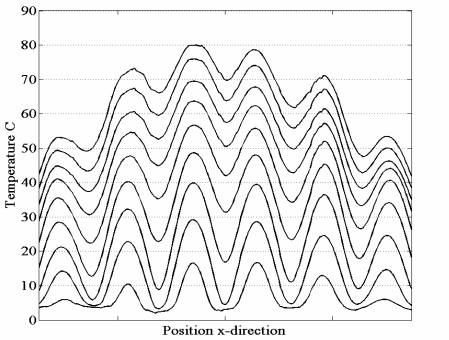

Fig. 7: Simulated surface temperature every 5 min during the heating.

CONCLUSIONS

The model accuracy and adequacy have been verified by a comparison using experimental measurement. The results show that FEM is a powerful tool in estimation of heat distribution when microwave heating is applied to wood. The model predicts the core temperature well. There is a difference between the model and the measurement regarding the surface temperature since the model does not handle all physical processes adequately, e.g., evaporation.

REFERENCES

[1] Perré, P. and Turner, I. (1997). Microwave drying of softwood in an oversized waveguide: Theory and experiment. AIChE Journal 43(10) pp 2579–2578.

[2] Antti, A.L. (1999) Heating and drying wood using microwave power (Doctoral thesis, 1999:35). Skellefteå: Luleå University of Technology, Division of wood physics.

[3] Zielonka, P. and Dolowy, K. (1998). Microwave drying of spruce: moisture content, temperature, and heat energy distribution. Forest Products Journal 48(6) pp 77–80.

[4] Hansson, L., Lundgren, N., Antti L. and Hagman O. (2005) FEM simulation of interactions between wood and microwaves. Submitted to Journal of Wood Science (March 2005)

[5] Hagman, O., Lundgren, N. and Johansson, J. (2004) Calibration for Frozen/Non-Frozen Conditions When Predicting Moisture Content and Density Distribution of Wood by Microwave Scanning of Sawn Timber. Forest Products Society 58th Annual meeting, Grand Rapids, June 27–30 2004.

[6] Torgovnikov, G.I. 1993. Dielectric Properties of Wood and Wood-Based Materials. Springer, Berlin.

[7] MacLean, J.D. 1941. Thermal conductivity of wood. Heating, Piping and Air Conditioning. Vol.13:380–391.

[8] Kollman, F.F.P. and Côté, W.A. 1984. Principle of Wood Science and Technology (Vol. 1. Solid wood). Springer. New York.

[9] Hansson, L. and Antti L. (2003) Design and performance of an industrial microwave drier for on-line drying of wood components. The 8th International IUFRO Wood Drying Conference. 24–29 August, Brasov, Romania, pp 156–158.

[10] Sorzano, C.O.S., Thévenaz, P. and Unser, M. (2005) Elastic Registration of Biological Images Using Vector-Spline Regularization. IEEE Transactions on Biomedical Engineering. In press.

[11] Comsol AB. Tegnérgatan 23 SE-11140 Stockholm. Home page: www.comsol.se

Paper V

J Wood Sci (2006)
DOI 10.1007/s10086-005-0724-9

ORIGINAL ARTICLE

Nils Lundgren · Olle Hagman · Jan Johansson

Predicting moisture content and density distribution of Scots pine by microwave scanning of sawn timber II: evaluation of models generated on a pixel level

Received: October 18, 2004 / Accepted: March 14, 2005

Abstract The purpose of this study was to use images from a microwave sensor on a pixel level for simultaneous prediction of moisture content and density of wood. The microwave sensor functions as a line-scan camera with a pixel size of 8 mm. Boards of Scots pine (*Pinus sylvestris*), 25 and 50 mm thick, were scanned at three different moisture contents. Dry density and moisture content for each pixel were calculated from measurements with a computed tomography scanner. It was possible to create models for prediction of density on a pixel level. Models for prediction of moisture content had to be based on average values over homogeneous regions. Accuracy will be improved if it is possible to make a classification of knots, heartwood, sapwood, etc., and calibrate different models for different types of wood. The limitations of the sensor used are high noise in amplitude measurements and the restriction to one period for phase measurements.

Key words Microwave scanning · Wood · Density · Moisture content

Introduction

There is an increasing need in the wood industry for precision on-line measurement of moisture content (MC) and density. This information could be used for individual drying of the boards or for quality and stress grading. A microwave signal will be affected by several properties such as density, MC, temperature, and grain angle when it is transmitted through wood. These properties have influence on attenuation, phase shift, and polarization of the signal. Moisture measurements can be improved by combining measurements of both attenuation and phase shift[1] or measurements of phase shift at two frequencies.[2] Another possibility is to use measurements of different microwave parameters for concurrent prediction of several wood properties from one noninvasive measurement. This has been done, for example, by Bolomey et al.[3] and Choffel et al.[4]

The present study is based on work by Johansson et al.[5] in which multivariate models to predict MC and density for boards of Scots pine (*Pinus sylvestris*) were calibrated using average values over the boards. The purpose of the present work was to evaluate and develop this method with models generated on a pixel level wherein each pixel was treated as one observation.

N. Lundgren (✉) · O. Hagman · J. Johansson
Division of Wood Technology, Luleå University of Technology, Skellefteå Campus, Skellefteå SE-931 87, Sweden
Tel. +46-910-58-5707; Fax +46-910-58-5399
e-mail: nils.lundgren@ltu.se

Theory

Consider a plane electromagnetic wave propagating through wood in the z-direction. If losses due to conductance and reflections are ignored, the attenuation and wavelength are governed by the factor $e^{-\gamma z}$, with the complex propagation constant,[6]

$$\gamma = j\omega\sqrt{\varepsilon^* \varepsilon_0 \mu' \mu_0} = \alpha + j\beta, \tag{1}$$

where ω is the angular frequency of the wave, $\varepsilon^* = \varepsilon' - j\varepsilon''$ is the complex dielectric constant, $\mu' \approx 1$ is the relative permeability of wood, and $\varepsilon_0 = 1/(\mu_0 c_0^2)$ is the permittivity of free space where c_0 is the speed of light in free space.

The real part of γ can be defined as an attenuation constant,

$$\alpha = \frac{\omega}{c_0}\left[\frac{\varepsilon'}{2}\left(\sqrt{1+\tan^2\delta}-1\right)\right]^{\frac{1}{2}} \tag{2}$$

and the imaginary part of γ as a phase constant,

$$\beta = \frac{\omega}{c_0}\left[\frac{\varepsilon'}{2}\left(\sqrt{1+\tan^2\delta}+1\right)\right]^{\frac{1}{2}} \tag{3}$$

where $\tan\delta = \varepsilon'/\varepsilon''$ is defined as the loss tangent.

For low moisture content ($\tan\delta << 1$) it has been shown by King[7] that these expressions for α and β can be simplified from binomial expansion of Eq. 1:

$$\gamma = j\beta_0\sqrt{\varepsilon'(1-j\tan\delta)} = j\beta_0\sqrt{\varepsilon'}\left[1-j\frac{\tan\delta}{2}+\frac{\tan^2\delta}{8}+\ldots\right] \quad (4)$$

where $\beta_0 = 2\pi/\lambda_0$ is the phase constant of air and λ_0 is the wavelength of the electromagnetic wave in air. Thus Eqs. 3 and 4 can be approximated as

$$\alpha = \frac{1}{2}\beta_0\sqrt{\varepsilon'}\tan\delta \quad (5)$$

and

$$\beta = \beta_0\sqrt{\varepsilon'}\left(1+\frac{1}{8}\tan^2\delta\right). \quad (6)$$

King[7] suggested that α should be used for prediction of MC and β should be used for prediction of density. However, tabulated values from Torgovnikov[8] plotted in Figs. 1 and 2 show that both ε' and $\tan\delta$ are correlated to wood density and moisture content. The complex relation between microwaves and wood properties indicates that multivariate methods are beneficial for simultaneous prediction of moisture content and dry density.

Material and methods

The study was based on 96 boards of Scots pine (*Pinus sylvestris)*, 48 with a cross section 150 × 50 mm and 48 with a cross section 150 × 25 mm. The 48 boards with a thickness of 50 mm consisted mainly of heartwood, while the amount of heartwood in the boards with a thickness of 25 mm varied from 0% to 100%. Examples of these variations are shown in Fig. 3.

The boards originated from two different parts of Sweden. Half of the boards of each dimension were sawn at a mill in Skellefteå (Wallmarks) situated in the northern part of Sweden. The other 48 boards were sawn at a mill in Ljungby (Vida), situated in the southern part of Sweden. Before scanning, each board was cut to a length of 1600 mm, and a 25-mm hole was drilled as a reference point.

The moisture content (MC) in some of the freshly sawn boards exceeded the dynamic measurement range of the microwave scanner. There was also a large variation in the moisture distribution at higher moisture contents. Therefore, this study is limited to measurements below the fiber saturation point (FSP), which corresponds to a MC of approximately 30%. The boards were dried from green condition to 7% MC. At three different moisture levels, the boards were removed from the kiln and scanned with microwaves and X-rays. Figure 4 shows an X-ray image of the scanned region from one board. The light regions in the image represent areas with high density.

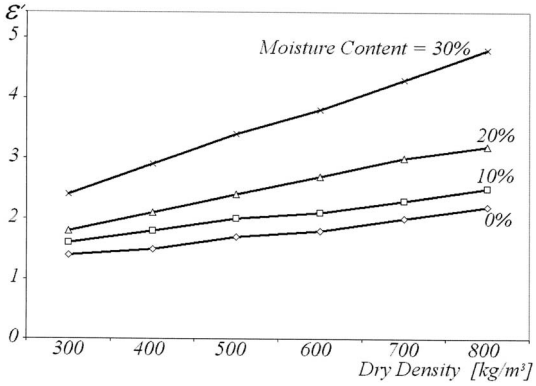

Fig. 1. Real part of the dielectric constant (ε') perpendicular to the grain as a function of dry density and moisture content at 10 GHz (data from Torgovnikov)[8]

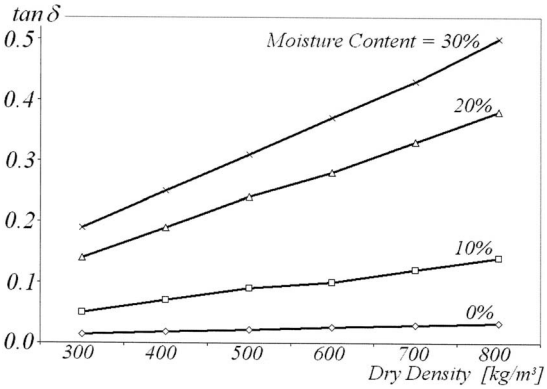

Fig. 2. Loss tangent ($\tan\delta$) perpendicular to the grain as a function of dry density and moisture content at 10 GHz (data from Torgovnikov)[8]

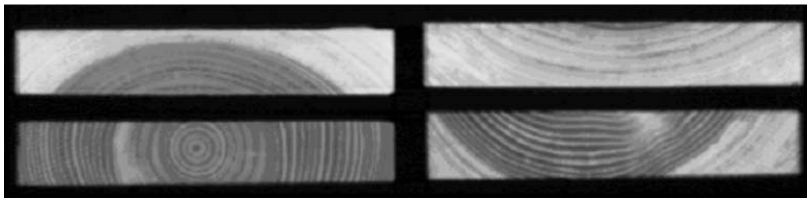

Fig. 3. Cross sections from computed tomography (CT) scanning of four different boards in green condition. The high moisture content (MC) gives high density in the sapwood compared with heartwood

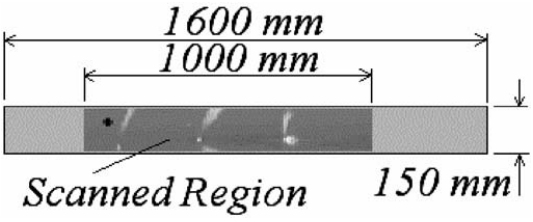

Fig. 4. Image of one board from the CT scanner after transformation to two dimensions. A length of 1 m of each board was scanned

Drying

The freshly sawn boards were dried in a small kiln. In order to determine the average moisture content for the boards, they were weighed after each drying step. The target moisture content at each drying step was set to 20%, 12%, and 7%. After the last scanning, the dry weight of each board was estimated from five samples taken at even intervals along the board. The moisture content was assumed to be evenly distributed in the boards after the last drying to 7% MC. From that assumption the dry density in each pixel was calculated using the density measured in a computed tomography (CT) scanner. The dry density was used to calculate MC in each pixel from the measured density in the remaining observations. No corrections were made for shrinkage, because the maximum shrinkage was less than one pixel.

X-ray scanner

A CT scanner (Siemens Somatom ART) was used to scan the boards every 8 mm with a 5-mm-wide X-ray beam. The scanner measures density in three dimensions with high accuracy.[9] The images from the CT scanner were transformed to two dimensions by taking mean values of density variations through the boards.

Microwave scanner

Using a transverse feeding direction, the boards were scanned with a microwave sensor (Satimo 9.375 GHz) in combination with a computer and a conveyer described by Johansson.[10] The system produces images with a pixel size of 8×8 mm. The sensor is based on electromagnetic transmission through the wood and a modulated scattering technique, which is described by Bolomey and Gardiol.[11] The sensor measures the real and imaginary part of the electromagnetic field in two orthogonal polarization angles. From these variables, the linear and decibel amplitude and the phase shift were calculated. All of these five variables were measured and calculated in four different polarization angles: horizontal, vertical, plus 45 degrees and minus 45 degrees. This gives a total of 20 variables describing attenuation, phase shift, and polarization of the transmitted field.

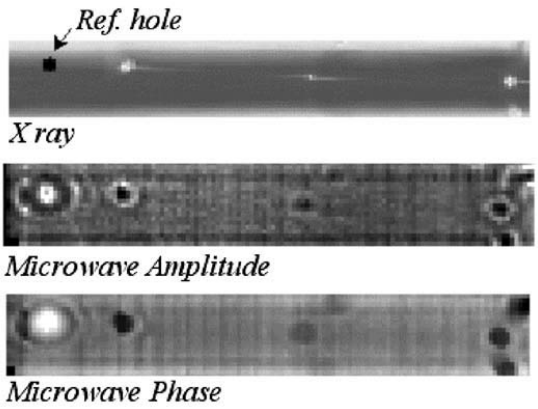

Fig. 5. Example of images from X-ray scanning and microwave measurements on phase shift and amplitude of one board. Several knots are visible in the images

Figure 5 shows an example of attenuation and phase shift measured in one direction with the microwave sensor compared with density measured with X-rays.

Multivariate models

Models for prediction of dry density and moisture content were calibrated using partial least squares (PLS) regression as described by Martens and Næs[12] using the Simca P+ 10.0 software from Umetrics. Average dry density and MC of the wood were calculated from CT images for each pixel in the microwave image and were used as response variables. The variables from the microwave scanner were used as predictors. Each variable was centered and scaled to unit variance. Using the PLS algorithm means that uncorrelated principal components (PC) are formed as linear combinations of the correlated variables from the microwave scanner. The numbers of PCs were optimized by the software to two or three depending on the response variable. The available amount of memory restricted the number of observations to 200 randomly selected pixels from each board. No distinction was made as to whether the points came from heartwood, sapwood, or knots. About 80% of the observations were used as a training set for calibrating the models. The remaining, randomly selected observations were used as a test set for verification of the models. This gave about 23 000 observations in the training set and 5700 observations in the test set for each thickness.

Results

Moisture content

Models based on values from randomly selected pixels turned out to be weak and noisy with a correlation coeffi-

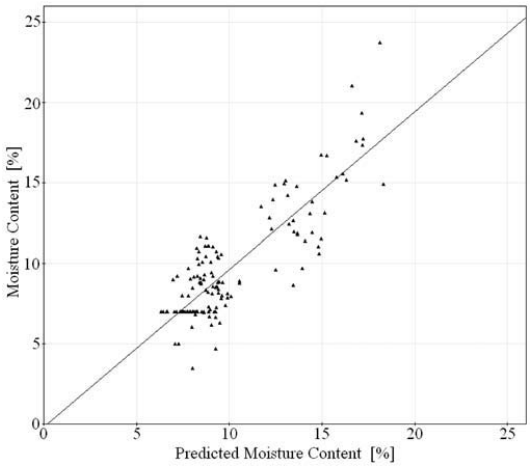

Fig. 6. Measured versus predicted moisture content for 25-mm boards based on mean values over five regions from each board

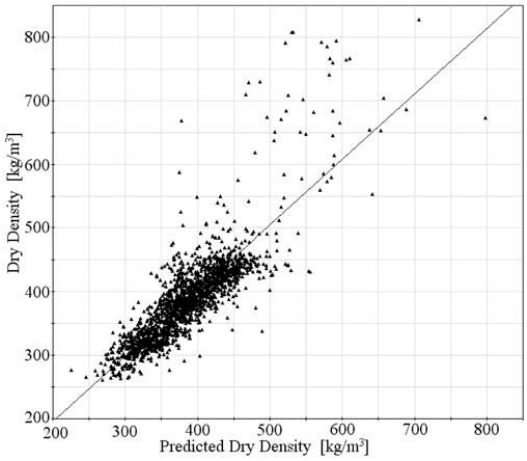

Fig. 8. Measured versus predicted dry density for 25-mm boards based on values from randomly selected pictures

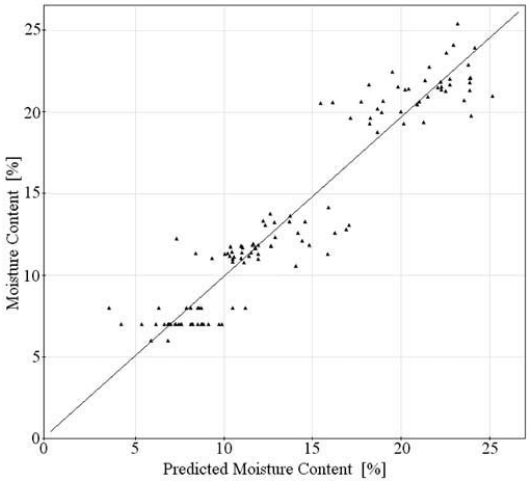

Fig. 7. Measured versus predicted moisture content for 50-mm boards based on mean values over five regions from each board

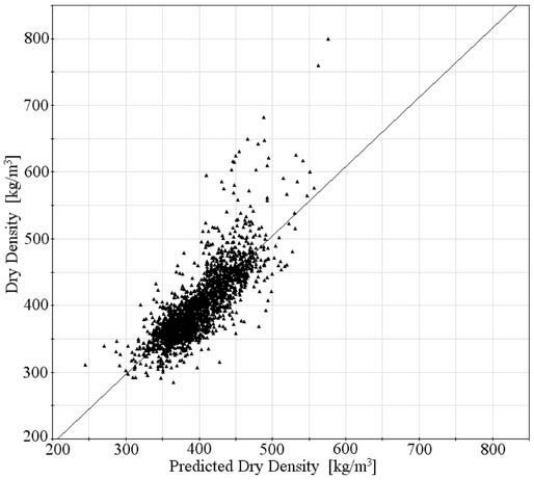

Fig. 9. Measured versus predicted dry density for 50-mm boards based on values from randomly selected pixels

cient R^2 of approximately 0.20. To avoid this problem, the models for MC shown in Figs. 6 and 7 are based on average values over five homogeneous regions from each board with sizes varying from 0.0025 to 0.015 m^2. This reduces the number of observations for each thickness to about 550 in the training set and 130 in the test set used for the verification that is shown in the figures. The model for prediction of MC for 25-mm boards has a correlation coefficient $R^2 = 0.72$ and estimated root mean square error RMSEP = 1.8% MC. The model for 50-mm boards has $R^2 = 0.90$ and RMSEP = 2.0% MC.

Density

The models for prediction of dry density shown in Figs. 8 and 9 are based on values from 200 pixels in each board. The model for prediction of dry density for 25-mm boards has $R^2 = 0.71$ and RMSEP = 38 kg/m^3. The model for 50-mm boards has $R^2 = 0.64$ and RMSEP = 32 kg/m^3. The randomly selected pixels also contain some high-density values from knots that the model is not able to describe properly.

Discussion

The 50-mm boards consisted mainly of heartwood, with the exception of three boards that showed up as outliers in the model and were excluded from the dataset. One board was also excluded because of rot. It would have been desirable to classify the amount of sapwood in the 25-mm boards in order to find correlations. This was not done, but five boards consisting mainly of heartwood were identified as outliers in the dataset and were excluded. There was no significant difference between the two groups of boards originating from different parts of Sweden.

The variables describing phase shift are periodic and the variation was more than one period between measurements at different MC. This made it impossible to compare these measurements without calibration to a known reference. Therefore, models for MC were mainly based on variables describing amplitude. It can be deduced from Eq. 5 in combination with Fig. 2 that MC should have a strong influence on amplitude. However, reflection and scattering at boundaries where the changes in dielectric properties are large caused large local variations in amplitude. This explains why models for MC could not be based on pixel values. Variations in phase shift caused by differences in dry density were less than one period. Therefore, the variables describing phase shift could be used as strong predictors for dry density.

Conclusions

A good model for prediction of density can be calibrated from pixel values. It is possible to calibrate a satisfactory model for moisture content from average values over homogenous regions, but not from pixel values. Edges, knots, and other regions where properties change will cause errors in the models. These errors can be reduced by taking the average over a large area. If algorithms that classify the regions could be created, it would be possible to use different prediction models for different regions. An improved microwave sensor for wood scanning should measure phase shift over several periods, for example, by using two frequencies. It should also produce less noise in the amplitude measurements.

References

1. Kraszewski A (1980) Microwave aquametry – a review. J Microwave Power 15:209–220
2. Zhang Y, Okamura S (1999) New density-independent moisture measurement using microwave phase shifts at two frequencies. IEEE Trans Instru Measurement 48:1208–1211
3. Bolomey JC, Cottard G, Lhiaubet GC, Ciccitelli J, Portala JF (1992) On-line control in wood and paper industries by means of rapid microwave linear sensor. Proceedings of 22nd European Microwave Conference, Espoo, 24–27 Aug 1992, Topic 16
4. Choffel D, Goy B, Martin P, Gapp D (1992) Interaction between wood and microwaves – automatic grading application. In: Lindgren O (ed) 1st International Seminar on Scanning Technology and Image Processing on Wood. Luleå University, Skellefteå, Sweden, pp 1–8
5. Johansson J, Hagman O, Fjellner B-A (2003) Predicting moisture content and density distribution of Scots pine by microwave scanning of sawn timber. J Wood Sci 49:312–316
6. Von Hippel A (1954) Dielectrics and waves. Wiley, New York
7. King RJ (1978) Microwave electromagnetic nondestructive testing of wood. Proceedings of 4th Symposium on Nondestructive Testing of Wood. Washington State University, Pullman, pp 121–134
8. Torgovnikov GI (1993) Dielectric properties of wood and wood-based materials. Springer, Berlin Heidelberg New York
9. Lindgren LO (1991) Medical CAT-scanning: X-ray absorbtion coefficients, CT-numbers and their relation to wood density. Wood Sci Technol 25:341–349
10. Johansson J (2001) Property predictions of wood using microwaves. Licentiate Thesis, Luleå University of Technology, LIC 2001:35
11. Bolomey JC, Gardiol FE (2001) Engineering applications of the modulated scatterer technique. Artech House
12. Martens H, Næs T (1989) Multivariate calibration. Wiley, New York, pp 22–163

Paper VI

Wood and Fiber Science 39(1)

PREDICTING THE STRENGTH OF NORWAY SPRUCE BY MICROWAVE SCANNING: A COMPARISON WITH OTHER SCANNING TECHNIQUES

Nils Lundgren[1]
Ph.D. Student

Mattias Brännström[1]
Ph.D. Student

Olle Hagman[1]
Professor

and

Johan Oja[1, 2]
Associate Professor

1. Luleå University of Technology, Division of Wood Technology, Skellefteå Campus, Skeria 3, SE-931 87 Skellefteå, Sweden

2. SP Swedish National Testing and Research Institute, Skeria 2, SE-931 87 Skellefteå, Sweden

ABSTRACT

In this study, 90 boards of Norway spruce (*Picea abies* (L.) Karst.) sized 48 x 148 mm in cross section, have been examined using different scanning and measurement techniques. All of the boards were originating from a sawmill located in southern Finland. Planar X-ray scanning, microwave scanning and grain-angle measurement have been performed. In addition, strength and elastic properties were assessed for each piece by four point bending. The purpose of the study was to relate the potential of microwave scanning compared to other, industrially available techniques and to explain the physiological background of the microwave responses. The results show that the microwave signal, after transmission through wood, contains information about the bending strength and the modulus of elasticity. The correlation to density is a key factor. Annual ring width was also found to be correlated both to microwave measurements and strength properties.

Keywords: wood, spruce, grading, microwave, x-ray, scanning, modulus of elasticity (MOE), modulus of rupture (MOR)

INTRODUCTION

There are several factors that influence the strength properties of sawn lumber. The variation that occurs between timbers of different species can usually be graded before the logs are taken into the sawmill. However, there is also a variation within the same species and even within a single tree. By visual grading of the sawn boards with either manual or automatic systems, it is possible to sort the material. Mechanical grading machines that measure bending stiffness are commonly used for strength prediction. The drawback of this method is the need for physical contact and moving parts in the machines.

According to Dinwoodie (2000), the correlation coefficient between density and compression strength is 0.9. This correlation has been used to predict strength from x-ray measurements by Oja et al. (2000) for classification of logs and by Schajer (2001) for classification of sawn lumber. Average density alone does not explain all the variation in strength. Leban and Haines (1999) have, for example, shown that there is a correlation in annual ring width and elasticity for larch. Such information about the structure can be obtained from x-ray measurements but x-rays can not be used to separate the dry wood density from moisture. Hence there still remains a need to develop other sensors that measure properties of wood.

Several studies have shown the potential of microwave scanning for prediction of density, moisture content and grain angle (GA) of a timber specimen. How variations in moisture content or dry density effects a transmitted microwave signal has been described by Lundgren et al. (2006) and by Hansson et al. (2005), among others. Shen et al. (1994) proposed a microwave method for measuring grain angle that has been verified by Sjödén et al. (2005). The influence of grain angle on the microwave signal has been used by Leicester and Craig (1996) to detect knots in combination with a conventional mechanical stress grader. Microwave measurements have also been combined with X-rays for strength grading in the Finnograder, which has been tested together with two bending machines and one machine based on the speed of sound in a study by Boström (1994). Boström concludes that the best prediction of bending strength was attained from the bending machine. However, he notes that the Finnograder is less sensitive to grading speed and that a better yield might be achieved by adjusting the setting values. The response from a microwave sensor has been related to elasticity by Choffel et al. (1992) and to bending strength in studies by Johansson (2001) and by Lundgren (2005).

The aim of the present study was to compare the microwave sensor used by Johansson and Lundgren to other scanning techniques for strength grading of sawn timber. Another aim was to quantify the correlation in the measurements from the microwave scanner with grain angle and density measurements.

MATERIAL AND METHODS

The timber raw material chosen for this study was Norway spruce (*Picea abies* (L.) Karst.) from southeastern Finnish stands. The logs where randomly selected from one sawmill on two different occasions. There was a natural variation within the material, since both butt and middle logs fulfilled the requirements of a predefined top diameter of about 200 mm measured 100 mm from the top of the log. Two center pieces were straight sawn from each log to the nominal dimension 50 X 150 mm and planed to 48 X 148 mm. This resulted in 90 boards with lengths between 3.5 and 5.5 meters. A conventional

channel kiln was used for drying of the boards. After drying, the boards were stored for several months in an even climate so that the moisture distribution could be assumed to be uniform during scanning.

The measurements were performed on different occasions. On each of these the weight of each board was recorded for moisture content correction. Grain angle was measured by a laser scattering technique and the tracheid effect as described by Nyström (2003). After sawing, drying and planing, a scan was performed on the sapwood side of each board. This measurement was done in the center of the board, roughly above the pith. The values represent the median grain angle for each board. X-ray scanning was done as planar X-ray in the longitudinal feeding direction on each board by a Microtec Golden Eye 706 strength-grading machine. The scanning speed was between 80 and 90 m/min.

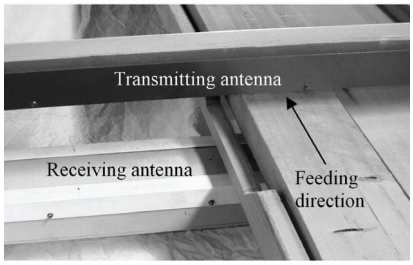

FIG. 1. Microwave scanner.

The boards were scanned with a microwave sensor from Satimo working at 9.375 GHz in combination with a computer and a conveyor as described by Johansson (2001). The scanner shown in Fig. 1 functions as a line-scan camera with a resolution of 8 mm. For the present study the boards were manually fed through the scanner with a speed of approximately 10 m/min. Each line in the resulting image represents average values from measurements covering a length of between 50 and 100 mm of the board. The sensor is based on electromagnetic transmission through the wood and modulated scattering technique, which is described by Bolomey and Gardiol (2001). The electromagnetic field was measured in two orthogonal polarization angles. From the measured variables the amplitude and the phase shift of the signal were calculated. Differences in the sensors were minimized by subtracting a measurement without an object in the scanner. The measured variables can be reduced to three components that describe amplitude, phase shift and polarization of the transmitted field. Finally, the modulus of rupture (MOR), the local and the global modulus of elasticity (MOE) in edgewise four-point loading were tested according to the European standard EN408 (2003). The test was performed on full-sized beams. It was recorded whether the most serious defects influencing strength were on the top or the bottom side of the board. A mean value for the annual ring width (ARW) was taken from a cross section close to the point of failure.

Multivariate modeling was done using Partial Least Squares (PLS) regression (Geladi and Kowalski 1986) and the software Simca P 10.0.2.0 (Anon. 2002) from Umetrics. The data were divided into a training set consisting of 80% of the observations, which the models were based upon, and a test set (the remaining 20%) to which the models were applied. Key figures used to evaluate the models are the goodness of fit (R^2) when the models were applied to training set and test set and the goodness of prediction (Q^2).

RESULTS

TABLE 1. *Average values of wood properties.*

	Density [kg/m^3]	ARW [mm]	MOR [MPa]	Local MOE [MPa]	Global MOE [MPa]	MC [%]
Mean	452	2.1	47	11500	10800	11.9
Std. Dev.	31	0.6	11.7	1560	1965	0.3

Three observations were removed from the data set prior to modeling due to scanning errors (first board in the microwave scanning sequence) and missing values. Average values and variation in some of the variables for the remaining observations are shown in Table 1. The correlation matrix in Table 2 shows that local MOE has a higher correlation with amplitude and phase from microwave measurements than with X-ray scanning.

TABLE 2. *Correlation matrix for the measured variables (R^2 values).*

	Amplitude	Phase	X-ray	ARW	GA	MOR	Local MOE
Amplitude	1.00						
Phase	0.81	1.00					
X-ray	0.79	0.86	1.00				
ARW	0.21	0.20	0.17	1.00			
GA	0.001	0.004	0.000	0.006	1.00		
MOR	0.32	0.26	0.17	0.41	0.08	1.00	
Local MOE	0.45	0.40	0.32	0.36	0.01	0.62	1.00

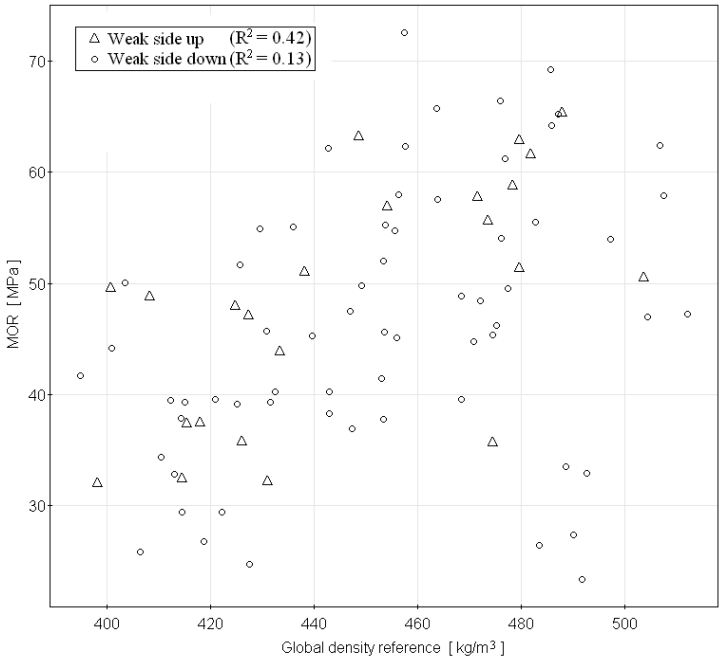

FIG. 2. Modulus of rupture (MOR) plotted against global density of the tested boards.

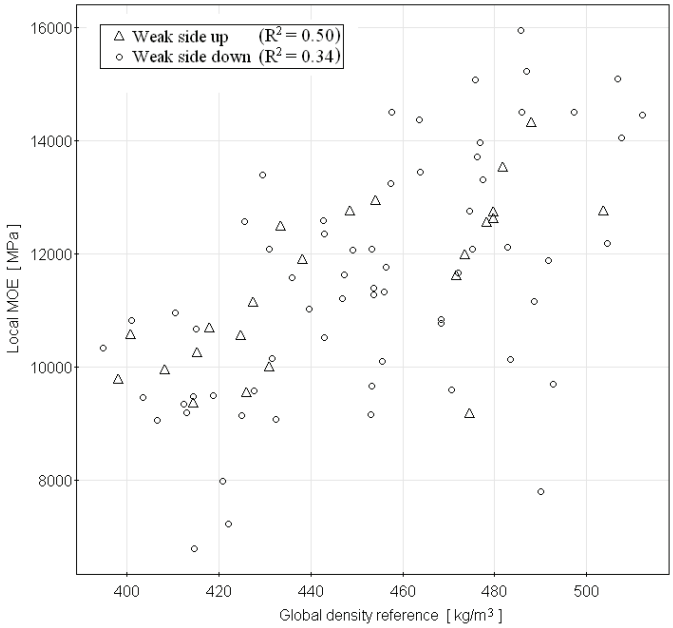

FIG. 3. Local Modulus of Elasticity (MOE) plotted against global density of the tested boards.

Since the result from destructive bending is affected by local defects, there will be deviations from the correlation to average density, as can be seen in Figs. 2 and 3. This was the case both when the largest defect was turned down (circles) and when it was turned up (triangles). Fig. 4 shows how some of the remaining variables are correlated to MOR and MOE.

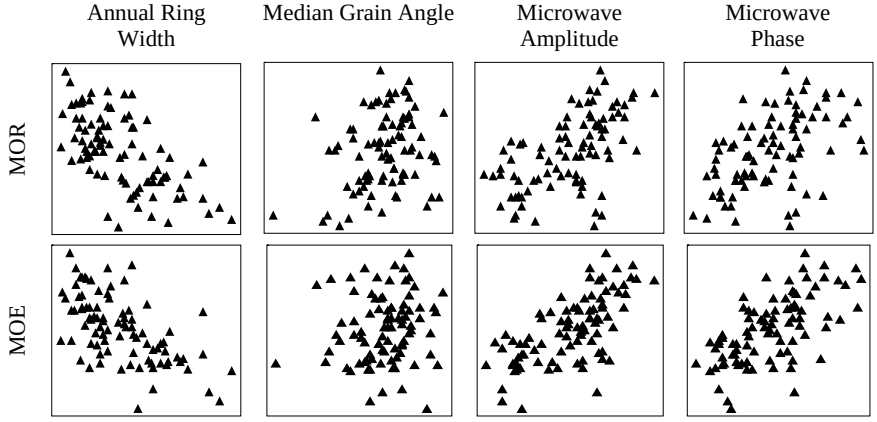

FIG. 4. Scatter plots for some of the variables in relation to modulus of rupture (MOR) and modulus of elasticity (MOE).

A principal component analysis (PCA) was performed in order to find correlations. The result is shown in Fig. 5 where the horizontal component, P1, explains most of the variation with $R^2 = 0.64$ and $Q^2 = 0.56$. These values increase to $R^2 = 0.80$ and $Q^2 = 0.63$ when P1 is combined with P2. The vertical component, P2, indicates a correlation in grain angle, annual ring width and MOR. However, Q^2 values are low, which means that this can not be generalized to other sets of data. The signal from the transmitting antenna was mainly polarized in one direction. Polarization was calculated as the relation between the signals in two orthogonal directions, but the amplitude in one of these directions was close to zero. Therefore, the measured signal in that direction consisted mainly of noise, and the polarization variable is strongly correlated to attenuation. No reliable model for prediction of grain angle from the microwave measurements could be established. Variations in moisture content were small, and hence the response, both in phase and in attenuation, was mainly governed by density.

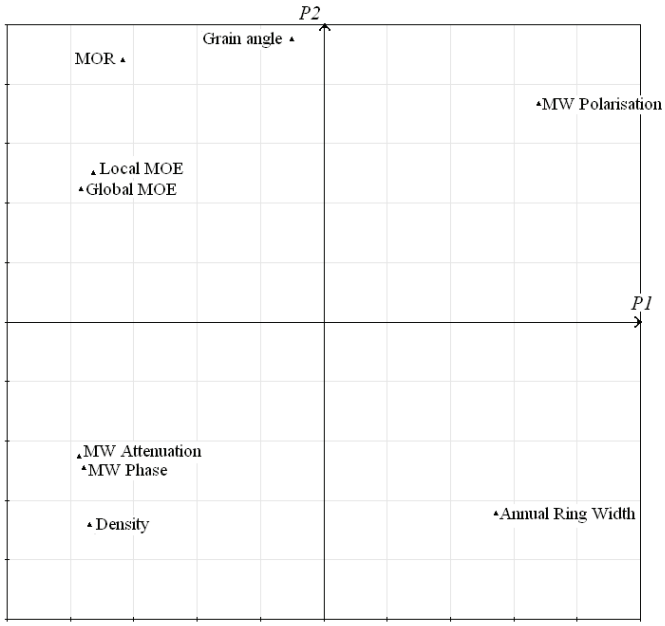

FIG. 5. Loading plot generated by Principal Component Analysis (PCA). The plot shows how microwave (MW) variables are correlated to other variables.

The ability of different responses to predict dry density was compared, and the result is presented in Table 3. The microwave variable with the strongest correlation to density was phase. The different models for prediction of local modulus of elasticity are compared in Table 4.

TABLE 3. *Density prediction using microwave (MW) response compared to X-rays.*

	Training set R^2 [%]	Training set Q^2 [%]	Test set R^2 [%]
X-ray	97.3	97.1	98.9
MW Amplitude	84.0	83.7	70.1
MW Phase	88.6	88.2	77.3

TABLE 4. *Prediction of local modulus of elasticity (MOE) using microwave (MW) response compared to X-rays in combination with grain angle and annual ring width.*

	Training set R^2 [%]	Training set Q^2 [%]	Test set R^2 [%]
MW Amplitude	42.5	40.7	55.2
MW Phase	36.6	35.8	51.3
X-ray	29.3	27.2	49.5
GA	3.2	-2.6	-
ARW	33.4	30.6	55.4
Amplitude, ARW	54.2	52.0	64.7
Amplitude, GA	43.2	38.6	52.0
Amplitude, ARW, GA	54.5	51.9	62.4
Phase, ARW	50.2	47.9	64.7
Phase, GA	37.2	33.4	44.8
Phase, ARW, GA	50.3	47.9	60.9
X-ray, ARW	46.4	43.6	64.5
X-ray, GA	32	26.6	42.4
X-ray, GA, ARW	47.6	44.2	60.1

DISCUSSION

As expected, a high correlation was found between x-rays and density. The correlation between density and MOE/MOR was lower for the boards where the weak side (largest defect) was turned down during the destructive bending. This was also expected, since the size and shape of defects on the tensile side affect the results more than defects on the compression side.

Some observations with high density but low elasticity were found in the training set used to calibrate the models. This could explain why better models for prediction of MOE were obtained from microwave scanning than from x-rays since properties other than average density are important. All models were improved when annual ring width was added as a variable. Annual ring width in combination with either microwaves or x-rays gave the best prediction when the models were applied to the test set. Microwaves in combination with annual ring width gave the highest correlation coefficients for the training set.

Some knots can be identified in the images obtained by microwave scanning, but if the aim is to find knots, a higher frequency should be used, since resolution in that case is more important than penetration depth.

CONCLUSIONS

The ability to predict elasticity from microwave scanning is mainly due to the correlation between density and elasticity but there is more information related to strength and elasticity in the microwave signal than can be obtained from density alone. All models for prediction of elasticity were improved when information about annual ring width was added. The microwave sensor that was used in this study cannot measure variations in grain angle but none of the models were improved when information about grain angle was added.

ACKNOWLEDGEMENTS

The project was financed by the SkeWood program, the Swedish Agency for Innovation Systems (Vinnova) and the Kempe foundation.

REFERENCES

ANON. (2002). Simca-P (Version 10.0.2.0). [Computer software]. Sweden, Umeå: Umetrics AB. Home page: http://www.umetrics.com/

BOLOMEY J. C. AND F. E. GARDIOL. 2001. Engineering applications of the modulated scatterer technique. Artech House Inc. ISBN: 1-58053-147-42004.

BOSTRÖM L. 1994. Machine Strength Grading - Comparison of Four Different Systems. Swedish National Testing and Research Institute, SP Report 1994:49.

CHOFFEL D., B. GOY, P. MARTIN AND D GAPP. 1992. Interaction between wood and microwaves – automatic grading application. In: Lindgren O. (ed) 1st International Seminar on Scanning Technology and Image Processing on Wood. Luleå University, Skellefteå, Sweden, pp 1.8.

DINWOODIE J. M. 2000. Timber: Its nature and behaviour. 2nd ed. E & FN Spon, London.

EUROPEAN STANDARD. 2003. Timber structures - Structural timber and glued laminated timber - Determination of some physical and mechanical properties. EN408: 2003.

GELADI P. AND B. R. KOWALSKI. 1986. Partial least squares regression: A tutorial. Analytica Chimica Acta 185(1986):1–17.

HANSSON L., N. LUNDGREN, A. L. ANTTI AND O. HAGMAN. 2005. Microwave penetration in wood using imaging sensor. Measurement 38:15–20.

JOHANSSON J. 2001. Property Predictions of Wood Using Microwaves. Licentiate Thesis, Luleå University of Technology. LIC 2001:35.

LEBAN J. M. AND D. W. HAINES. 1999. The modulus of elasticity of hybrid larch predicted by density, rings per centimeter and age. Wood Fiber Sci. 31(4):394–402

LEICESTER R. H. AND A. S. CRAIG. 1996. “Microwave scanners in stress grading operations”. 25th Forest products research conference. CSIRO division of forestry and forest products, Clayton, Victoria, Australia.

LUNDGREN N. 2005. Modelling Microwave Measurements in Wood. Licentiate Thesis, Luleå University of Technology. LIC 2005:61.

———, O. HAGMAN AND J. JOHANSSON. 2006. Predicting moisture content and density distribution of Scots pine by microwave scanning of sawn timber II: evaluation of models generated on a pixel level. J Wood Sci. 52:39-43.

NYSTRÖM J. 2003. Automatic measurement of fiber orientation in softwoods by using the tracheid effect. Comput Electron Ag. 41(1–3):91–99.

OJA J., S. GRUNDBERG AND A. GRÖNLUND. 2000. Predicting the strength of sawn products by X-ray scanning of logs: A preliminary study. Wood Fiber Sci. 32(2):203–208.

SCHAJER G. S. 2001. Lumber strength grading using x-ray scanning. Forest Prod. J. 51(1):43–50.

SHEN J., G. SCHAJER AND R. PARKER. 1994. Theory and practice in measuring wood grain angle using microwaves. IEEE Transactions on instrumentation and measurement. 43(6):803-809.

SJÖDEN T., B. NILSSON AND S. NORDEBO. 2005. Microwave modelling and measurements for early detection of spiral grain in wood. 14th International Symposium on Nondestructive Testing of Wood, May 2nd to 4th 2005, Hannover, Germany.

Paper VII

An Online Microwave Scanner for Sawn Wood

Nils Lundgren, Vasily Gerasimov, Tatyana Kozlova, Evgeny Zorin
Luleå University of Technology, Skellefteå Campus, nils.lundgren@ltu.se

Abstract

This article presents the results from preliminary tests of a microwave scanner. The ability to measure variations in density and moisture content (MC) has been related to results from previous measurements using the same type of sensor. Density variations gave a response that was similar to the response from the old sensor. Variations in moisture content were too small in each piece to be separated from measurement noise. The results show that the main benefit with the new sensor is increased scanning speed.

Introduction

There are several studies showing the potential of microwave scanners in wood industries. Microwaves can be used for online prediction of dry basis moisture content (MC) and density distribution in sawn lumber. The interactions have been investigated by Hansson et. al (2005) among others. Response from a microwave sensor has also been related to mechanical properties in the wood, for example by Choffel et. al (1992). The purpose of the present work was to evaluate a new microwave scanner, based on the same technique as used by Hansson. This new scanner is developed for online quality control of stone wool but has a potential for wood scanning.

Material

Four pieces of wood, shown in Fig.1 were scanned. They were chosen in order to investigate the response to variations in density, MC and thickness. Further information about dimensions and weight is provided in Appendix I.

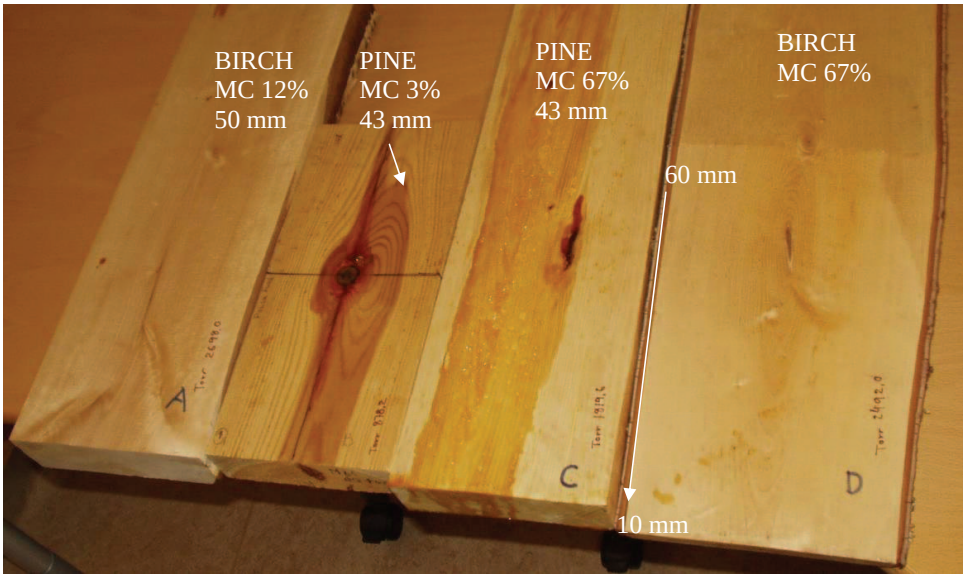

Fig. 1. The four pieces that were scanned, their average moisture content (MC) and thickness.

Experimental Design

The aim was to relate the distribution of dry density and moisture to the response from the microwave scanner.
The following measurements were made;

1. CT scanning and weighting.
   Skellefteå 2006-05-09.
2. Microwave scanning.
   Courtaboeuf 2006-05-11.
3. CT-scanning (no scale available).
   Skellefteå
   2006-05-12.
4. Drying at 102° C for 24 hours.
5. CT scanning and weighting.
   Skellefteå 2006-05-20.
6. Drying to zero MC.
7. CT scanning and weighting
   Skellefteå 2006-06-21.

The measurements in points 4 and 5 were performed to get a first overview of the data but have not been used for the analysis in this report since there was moisture remaining in the wood. The CT-scans made at point 3 and 7 were used to estimate the distribution of moisture and dry density in the wood. Resins were transported to the surface, especially for the fresh sawn pine (C), during drying. This means that the moisture distribution calculated from CT images also includes resin losses. Weight and estimated average moisture content at the different occasions are presented in appendix I.

Microwave Scanning

A microwave scanning system, developed for quality control of stone wool by Satimo (Anon 2006), was used for the microwave measurements. Fig. 2 shows how the transmitting and receiving antennas are positioned in the scanner while Fig. 3 illustrates how defects can be detected. The system is based on modulated scattering technique as described by Bolomey and Gardiold (2001). The pieces of wood were placed on Styrofoam and manually fed through the scanner as is shown in Fig. 4. Real and imaginary parts of the transmitted field were continuously measured at every 10^{th} mm with a speed of approximately 30 lines per second.

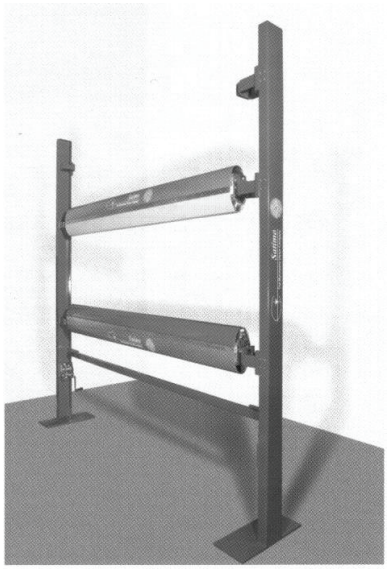

Fig. 2. Microwave antennas

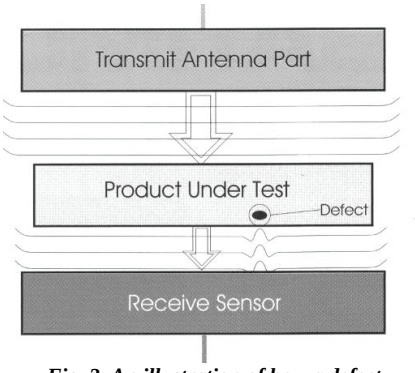

Fig. 3. An illustration of how a defect changes the field.

Fig. 4. Each piece of wood was placed on Styrofoam and manually fed through the scanner.

Results for Density

Fig. 5 shows the raw data images of piece B (Polish pine) obtained from the new and old sensors. Further comparisons of measurements on this piece are shown in appendix II. Some measurements on piece D (with varying thickness) are shown in appendix III. The influence from thickness on these measurements is surprisingly small. This could mean that the signal does not penetrate the wood. It could also be an effect from moisture condensed on the surface since the pieces were wrapped in plastic foil. The main impression from the new sensor in comparison with the old one is that;

- The new sensor gives lower quality images. This could be caused by varying feeding speed, disturbances from hands and other body parts or by fewer measurement points.
- Measurements are done in real time.

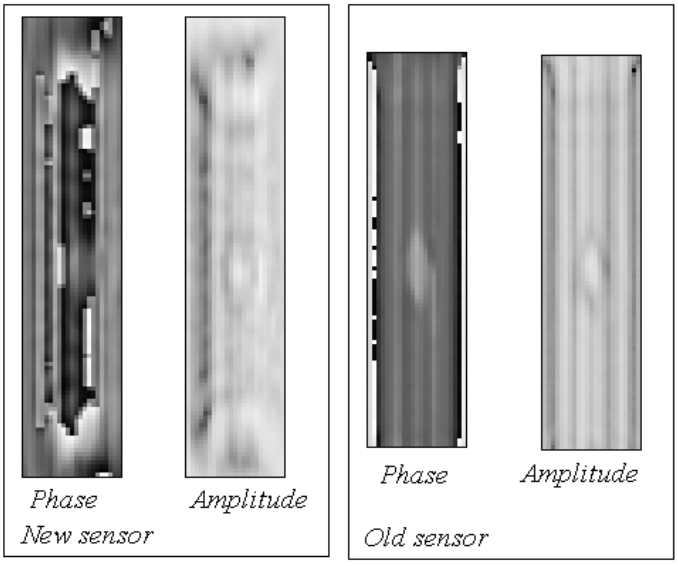

Fig. 5. Measurements on Polish pine with the new sensor compared to measurements with the old sensor.

Results for Moisture

Variations in the images due to boundary effects and other disturbances in each piece exceed the variations caused by moisture. It was also difficult to separate moisture distribution in the CT images of the green pieces from resins that were transported to the surface during drying. Hence there is no certain result about the ability to predict moisture content but the main impression from this study is that this ability is approximately the same as with the old sensor.

Conclusions

The ability to predict density or moisture content from measurements with the new and old sensor seems to be approximately equal. Hence the quality of images obtained with the new sensor should be comparable to images from the old sensor, evaluated by Lundgren et. al (2006) if feeding and positioning are controlled. The main benefit from using the new sensor is speed. It should also be expected to have a higher dynamic range but such conclusions can not be made from these measurements. The influences on the result of variations in the surface structure need further examination.

Acknowledgements

The project was financed by the Skewood program, the Swedish Agency for Innovation Systems (Vinnova) and the Kempe foundation. The microwave sensor and assistance in scanning was provided by Satimo.

References

Anon. (2006). SATIMO, Courtaboeuf 91953 France. Home page: http://www.satimo.fr/

BOLOMEY J. C. AND F. E. GARDIOL. 2001. Engineering applications of the modulated scatterer technique. Artech House Inc. ISBN: 1-58053-147-42004.

CHOFFEL D., B. GOY, P. MARTIN AND D GAPP. 1992. Interaction between wood and microwaves – automatic grading application. In: Lindgren O. (ed) 1st International Seminar on Scanning Technology and Image Processing on Wood. Luleå University, Skellefteå, Sweden, pp 1.8.

HANSSON L., N. LUNDGREN, A. L. ANTTI AND O. HAGMAN. 2005. Microwave penetration in wood using imaging sensor. Measurement 38:15–20.

LUNDGREN N., O. HAGMAN AND J. JOHANSSON. 2006. Predicting moisture content and density distribution of Scots pine by microwave scanning of sawn timber II: evaluation of models generated on a pixel level. J Wood Sci. 52:39-43.

Appendix I

Description of the pieces.

A. Birch, thickness 50 mm, size. Average MC 12%.
B. Pine, Average MC 3%.
C. Pine, Average MC 67%.
D. Birch, with thickness from 60 to 10 mm. Average MC 67%.

Dimensions

Piece	Specie	Thickness (mm)	Width (mm)	Length (mm)
A	Birch	50	177	495
Polish Pine (B)	Pine	43	150	320
C	Pine	43	155	500
D	Birch	60 to 10	210	500

Weight and average moisture content.

Before visit to Satimo. CT scanning 1				
PIECE	A	POLISH PINE (B)	C	D
MASS	3.0260	0.9060	3.0470	4.1920
MC(%)	12.1572	3.1656	67.4544	68.2183

At Satimo (Paris). Microwave scanning				
PIECE	A	POLISH PINE (B)	C	D
MASS (approximate)	3.00	0.90	3.05	4.15
MC(%)	11.19	2.48	67.62	66.53

Before drying (Skellefteå). CT scanning 2				
PIECE	A	POLISH PINE (B)	C	D
MASS	3.0000	0.9110	3.0390	4.1890
MC(%)	11.1935	3.7349	67.0147	68.0979

After first drying. CT scanning 3				
PIECE	A	POLISH PINE (B)	C	D
MASS	2.7740	0.8855	2.2050	3.1270
MC (%)	2.8169	0.8312	21.1805	25.4815

After second drying (June). CT scanning 4				
PIECE	A	POLISH PINE (B)	C	D
MASS	2.6980	0.8782	1.8196	2.4920
MC(%)				

Appendix II

Results from measurements on piece B (Polish Pine). The left column illustrates previous results obtained from measurements with the old microwave scanner and finite element modelling. The right column shows the same cross section in this measurement. The vertical scale is the same in both columns.

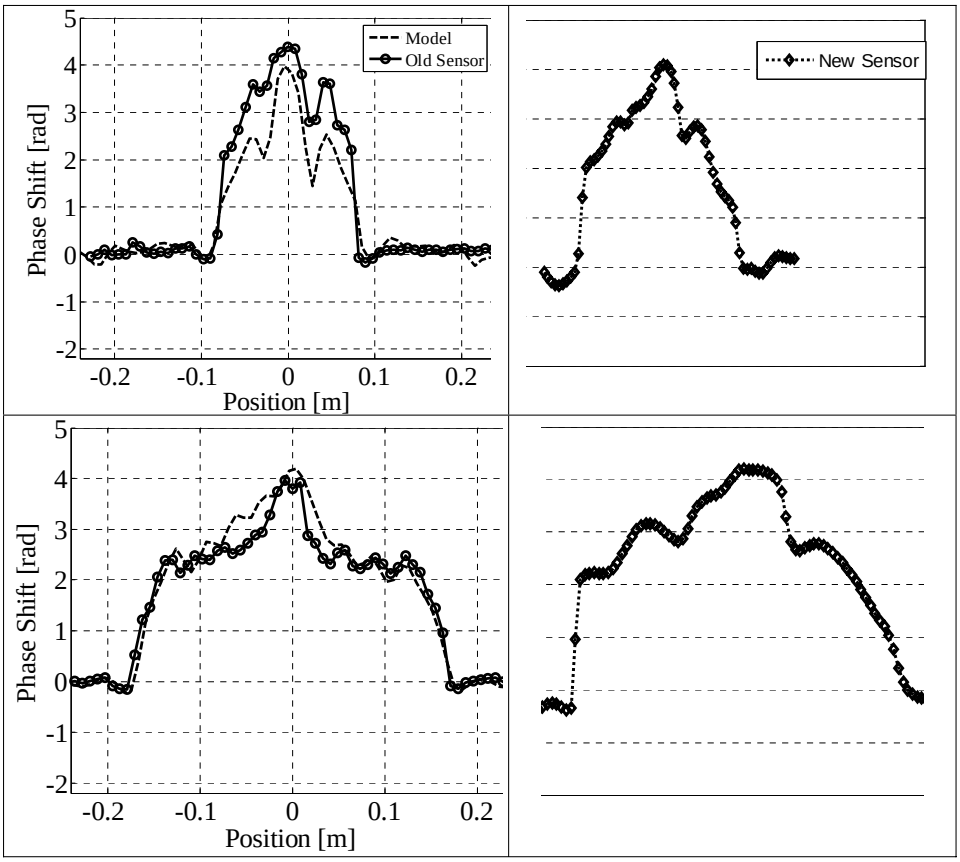

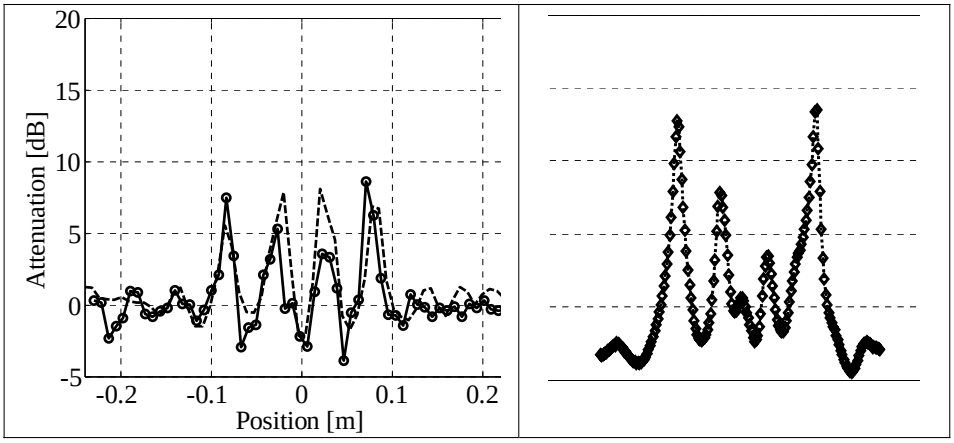

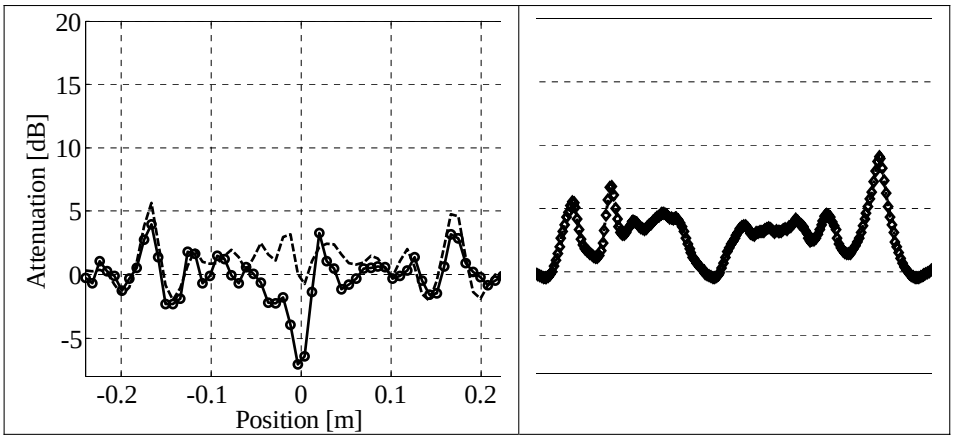
20
15
10
5
0
-5
Attenuation [dB]
-0.2
-0.1
0
0.1
0.2
Position [m]

Appendix III

Results for Piece D (green birch with varying thickness from 10 to 60 mm)
The variation in thickness has a lower influence on the results from the new scanner than expected. Piece D was scanned with the old scanner after drying in order to compare the results.

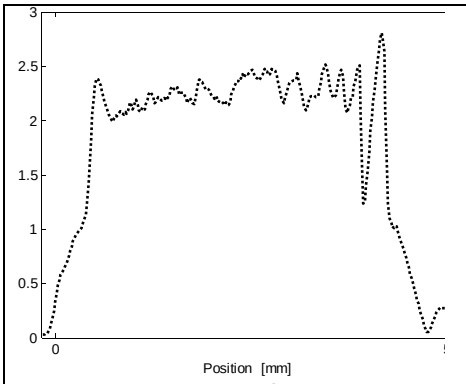

New scanner, Phase Shift in radians.
Piece D in green condition.

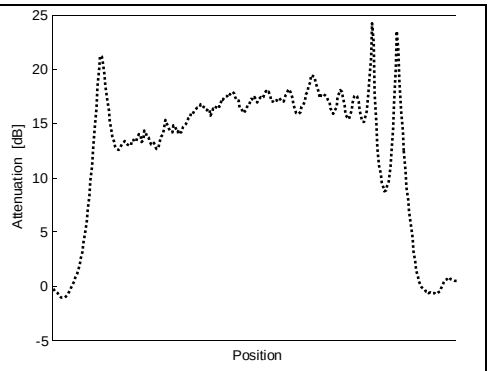

New scanner, Attenuation in decibels.
Piece D in green condition.

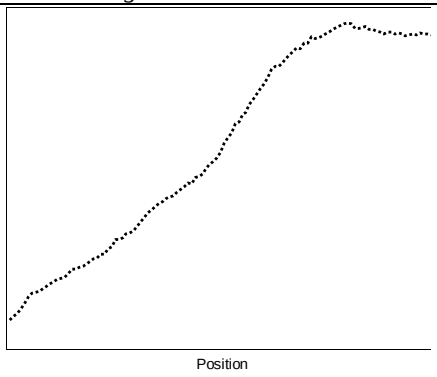

Old scanner, Phase Shift.
0 - 360 mm from thin end of piece D
(after drying).

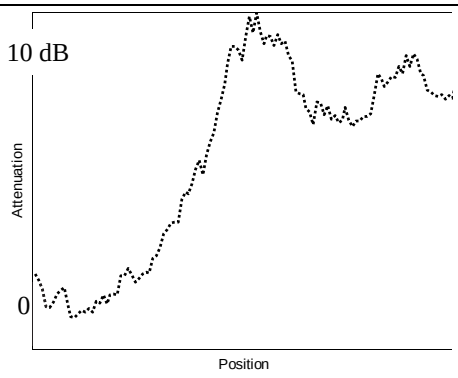

Old scanner, Attenuation.
0 - 360 mm from thin end of piece D
(after drying).